

Biophysical Investigations of Boranophosphate siRNA for use in RNA Interference

Against Human Disease

by

Laura W Moussa

Department of Chemistry
Duke University

Date: _____

Approved:

Barbara Ramsay Shaw, Supervisor

Richard MacPhail

Boris Akhremitchev

Jiyong Hong

Dissertation submitted in partial fulfillment of
the requirements for the degree of Doctor
of Philosophy in the Department of
Chemistry in the Graduate School
of Duke University

2009

ABSTRACT

Biophysical Investigations of Boranophosphate siRNA for use in RNA Interference

Against Human Disease

by

Laura Moussa

Department of Chemistry
Duke University

Date: _____

Approved:

Barbara Ramsay Shaw, Supervisor

Richard MacPhail

Boris Akhremitchev

Jiyong Hong

An abstract of a dissertation submitted in partial
fulfillment of the requirements for the degree
of Ph.D. in the Department of
Chemistry in the Graduate School
of Duke University

2009

Copyright by
Laura W Moussa
2009

Abstract

This project is predicated on the ability of the boranophosphate modification of siRNA to increase its therapeutic applicability for gene silencing in *in vitro* and *in vivo* systems. It has been shown that the boranophosphate ($\text{BH}_3\text{-PO}_3$) can overcome many of the limitations that are traditionally found when using RNAi, namely nuclease stability. The synthesis of siRNA modified with 5'-(α -P-borano)-nucleoside triphosphates (NTP) analogs alone and in combination with 2'-deoxy-2'-fluoro nucleoside triphosphate analogs were performed and optimized. It was found that normal RNA transcriptions showed the highest yield with higher NTP concentrations and shorter incubation times. Boranophosphate modified RNA and 2'F/borano modified RNA transcription yield was optimal at lower NTP concentrations and extended incubations. The boranophosphate NTPs and RNA were characterized with high performance liquid chromatography, mass spectrometry, and nuclear magnetic resonance, indicating successful synthesis of NTP α B and 2'F NTPs. PAGE and mass spectrometry analysis were performed to ensure full-length transcription of the modified siRNA molecules. The effects of these modifications were explored with respect to the biophysical properties of the modified homoduplex and heteroduplex siRNA. The techniques used in this work included hybridization affinity assays (melting temperature), secondary structure determination

(circular dichroism), nuclease stability assays, and assessment of the lipophilicity of the modified siRNA by determining partition coefficients.

Modification of siRNA with boranophosphate and 2'fluoro/borano modified NTPs appears to have caused the homoduplexes and heteroduplexes to adopt a more B form-like helix that had lower T_m compared to unmodified RNA. The stability of the siRNA transcript to enzymatic hydrolysis by Exonuclease T was on the order of 2'fluoro/borano > normal = boranophosphate. Boranophosphate modification increased the stability of the transcript to enzymatic hydrolysis by the endonuclease RNase A, compared to both normal and 2' fluoro modified siRNA. Overall, the 2' fluoro/borano modified siRNA showed the greatest biological stability. Modification of the siRNA with increasing percentages of boranophosphates resulted in increasing lipophilicity of the molecule up to 60-fold, compared to both normal and 2' fluoro RNA.

A method to site-specifically modify the boranophosphate siRNA using T4 RNA ligase was also investigated. Finally, the siRNA in this work was tested in several *in vitro* systems, yielding promising results for the usage of boranophosphate siRNA for use against human viruses and cancers. It was shown that in for *in vitro* systems for human papillomavirus gene expression (HeLa, SiHa, and W12E) and luciferase expression (B16F10 cells), boranophosphate modified siRNA can specifically downregulate gene expression, and in the case of human papillomavirus, can downregulate cell growth.

Contents

Abstract	iv
List of Tables	xi
List of Figures	xiii
List of Schemes	xvi
List of Abbreviations	xvii
Acknowledgements	xxi
1. Introduction.....	1
1.1 RNA.....	1
1.1.1 The Central Dogma	1
1.1.2 Structure and Properties of Nucleic Acids.....	2
1.2 RNA Interference (RNAi).....	5
1.3 Modification of RNA.....	11
1.4 Project definition.....	14
2. Materials and Methods.....	15
2.1 Instruments.....	15
2.2 Chemicals, Enzymes, and Nucleic Acids	23
2.2.1 Chemicals	23
2.2.2 Buffers	25
2.2.3 Enzymes and Kits.....	29
2.2.4 Nucleosides, Nucleotides, and Nucleic Acids.....	34

2.3 General Methodology	40
2.3.1 Concentration determination of nucleic acids.....	40
2.3.2 DNA Template Preparation and RNA Transcription	41
2.3.3 Agarose Gels	43
2.3.4 Polyacrylamide Gel Electrophoresis (PAGE)	44
3. Synthesis and Purification of Normal and Chemically Modified Nucleotides and Oligonucleotides	47
3.1 Introduction.....	47
3.1.1 Synthesis of modified nucleotide triphosphates.....	47
3.1.2 Synthesis of modified oligonucleotides	48
3.1.2.1 Chemical synthesis of oligonucleotides.....	49
3.1.2.2 Enzymatic Synthesis of oligonucleotides	50
3.2 Synthesis of NTP α B Modified and 2' F Modified Triphosphates.....	54
3.2.1 Experimental Procedures	54
3.2.2 Results and Discussion	58
3.3 Purification of NTP α B and 2'F-NTP Modified Triphosphates	65
3.3.1 Experimental Procedures	65
3.3.2 Results and Discussion	67
3.4 Enzymatic Synthesis of Normal and Chemically Modified Ribonucleic Acids	73
3.4.1. Experimental Procedures	73
3.4.2 Results and Discussion	77
3.5 Purification of Enzymatically Synthesized Normal and Chemically Modified Oligonucleotides.....	84

3.5.1	Experimental Procedures	84
3.5.2	Results and Discussion	86
3.5	Chapter Summary	91
4.	Investigations of modified siRNA duplex in regards to secondary structure.....	93
4.1	Background Overview	93
4.2	Thermal stability of modified RNA duplexes	95
4.2.1.	Introduction.....	95
4.2.2.	Experimental Procedures	97
4.2.3	Results	101
4.2.4	Discussion.....	107
4.3	Circular Dichroism	113
4.3.1.	Introduction.....	113
4.3.2.	Experimental Procedures	114
4.3.3	Results.....	115
4.3.4.	Discussion.....	120
4.4	Chapter Summary	122
5.	Chemical and Biological Properties of Boranophosphate siRNA	124
5.1	Chemical Stability of Boranophosphate Modified siRNA.....	124
5.1.1	Introduction.....	124
5.1.2	Experimental Procedures	125
5.1.3	Results	127
5.1.4	Discussion.....	130

5.2 Enzymatic Stability of Boranophosphate Modified siRNA.....	131
5.2.1. Introduction.....	131
5.2.1.1 Ribonuclease A.....	132
5.2.1.2 Exonuclease T.....	133
5.2.2 Experimental Procedures.....	133
5.2.3 Results and Discussion.....	135
5.2.3.1. Ribonuclease A.....	135
5.2.3.2 Exonuclease T.....	139
5.3 Lipophilicity of modified siRNA.....	144
5.3.1 Introduction.....	144
5.3.2 Experimental Procedures.....	145
5.3.3 Results and Discussion.....	147
5.4 Chapter Summary.....	150
6. Site specific modification of boranophosphate siRNA using T4 RNA ligase.....	152
6.1 Introduction.....	152
6.2 Experimental Procedures.....	155
6.3 Results.....	159
6.4 Discussion.....	163
6.5 Chapter Summary and Future Work.....	165
7. Biological Applications of Boranophosphate siRNA.....	167
7.1 Boranophosphate siRNA for use against human papillomavirus.....	167
7.1.1 Introduction.....	167

7.1.2 Experimental Procedures	170
7.1.3 Results and Discussion	172
7.1.4 Summary	178
7.2 Efforts toward cellular delivery of boranophosphate siRNA	178
7.2.1 Introduction.....	179
7.2.2 Experimental Procedures	180
7.2.3 Results and Discussion	183
7.2.4 Summary	189
8. Summary and Future Work.....	191
Appendix I	195
Appendix II.....	200
References	203
Biography.....	214

List of Tables

Table 2-1. Nucleoside, nucleotide monophosphate, nucleotide diphosphate, and nucleotide triphosphate molecular weights.....	36
Table: 2-2. DNA and RNA sequences with source, purity, molecular weight, and molar extinction coefficient (ϵ_{\max}).....	38
Table 2-3. Maximum absorbance wavelength (λ_{\max}) and molar extinction coefficient (ϵ_{\max}) for the four nitrogenous bases of RNA	40
Table 2-4. PAGE gel percentages and corresponding ranges of separation.....	45
Table 3-1. Yields of NTP α B syntheses by weight and by UV absorbance.....	60
Table 3-2. Optimal preparative scale purification conditions for the four NTP α Bs.....	70
Table 3-3. HPV 16+24 AS sequence 21mer RNA transcripts were used for comparison of yield under different conditions.....	75
Table 4-1. Modified RNA sequences used for the melting temperature and circular dichroism experiments.....	99
Table 4-2. T_m values for the homo- and hetero- duplexes.....	105
Table 4-3. Comparison of effect of modification on T_m for homoduplexes.....	106
Table 4-4. Comparison of effect of modification on T_m for heteroduplexes.....	107
Table 5-1. Enzymatically transcribed 21mer RNA used in thermodynamic and enzymatic stability assays, as well as lipophilicity assays.....	126
Table 5-2. Kinetics of RNase A digestion of ^{32}P endlabeled modified HPV 16+24 AS RNA over time.....	136
.Table 5-3. Kinetics of Exo T digestion of natural and modified RNA over time.	141
Table 5-4. Partition coefficients for natural and modified ^{32}P -labeled HPV 16+24 siRNA.. ..	148
Table 6-1. The four sets of ligation reaction conditions that were tested to achieve ligation of 11mer boranophosphate RNA donor molecules to 11mer unmodified acceptor molecules using T4 RNA ligase.....	161
Table 7-1. siRNA sequences used in HeLa cell culture assays	171
Table 7-2. Modifications of HPV 16+24+G siRNA used in cell proliferation assays.....	175

Table 7-3. Luciferase sequences used in melanoma cell lines.....	181
Table 7-4. Enzymatically transcribed 19 nt duplexes with 3' UU overhangs used in the luciferase assays in B16F10 cells.	184

List of Figures

Figure 1-1. The central dogma of molecular biology.....	1
Figure 1-2. The four nucleotides of RNA.....	3
Figure 1-3. Base pairing and the double helix.....	4
Figure 1-4. T7 RNA polymerase promoter region.....	5
Figure 1-5. Different methods of gene silencing.....	6
Figure 1-6. The endogenous pathway of RNA Interference.....	8
Figure 1-7. Positions available for modification on a nucleoside triphosphate..	11
Figure 1-8. Selected modifications of the phosphate backbone.....	12
Figure 3-1. T7 RNA Polymerase.....	52
Figure 3-2. A ribbon diagram showing the overall structure of T7 RNA polymerase.....	53
Figure 3-3. Starting materials for the chemical syntheses of NTP α Bs.....	55
Figure 3-4. Starting protected nucleosides for synthesis of 2'F modified triphosphates..	57
.....	
Figure 3-5. The four rNTP α Bs.	59
Figure 3-6. Characterization by UV and ESI-MS of the final products of NTP α B synthesis.	61
Figure 3-7. Characterization by NMR of final products from NTP α B synthesis	62
Figure 3-8. 2'F NTPs.....	63
Figure 3-9. Characterization by UV and ESI-MS of the final products of 2'F NTP synthesis.	64
Figure 3-10. Rp and Sp stereoisomers that result from the introduction of the chiral center by substitution of a non-bridging oxygen with a borane group	67
Figure 3-11. Separation profiles of the four NTP α B stereoisomers, where time is plotted versus absorbance.	71
Figure 3-12. Representative analytical RP-HPLC spectra..	72
Figure 3-13. Analytical spectra of 2'F UTP.	73

Figure 3-14. MALDI-MS of enzymatically synthesized normal siRNA and boranophosphate siRNA using <i>Rp</i> -GTP α B.	79
Figure 3-15. Yield comparisons of 21mer normal and boranophosphate modified RNA.	81
Figure 3-16. Retention times of dT standards (5, 10, 15, 20, 30 nt) on reverse phase HPLC column.	87
Figure 3-17. 20% PAGE/7M Urea Analysis of enzymatically transcribed, radiolabeled unpurified and purified 21mer HPV 16+24 AS RNA.	90
Figure 4-1. Base interactions in oligonucleotide duplexes.	95
Figure 4-2. Hyperchromicity)	96
Figure 4-3. Lower and upper limits for hyperchromicity calculations of T_m	100
Figure 4-4. HPV 16+24 RNA:RNA duplex.	102
Figure 4-5. Representative melting curves of modified duplexes at a final concentration of 2 μ M in 0.1 M potassium phosphate, pH 7.4.	103
Figure 4-6. C2' endo and C3' endo sugar conformations of DNA and RNA.	112
Figure 4-7. Representative CD spectra for three types of helical structures.	113
Figure 4-8. CD spectra of single stranded RNAs.	116
Figure 4-9. CD spectra of homoduplex RNA.	118
Figure 4-10. CD spectra of heteroduplex RNA.	119
Figure 4-11. Secondary structure of single stranded HPV 16+24 antisense RNA.	121
Figure 5-1. Thermodynamic hydrolysis of RNA.	125
Figure 5-2. 20% PAGE/ 7 M urea analysis of the stability of single stranded siRNA at 37°C and pH 7.4, incubated over 24 hours.	128
Figure 5-3. Chemical hydrolysis of RNA over 24 hours under physiological temperature and pH.	129
Figure 5-4. Mechanism of RNase A catalyzed cleavage of the phosphodiester bond. ...	132
Figure 5-5. 20% PAGE/7 M urea gel analysis of natural and modified RNA stability to RNase A hydrolysis assay.	137
Figure 5-6. Kinetics of natural and modified RNA against RNase A degradation assays.	138

Figure 5-7. . 20% PAGE/7 M urea gel analysis of natural and modified RNA stability to Exonuclease T hydrolysis assay.....	140
Figure 5-8. Kinetics of natural and modified RNA against Exonuclease T degradation assays.....	142
Figure 5-9. Effect of boranophosphate modification on the partition coefficients of siRNA.	149
Figure 6-1. Experimental flow for the T4 RNA ligation experiments using normal and boranophosphate modified siRNA.	156
Figure 6-2. Expected product of the T4 RNA ligase reaction with boranophosphate RNA..	159
Figure 6-3. Products of ligation of a normal acceptor and a boranophosphate donor using T4 RNA ligase were run on 20% PAGE/7 M urea	160
Figure 7-1. The proteins encoded by the HPV genome.....	168
Figure 7-2. HPV oncoprotein E7	168
Figure 7-3. HPV oncoprotein E6.	169
Figure 7-4. Products of T7 RNA polymerase transcription using normal and modified NTPs on 20% PAGE/7 M urea gels.....	173
Figure 7-5. W12E cell proliferation assay after administration of 20 nM HPV 16+24+G siRNA.	174
Figure 7-6. SiHa cell proliferation assay after administration of 20 nM modified single stranded siRNA.....	176
Figure 7-7. Formation of LPD nanoparticles.....	180
Figure 7-8. Enzymatically transcribed sense and antisense luciferase single stranded siRNA products analyzed on 20% PAGE/7 M urea.....	182
Figure 7-9. Downregulation of luciferase activity by anti-luciferase modified siRNA.	186
Figure 7-10. Silencing of luciferase activity by boranophosphate modified siRNA duplexes compared to chemically synthesized duplexes with dTdT overhangs.	187
Figure 7-11. Comparison of the effect of overhang composition on luciferase activity decrease by anti-luciferase chemically and enzymatically synthesized unmodified siRNA duplexes. with UU overhangs.....	188

List of Schemes

Scheme 3-1. Sal-P-chloride approach to chemical synthesis of adenosine 5'-(α -P-borano) triphosphate.....	48
Scheme 3-2. Chemical synthesis of oligonucleotides.....	50
Scheme 6-1. Ligation reaction using T4 RNA ligase.....	154
Scheme 6-2. T4 RNA ligase mechanism.....	154

List of Abbreviations

α -P-borano	Nucleotides and oligonucleotides modified with BH_3 on the α phosphorus
A_{260}	UV Absorbance at 260 nanometers
Ac	Acetyl
AP	Antarctic Phosphatase
bp	Base pairs
BP	Boranophosphate
BP-RNA	Boranophosphate modified RNA
CD	Circular Dichroism
dATP	2'-Deoxyadenosine 5'-triphosphate
dCTP	2'-Deoxycytidine 5'-triphosphate
dGTP	2'-Deoxyguanosine 5'-triphosphate
dTTP (TTP)	Thymidine 5'-triphosphate
dNTP	dATP + dCTP + dGTP + dTTP
DCM	Dichloromethane
DEPC	Diethylpyrocarbonate
DI Water	Deionized water
DMF	N,N-Dimethylformamide

DMT	4,4'-Dimethoxytrityl
DNA	Deoxyribonucleic acid
DNase	Deoxyribonuclease
DTT	Dithiothreitol
ϵ_{260}	Molar absorptivity at 260 nanometers
E2F	Transcription factor that up-regulates expression of genes involved in DNA replication, DNA repair and mitosis
E6	Human papillomavirus oncoprotein, binds to p53
E6AP	E6 associated protein
E7	Human papillomavirus oncoprotein, binds to pRB
EDTA	Ethylenediaminetetraacetic acid
ESI-MS	Electrospray ionization mass spectrometry
FAM	Fluorescein isothiocyanate
HPFC	High performance flash chromatography
HPLC	High performance liquid chromatography
HPV	Human papillomavirus
LPD	Liposome-protamine-DNA
MALDI-MS	Matrix assisted laser desorption/ionization mass spectrometry
mRNA	Messenger RNA
NMR	Nuclear magnetic resonance spectroscopy

NDP	Nucleotide diphosphate
NMP	Nucleotide monophosphate
NTP	Nucleotide triphosphate
nt	Nucleotide
OD ₂₆₀	Optical density unit at 260 nanometers; 1 OD ₂₆₀ compound, when dissolved in 1 mL solution, has an A ₂₆₀ of 1 at 260 nanometers and a 1 cm light path length
ODN	Oligodeoxynucleotide (DNA backbone)
ON	Oligonucleotide (RNA backbone)
PAGE	Polyacrylamide gel electrophoresis
PDE	Phosphodiester
PNK	Polynucleotide Kinase
p53	Protein 53
pRB	Retinoblastoma protein
PS	Phosphorothioate
PTGS	Post-transcriptional gene silencing
Py	Pyridine
RNA	Ribonucleic acid
RNase	Ribonuclease
RNAi	RNA interference

r.t.	Room temperature
SD	Standard deviation
siRNA	Small interfering RNA
TEA	Triethylamine
TEAA	Triethylamine acetate
TEAB	Triethylammonium bicarbonate
TEMED	N,N,N',N'-Tetramethylethylenediamine
THF	Tetrahydrofuran
T _m	Melting temperature
Tris	Tris(hydroxymethyl)aminomethane
UV	Ultraviolet

Acknowledgements

I would like to express my sincere appreciation of my advisor, Dr. Barbara Ramsay Shaw for her guidance and support throughout my graduate studies. The Shaw group has been a very open place to conduct research, and I have been very lucky to have wonderful co-workers, both past and present. Dr. Nadeem Hashmi, Dr. Shoeb Kahn, and Marcus Cheek contributed invaluable help with the synthesis of materials. Dr. Chrissy Prater was instrumental in helping me set up the molecular biology experiments. Dr. Charlotta Wennefors and Mariam Sharaf have been my partners-in-research and partners-in-crime during the time we shared as graduate students.

The Alexander Lab the University of Chicago and the Huang Lab at UNC-CH both deserve my deepest thanks for fruitful collaborations that enabled the *in vitro* tests. I would also like to thank Dr. Jiyong Hong, Dr. Richard MacPhail, Dr. Boris Akhremitchev, and Dr. Ken Alexander for participating as my committee members.

It is my belief that my parents, Patricia and Wisam Moussa, should be listed as co-authors of this dissertation, because it is their love and support that have been the motivation and foundation for everything that I have done and will do. My siblings Nader and Faye have provided much needed moral support during the dark days that preceded the completion of this thesis. Thanks to Dr. Christopher Rinderspacher, for late night phone calls and early morning morale boosts.

Dedicated to my family

1. Introduction

1.1 RNA

During the life cycle of an organism, the genetic information encoded in the nucleus must make its way into the cytoplasm, where machinery exists to synthesize the proteins necessary for day-to-day tasks. The molecule that is responsible for the transition from DNA sequence to functional protein is known as messenger ribonucleic acid, or mRNA.

1.1.1 The Central Dogma

The central dogma of molecular biology illustrates the storage and transfer of genetic information. The process, demonstrated in Figure 1-1, utilizes double-stranded DNA as the storage molecule for genetic information and single stranded RNA as an information transfer molecule.

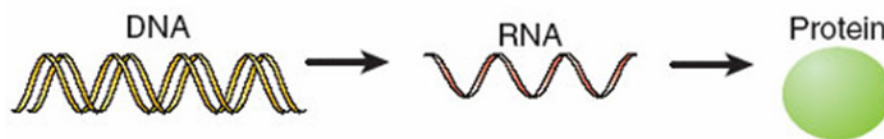


Figure 1-1. The central dogma of molecular biology. The genetic information stored in the DNA is transferred via transcription into RNA. The RNA travels from the nucleus of the cell into the cytoplasm, where it is translated into protein.

The DNA is transcribed to mRNA in the nucleus and then processed, capped and exported into the cytoplasm, where translation machinery decodes the triplet codons (three nucleotides) into an amino acid sequence to create proteins. Once they are

synthesized, proteins perform the biological functions necessary for life in the cell, namely by participating in signaling cascades that regulate gene expression and by catalyzing biochemical reactions required for energy metabolism and cell reproduction (Davidson 1976).

1.1.2 Structure and Properties of Nucleic Acids

The ability of nucleic acids to lend themselves easily to decoding is due to their unique structure. First noted by Watson and Crick, the double helix structure of DNA that is formed by complementary base pairing between the two strands intuitively “suggests a possible copying mechanism for the genetic material.” (Watson and Crick 1953). The double helix allows for easy replication and transfer of the genome via the central dogma.

DNA and RNA contain subunits, called nucleotide triphosphates (NTPs), which consist of one of four nitrogenous bases, a sugar ring, and phosphodiester linkages to form linear polymers. The base composition of the nucleotide sequence encodes the genetic information necessary for the construction of proteins. DNA and RNA differ in two important structural aspects; 1) In DNA, the four nitrogenous bases are adenine (A), guanine (G), cytosine (C), and thymine (T), while in RNA, the thymine is substituted by uracil (U), and 2) DNA utilizes deoxyribose as its sugar ring, while RNA uses ribose (Davidson 1976). These divergences result in different biophysical and biological properties of the RNA:RNA, DNA:DNA, and RNA:DNA duplexes (Calladine and Drew 1992). The structures of the four RNA nucleotide triphosphates are shown in Figure 1-2.

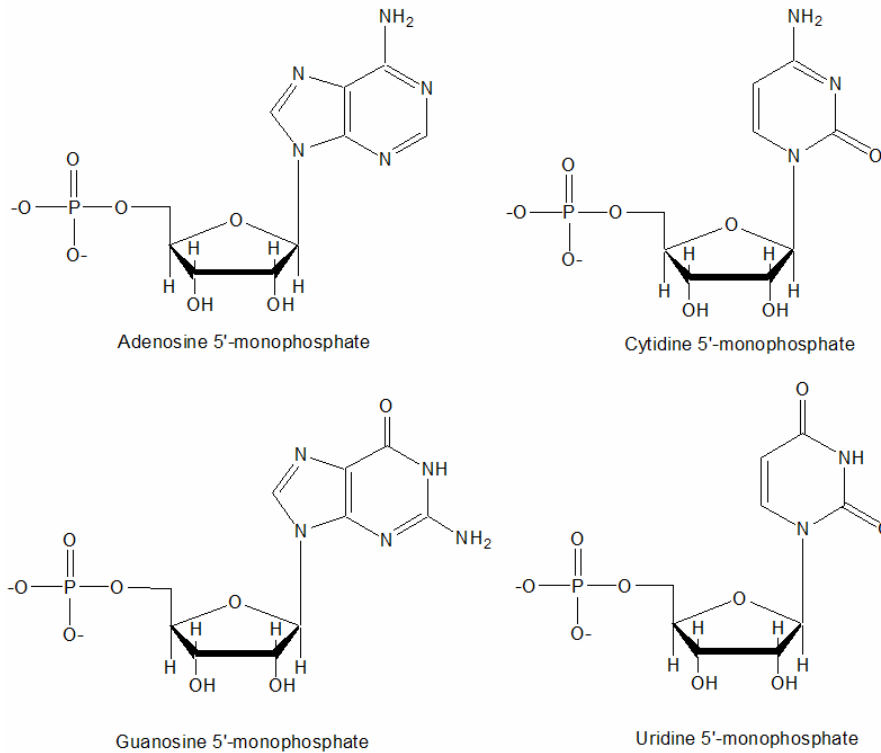


Figure 1-2. The four nucleotides of RNA. The nucleotide is made of a nitrogenous base, a sugar ring, and a phosphate (mono-, di-, and tri-). Adenosine and guanine are purines and cytosine and uridine are pyrimidines.

The assembly of mRNA is dictated by the arrangement of the constituent bases of its DNA template; therefore, RNA carries the complement of the genetic information stored in the DNA, albeit in a modified version. The bases of DNA and RNA are capable of hydrogen bonding to each other via canonical (i.e. Watson-Crick) base pairs, A-U and G-C to form a double helix. The phosphate moiety and the sugar form the backbone of the helix. Each nucleic acid strand has polarity, or sense, and pairing occurs with one strand in the 5'→3' orientation and the other strand in the 3'→5' orientation to form a double stranded duplex (Figure 1-3) (Smith et al 1983). There are differences in the thermal stability of the duplex depending on the type of nucleic acid it is made from.

The melting temperature (T_m) of the RNA:RNA duplex is usually higher than that of a DNA:DNA duplex; however, specific T_m values must be calculated based on oligonucleotide concentration, salt concentration, and sequence.

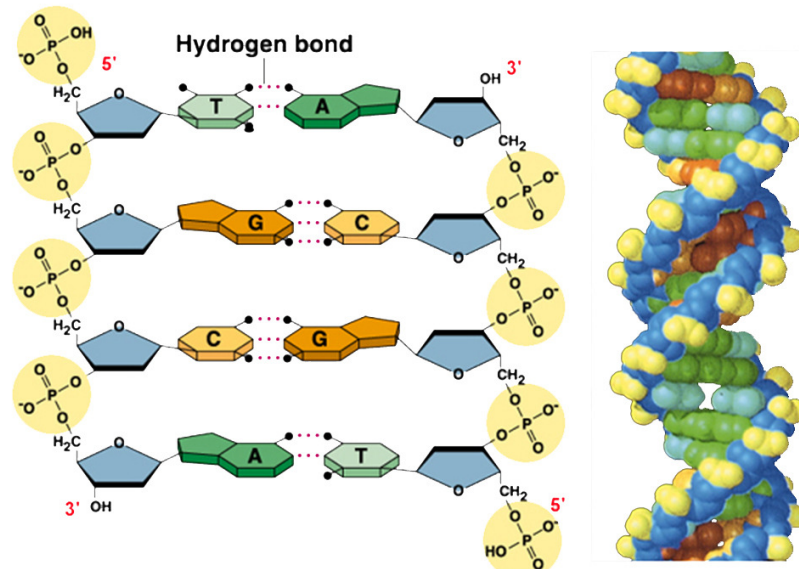


Figure 1-3. Base pairing and the double helix. Watson-Crick base pairing allows for easy storage, replication, and transfer of genetic information. Double stranded oligonucleotides form a double helix with the two strands having opposite polarity.

Transcription is the enzymatic synthesis of mRNA that is complementary in sequence to a DNA template. The enzymes responsible for transcription are known as RNA polymerases (RNA pol). Working in the nucleus, RNA pol's produce pre-mRNA in a 5' → 3' direction, which is then processed into mRNA, capped, and exported into the cytoplasm. Bacteriophage T7 RNA polymerase (T7 RNA pol) is the most extensively studied enzyme used for *in vitro* transcription of RNA (Kochetkov, et al 1998; Sousa and Mukherjee 2003; Wan and Shaw 2005). T7 RNA pol utilizes a specific promoter

sequence in order to recognize DNA templates, shown in Figure 1-4. Once the promoter region is recognized, the polymerase can bind the double stranded DNA template and begin transcription of the template strand.

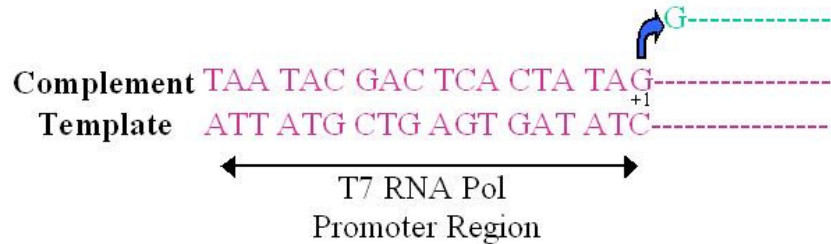


Figure 1-4. T7 RNA polymerase promoter region. T7 RNA pol recognizes a specific sequence of double stranded DNA template to begin transcription at the +1 position. DNA is shown in purple and RNA is shown in green.

1.2 RNA Interference (RNAi)

Anomalous host cell gene expression is associated with human disease, notably viral infections and cancers. Often, this deregulated gene expression results in deregulated cell growth coupled with an inhibition of cell death (apoptosis). Therefore, one therapeutic approach to treating diseases is to artificially control the ability of certain genes (known as oncogenes) to form proteins that lead to maladaptive behavior for the organism (cancerous transformation). The unique structures of nucleic acid polymers suggest several strategies for modulating gene expression. It has been shown that administration of complementary nucleic acid sequences to the gene of interest can result in specific silencing of that gene's message (Hélène 1990; Fire 1998; Fire 1999). This is known as homology dependent gene silencing.

Homology dependent gene silencing can occur by one of two mechanisms. (Figure 1-5) The first mechanism, transcriptional gene silencing (TGS), interferes with DNA to block transcription. The second mechanism, post-transcriptional gene silencing (PTGS), decreases the half-life of target mRNA to block translation. The Nobel Prize in 2006 was awarded for the discovery of RNA interference (RNAi), a form of homology dependent PTGS, where expression of a gene is turned off due to the introduction of exogenous oligonucleotide sequences that is a match to the sequence of the gene and is complementary to the gene's mRNA. All homologous mRNAs in the cell with at least 80% sequence match are degraded.

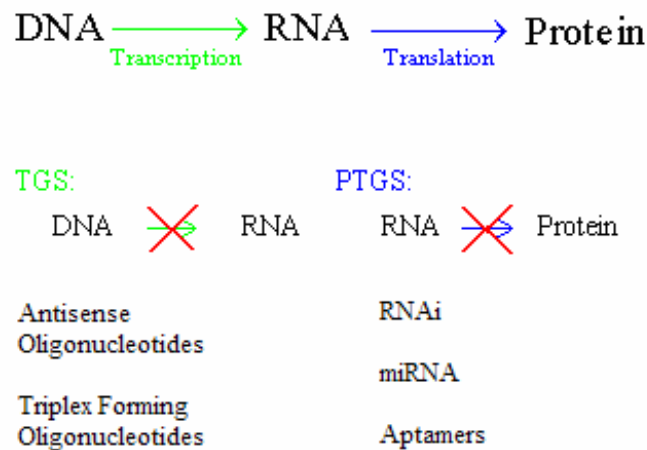


Figure 1-5. Different methods of gene silencing. Transcriptional gene silencing blocks the synthesis of RNA and post-transcriptional gene silencing blocks the synthesis of proteins. Both methods can be achieved using several different techniques.

RNAi has several interesting and unique properties. To begin with, the application of RNAi results in a phenotype identical to the genetic null mutant (Alberts, et al. 2002). Genes with the sequence corresponding to exogenous sequence are silenced

with no effect on DNA lacking homology. Therefore, the mechanism of RNAi does not represent genetic change and is highly specific (Fire 1999). It has been shown that double stranded RNA (dsRNA) is important in the mechanism of RNAi, as observed in the experiment of dsRNA by Fire, et al in 1998 in *C. elegans*. Injection of single stranded RNA (ssRNA) with sense and antisense polarity into the organism showed marginal silencing activity while the injection of both showed interference two orders of magnitude higher (Fire, et al. 1998). The increased potency of the mixture was attributed to the formation of dsRNA from the ssRNA. With few exceptions, dsRNA was shown to be most effective in gene silencing of the corresponding gene compared to ssRNA, and RNAi effects have been shown to carry over into the F1 generation but are usually lost by the F2 generation (Fire 1999).

The RNAi effect is the result of a distinct host cell mechanism (Haley and Zamore 2004). Figure 1-6 shows a representation of the pathway from the dsRNA trigger to the gene silencing. The first step is the introduction of dsRNA that is greater than 500 base pairs in length into the cell. The second step of the mechanism requires an enzyme termed Dicer. Dicer is an RNase III homologue, a dsRNA-specific endonuclease, and has homologues in many organisms. Dicer cleaves the dsRNA strand into 20-25 nucleotide dsRNA segments called small interfering RNA (siRNA). Each siRNA is double stranded, containing a guide strand and a passenger strand. The guide strand is complementary to the target mRNA and the passenger strand is identical to the target

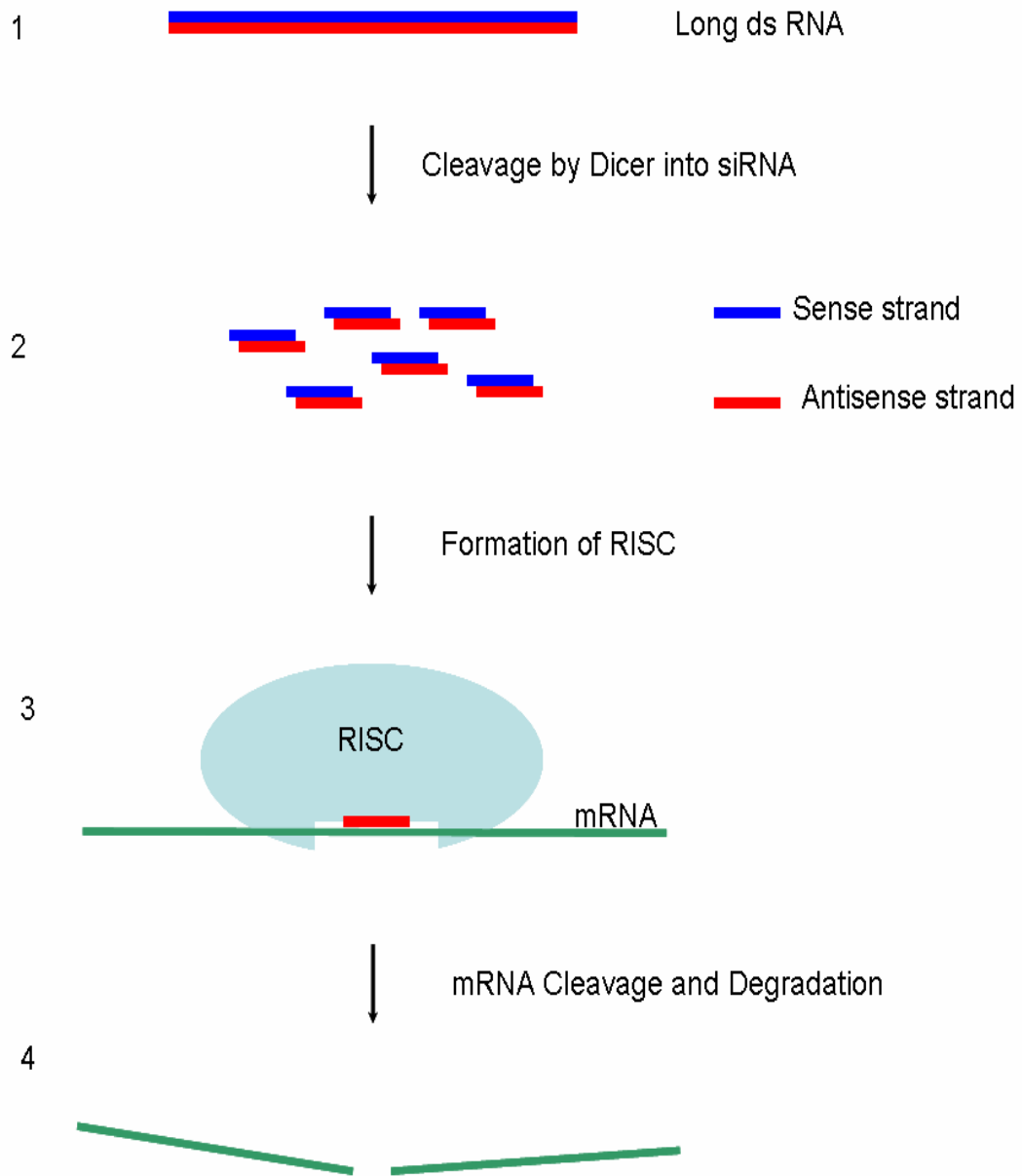


Figure 1-6. The endogenous pathway of RNA Interference. 1) Long, double stranded RNA is introduced into the cell; 2) The endonuclease Dicer cleaves the dsRNA into small interfering RNA (siRNA); 3) The ribonucleoprotein assembly known as RNA-induced Silencing Complex (RISC) incorporates the antisense strand of the siRNA to guide cleavage; 4) Target mRNA is cleaved in a sequence-specific manner, leading to further degradation by cellular nucleases and silencing of the message.

mRNA sequence. The double stranded siRNA have 2-3 nucleotide 3' overhanging ends that are required for RNAi activity. In the third step of the mechanism, the siRNA are incorporated into the RNA-induced silencing complex (RISC). The RISC is a ribonucleoprotein (RNP) complex with endonuclease activity (Filipowicz 2002). RISC uses the siRNA guide strand to recognize and bind the target mRNA based on hybridization. The final step is the cleavage of the target mRNA from the center of the guide siRNA, followed by degradation by cellular nucleases. The cleavage site of the RISC ribonucleoprotein complex has been shown to be defined by the 5' end of the guide siRNA rather than the 3' end; cleavage occurs 10 nucleotides upstream from the base at the 5' end of the guide strand (Elbashir, et al. 2001). With the mRNA degraded, the protein cannot be formed, and so the gene is silenced. It has been postulated that the mechanism of RNAi is a viral defense mechanism, as RNA viruses begin infection of a cell by injecting long, double stranded RNA genomes into the host (Fire 1999).

The machinery of RISC has been shown to recognize synthetic siRNA, bypassing the Dicer step (Preall and Sontheimer 2005). This allows the therapeutic application of synthetic double stranded siRNA to specifically downregulate the expression of a gene of interest. The RNAi approach has been shown to be a successful therapy in many different laboratories. Recent work in hepatitis B (HBV) infected cells has shown that RNAi can be used to trigger potent silencing of HBV transcripts (Snydera, et al. 2008). Other work targeting human immunodeficiency virus (HIV) has shown the ability to directly target siRNA molecules to the cells of interest (Kirchoff

2008). In the case of human papillomavirus (HPV), siRNAs that targeted the viral oncoproteins were able to reduce expression of viral oncoprotein E7 and restore the normal expression of host proteins (Caberg, et al. 2008).

Over the past 15 years, many scientists have been able to utilize RNAi as a tool for basic research. However, as a therapy, RNA has several disadvantages. The first is the susceptibility of RNA to a class of enzymes known as ribonucleases. Ribonucleases (RNases) accelerate the hydrolysis of the phosphodiester backbone of RNA, either by destroying the internucleoside linkages at the ends of the RNA (exonucleases) or by internally cleaving the RNA into fragments (endonucleases) (Krieg 1996). Secondly, injection of foreign nucleic acids may cause an immune response, via either systemic or cellular immunity (Marques and Williams 2005). Thirdly, any drug that is taken orally is subject to the “first pass effect” of the liver, which breaks down contaminants and then excretes them. The fourth, and most important, hurdle for any oligonucleotide therapy is delivery (Juliano, et al. 2008). Since oligonucleotides are highly charged, they have trouble moving across cell membranes. The RISC machinery is located in the cytoplasm, allowing for easier delivery when compared to antisense oligonucleotide approaches, which must be delivered to the nucleus. Nevertheless, delivery remains the major obstacle to the use of RNAi therapeutics. Therefore, to be therapeutically viable, synthetic siRNA must be potent, ribonuclease-resistant, non-immunoactivating, and will probably have to be delivered intravenously. Also, the siRNA must pass the acid test of cellular uptake.

1.3 Modification of RNA

In human cells, the average half-life of mRNA is reported to be ~600 min (10 hours). However, this mRNA is processed and capped, allowing increased stability versus unmodified RNA. In order to satisfy the requirements for use of siRNAs in a therapeutic manner, the applicability of RNAi can be expanded with chemical modification of the nucleoside triphosphate. By this method, the siRNA can exhibit improved nuclease resistance, cellular uptake, and hybridization affinity (de Fougères 2007). Figures 1-7 shows the positions that available for modification on a nucleoside triphosphate. Modifications have been implemented at positions on the sugar, the base, and the phosphate moieties. The best-studied modifications are the “first-generation” backbone modified NTP analogs (Ludwig and Eckstein 1989; Manoharan 2007). Figure 1-8 show the structures of several types of these backbone modifications.

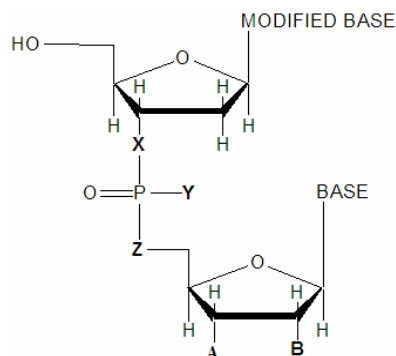


Figure 1-7. Positions available for modification on a nucleoside triphosphate. Positions A and B show modifications on the sugar that act as obligatory and non-obligatory chain terminators, respectively. Positions X, Y, and Z show modifications on the bridging and non-bridging oxygens. Positions on the nitrogenous base may also be modified.

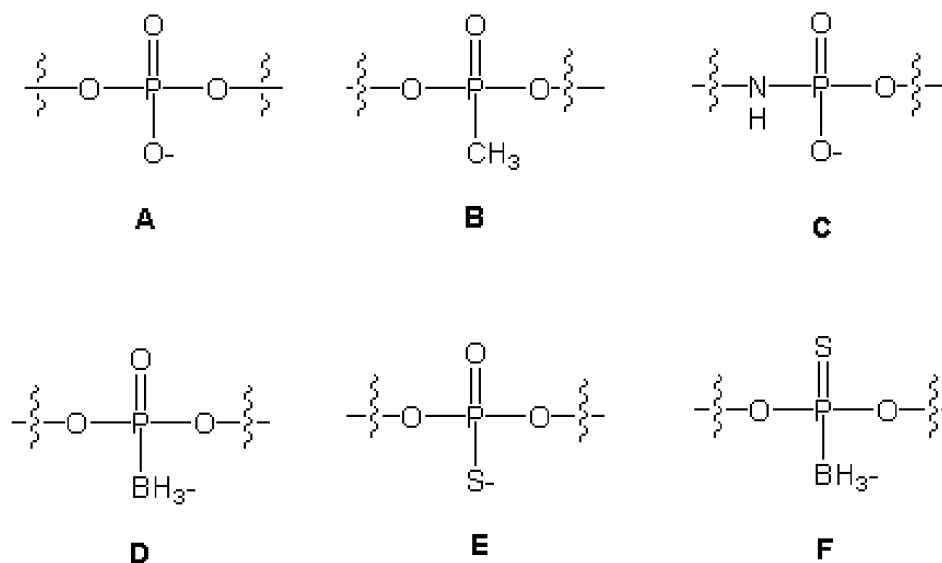


Figure 1-8. Selected modifications of the phosphate backbone. A) normal phosphate, B) methylphosphonates, C) phosphoamidate, D) boranophosphate, E) phosphorothioate, F) boranophosphorothioate.

Backbone modifications of siRNA, including the phosphorothioate and 2'-O-methyl, have been shown to increase the persistence of gene silencing and potency (Amarzguioui, et al. 2003). This dissertation will describe the synthesis of boranophosphate-modified siRNA, where there is exchange of a non-bridging oxygen for a borane ($\text{-BH}_3\text{-}$) group.

Boranophosphates have great potential as therapeutic and diagnostic agents, as the modification confers many unique properties (Sood, et al. 1990; Shaw, et al. 2003). The boranophosphate resembles the normal phosphate in that the negative charge is retained; however, the polarity of the molecule changes because the negative charge is localized on the remaining non-bridging oxygen (He, et al. 1998; Summers, et al. 1998). Partitioning experiments have demonstrated that boranophosphates are more lipophilic

than normal phosphates; this could allow for increased cellular uptake and targeted delivery (He 2000; Wan 2005). In addition, boranophosphates have increased nuclease resistance without affecting activation of RNase H cleavage of RNA in RNA: boranophosphate hybrids (Shaw, et al. 2000; Wang 2004). Importantly, the stability of the boranophosphate allows its administration as a single-stranded siRNA (ss-siRNA), which may allow for increased ease of delivery (due to decreased charge and size) and decreased immunoactivation (Hall, et al. 2006).

Increasingly, the trend in RNAi therapeutics has been to combine modifications on the guide strand of the siRNA in order to maximize the benefit of each modification (Zhang, et al. 2006). Often a backbone modification is combined with a sugar modification, which is known as second generation siRNA. One popular sugar modification is the 2'-deoxy-2'fluororibonucleoside triphosphate (2'F NTP), first described by Codington (Codington, et al. 1964). This modification imparts significant stability to nucleases versus unmodified RNA, and should act to increase the thermal stability of the duplex (Williams, et al. 1991; Kawasaki, et al. 1993; Manoharan 1999; Blidner 2007). The combination of the boranophosphate modifications with 2'fluoro modifications will be investigated in this work to create optimized siRNA molecules for highly potent, specific, and persistent gene silencing in human systems.

1.4 Project definition

The overall goal of this project is to create modified siRNA that show enhanced properties for therapeutic applications. This project investigates the synthesis and properties of boranophosphate modified and 2'F/boranophosphate modified siRNA with respect to the effects of modification on secondary structure, chemical and biological stability, and lipophilicity, and investigates the ability of the modified siRNA to induce gene silencing *in vitro*. Chapter 2 described the instruments, materials, and general methodology that were used in this dissertation. In Chapter 3, the synthesis and purification of the NTP α B triphosphates and 2'F NTPs will be discussed. The synthesis and purification of short 21 and 22 nucleotide RNAs with borano, fluoro, and fluoro/borano modifications will also be discussed. In Chapter 4, the effects of the modifications on the secondary structure and duplex stability will be investigated. In Chapter 5, the effects of the modifications on chemical, endonuclease, and exonuclease stability are discussed and the effects of the modifications on the lipophilicity of the siRNA are investigated. Chapter 6 discusses attempts that were made to synthesize modified RNA with site-specific placement of the boranophosphate modification. Chapter 7 is a summary of the biological applications of the boranophosphate siRNA in two different cell systems to determine its therapeutic efficacy. Chapter 8 summarizes the dissertation and discusses possible avenues of future investigation.

2. Materials and Methods

2.1 Instruments

Centrifuges

A Fisher Scientific Minicentrifuge personal benchtop centrifuge (Fisher Scientific) was used for 10 second spin downs of liquid samples in 0.5 and 1.5 ml plastic centrifuge tubes. Centrifugation of samples after phenol extraction (Section 2.3.2) was done using an Eppendorf MiniSpin Plus centrifuge with dimensions as follows: 9" W x 4.75" H x 9.5" D (Eppendorf). Centrifugation of RNA samples after ethanol precipitation to produce a solid RNA pellet required that the sample be kept at 4°C. For this purpose, the Baxter/Heraeus Biofuge 22R with HFA 6.15, 24 place fixed rotor was used (Baxter Scientific Products). For centrifugation of samples in 15 or 50 ml plastic centrifuge tubes, the Sorvall RC 5 Superspeed Refrigerated Centrifuge with an HS-4 4 place swinging bucket rotor was used (Dupont). The centrifuge speed for all the centrifuges used in this work was determined using the online calculator from Eppendorf located at <http://www.eppendorfna.com/support/online-calculator.asp>. This allowed determination of the relative centrifugal force as long as the diameter of the rotor was known.

UV Spectrometer

The concentrations of nucleotides and nucleic acids used in this work were determined by measuring their UV absorbances at base-specific wavelengths. Measurements were performed using a Varian Cary 500 spectrometer supported with Cary WinUV software or using a Nanodrop ND-100 Spectrometer. For concentration determinations using the Varian Spectrometer, sample solutions were loaded into 80 μ L quartz microcells with Teflon stoppers (Varian 6610014900). These cells are self-masking and have a 4 mm aperture width and 10 mm light path lengths. One of these quartz microcells was used as the reference cell and contained a solvent blank. Both cells were placed in the 6 x 6 Peltier thermostable multicell holder. The Cary electrothermal temperature controller with built-in water reservoir was used for UV thermal melting experiments. For concentration determination using the Nanodrop, the sample holder was thoroughly cleaned using Kimwipes and deionized water 3-5 times before loading a 2 μ L sample onto the pedestal. After measurements, samples were wiped off the pedestals with a Kimwipe. The pedestal was cleaned with DI water and Kimwipes in between samples.

Gel Electrophoresis

Agarose gels (4%) were used to assay double stranded DNA templates. To cast and run an agarose gel, the Horizontal Gel Rig Model MPH (International Biotechnology, Inc) was used, with dimensions as follows: 10 cm (w) x 15 cm (l). The 10-

well comb was 10 cm wide and each well was 0.6 cm wide. A PS 3000 DC power supply (Hoefer, Inc.) was used to supply the necessary voltage (7 V/cm).

Polyacrylamide gels were used to qualify and purify single stranded RNA. For 21mer RNA, 20% PAGE gels were made using 40% acrylamide/bisacrylamide (19:1) purchased from VWR. The gel casting is described fully in Section 2.3.4. Two types of gel rigs were used for PAGE analysis, sequencing gels and short gels. The GIBCO BRL SA-32 sequencing system (Life Technologies) was used for sequencing gels, with dimensions as follows: 20 cm (w) x 32 cm (l). The sequencing gel comb created 16 wells that were 1 cm wide and had dimensions as follows: 20 cm (w) x 0.4 mm (t) The Hoefer SE600 Standard Vertical Electrophoresis Unit (Hoefer, Inc.) was used for short gels with dimensions as follows: 18 cm (w) x 16 cm (l). Both systems used a PS 3000 DC power supply (Hoefer, Inc) to supply 30W of power for the 2 hour run times.

Imaging System

A *UVP Bioimaging System* was used to image nucleic acids present in agarose and polyacrylamide gels that had been stained with ethidium bromide. This system consisted of an Epi Chem II Darkroom (imaging box), a CoolSNAP-ProCF Monochrome camera, and a 2UV Transilluminator. The instrument was controlled by the Labworks Imaging and Analysis Software V 4.0. Gels were stained using the fluorescent dye ethidium bromide and were scanned with an orange filter to monitor the fluorescence.

The digital images were saved as JPEG files and bands were quantified using the Labworks software.

A *Typhoon 9410 Variable Mode Imager* (Amersham Biosciences) was used to image gels containing fluorescent or radioactive samples. This instrument is capable of detecting fluorescence (fluorescently-labeled samples) and storage phosphorescence (radioactively labeled samples) at very low concentration (nanomolar). The instrument was controlled by Typhoon Scanner Control Software, V 4.0 (Amersham) installed on a Dell Optoplex computer. Gels that contained FAM-labeled fluorescent samples were run "as is" in the gel sandwich and the fluorescence was detected using an excitation wavelength of 494 nm and an emission wavelength of 520 nm. Gels that contained radioactive samples were exposed overnight to a low energy autoradiography screen inside a light-blocking cassette. The screen was then imaged on the Typhoon using the storage phosphorescence setting. The Typhoon has a dynamic range of five orders of magnitude and has spatial resolution of 2 line pairs per millimeter. The pixel accuracy is $\pm 0.15\%$ and the uniformity is $\pm 5\%$ over the entire area scanned. The digital images were saved as .gel files and band intensities were quantified using ImageQuant 5.2 software.

Liquid Scintillation Counter

Radiation in liquid samples containing ^{32}P -labeled nucleic acid was determined using a Beckman Coulter LS-6000 Scintillation Counter (Beckman Coulter) located in the laboratory of Dr. Xinnian Dong, Department of Biology, Duke University. A Wyse

Winterm computer supported by LS WinConnection Suite was used to collect and store data. Radioactive samples were dissolved in a counting cocktail solution, ScintiSafe 30% (Fisher Scientific). The counting solution contains fluors that emit light when excited. The radioactive ^{32}P emits beta particles in the solution, resulting in flashes of light that are detected by the photomultiplier tubes in the L-6000. The photomultiplier tubes convert flashes of light to amplified electrical pulses, which results in data that is reported in counts per minutes, a measure of radioactive decay. The counting efficiency of ^{32}P is nearly 100%, as it is a high-beta emitter. The resolution of the instrument is 0.06 keV

Temperature Controlling Apparatus

Samples were heated to and incubated at specific temperatures, often 37°C , for optimum enzymatic results. Heating of samples in small tubes (0.5 or 1.5 mL centrifuge tubes) was done using a Dry Bath Block Heater (Fisher Scientific), monitored with an external thermometer that was accurate to 0.1°C . Heating of samples in large tubes (15 mL or 50 mL centrifuge tubes) was done using a VWR Scientific Model 1220T Water bath (VWR), monitored with an external thermometer accurate to 0.1°C .

pH meter

To determine the pH of buffers and sample solutions, a Fishernet Accumet pH meter (model 620) and a Beckman electrode (Futura) were used. Three certified buffer solutions (Fisher) were used to standardize the pH meter: pH = 4.00 (± 0.01 at 25°C), pH =

7.00 (± 0.01 at 25°C), and pH = 10.00 (± 0.01 at 25°C). The instrument was standardized upon each usage.

Ion Exchange Chromatography

Purification of the nucleotide triphosphates (NTP α B) compounds from nucleotide diphosphates (NDP α B) and nucleotide monophosphates (NMPB) compounds was performed on an ISCO system (Teledyne Isco, Inc.), which included a TRIS™ peristaltic pump, a UA-6 absorbance detector, and a Foxy 200 fraction collector. The column was composed of QA-52 quaternary ammonium cellulose (Whatman) with dimensions as follows: 30 cm (l) x 1.5 cm (d). The columns were packed by hand by filling the glass column with pre-swollen QA-52 media and using a hand pump to remove the buffer solution from the column. The column was filled with 5 mM ammonium bicarbonate (ABC), equilibrated with 2-3 column volumes of the same buffer, and was used no more than 5 times. A concentration gradient of 5 mM \rightarrow 400 mM ABC was used to elute the samples.

High Performance Liquid Chromatography (HPLC) Systems

To separate the NTP α B stereoisomers in preparative scale, the Waters Delta 600 HPLC system was used, which consisted of a Waters 996 Photodiode Array, with a range of 190-800 nm \pm 1 nm, and a Waters 600E Multisolvent Delivery system (including a 600s controller and a Rheodyne 7725i manual injector). The HPLC was controlled by Dell Dimension desktop computer equipped with Millennium³² software (Version 3.20).

For milligram scale separation, a semi-preparative C-18 PrepPak Cartridge (Waters Corp) column was used, with dimensions as follows: 40 mm (d) x 100 mm (l), 15-20 μm column diameters, and 125 \AA particle size. The column was placed in a Prep LC Universal Base (Waters Corp) that was attached to the solvent delivery module. The detector flow cell had a 10 mm path length and 0.009 inch tubing. Spectra were recorded as 3D data (time-wavelength-absorbance) and chromatographic profiles were extracted at specific wavelengths, depending on the base.

For analysis of purity for the *Rp*-NTP α B stereoisomers, the Varian Prostar HPLC was used, which consisted of a 330.71 Photodiode Array detector, a solvent delivery module, and a 430 Autosampler (Varian). For analysis, a C-18 DeltaPak column (Waters Corp) was used with dimensions as follows: 3.9 mm (d) x 300 mm (l), 15 μm column diameter and 100 \AA particle size. The instrument was fitted with a guard column to prevent large particles from clogging the analytical column.

All solvents were filtered through a 0.2-micron filter (Millipore) and included methanol, acetonitrile, deionized water, 50 mM tetraethyl ammonium acetate (TEAA), and 100 mM triethyl ammonium bicarbonate (TEAB). These buffers were used to form either isocratic conditions or linear gradients for sample elution.

Circular Dichroism Spectrometer

Circular dichroism (CD) spectra were recorded using AVIV 202 Circular Dichroism spectrometer, which is a shared instrument in the laboratory of Dr. Terry

Oas, Department of Biochemistry, Duke University. Samples were loaded into a quartz microcell (#6610012700, Varian) with dimensions as follows: 4 mm x 10 mm and a volume of 0.9 mL. The same cell was used for both background and sample measurements so that no error due to individual cell fluorescence could be introduced into the spectra. The temperature of the sample was held constant at 25°C using a Neslab Coolflow CFT-33 refrigerated recirculator.

Electrospray Ionization Mass Spectrometer (ESI-MS)

The mass spectra of individual NTP α B samples were obtained using an Agilent 1100 series Liquid Chromatograph/Mass Selective Detector (LC/MSD), controlled by a LC/MSD Software 5.3 (Applied Biosystems) on a Dell computer. The instrument was located in the Chemistry Department Instrument room maintained by Dr. George Dubai. A Harvard Apparatus 22 Model Standard Infusion Syringe Pump was used to directly inject samples into the mass trap, bypassing the HPLC mode. Approximately 100-200 μ L of sample was required for each injection. Sample concentration was in the low micromolar range.

Matrix Assisted Laser Desorption/Ionization Mass Spectrometer (MALDI-MS)

The mass spectra of nucleic acids containing boranophosphate modifications were obtained using a Voyager-DE PRO Biospectrometry Workstation (Applied Biosystems). The instrument was located in the Chemistry Department Instrument room maintained by Dr. George Dubai. Samples were combined with different

matrices, loaded onto MALDI-TOF gold or steel sample carriers, and loaded into the instrument. The matrices 5-methoxysalicylic acid (5-MSA) and 3-hydroxypicolinic acid (3-HPA) were investigated. To acquire the spectra, the sample spot was rastered across and the shots were averaged. The Dell Optiplex G workstation was supported by Voyager Instrument Control Panel 5.10 software (Applied Biosystems).

2.2 Chemicals, Enzymes, and Nucleic Acids

2.2.1 Chemicals

RNase-free chemicals were used wherever possible for all the experiments described in this work. In this section, they are listed alphabetically by name with their abbreviations and sources.

Acetic acid, glacial, Mallinckrodt AR

Acetonitrile (CH₃CN), HPLC grade, Fisher

Acrylamide:bis-acrylamide 19:1, 40% solution, electrophoresis grade, EMD

Chemicals

Agarose, NuSieve GTG, Lonza

Ammonium bicarbonate, Sigma

Ammonium citrate, MP Biomedicals

Ammonium persulfate (APS), electrophoresis purity reagent, Acros

Borane-dimethyl sulfide complex, 2.0 M in THF (BMS), Aldrich

Bromophenol blue (BB), electrophoresis purity reagent, Bio-Rad

2-Chloro-4*H*-1,3,2-benzodioxaphosphorin-4-one (Sal-p-Cl), Aldrich

Chloroform, Acros Organics

Coomassie Blue, Bio-Rad

DEPC Water, Ambion

Diammonium citrate, Sigma Aldrich

Dichloromethane (DCM, CH₂Cl₂), HPLC grade, Fisher

Diethyl ether, Fisher

Dichlorodimethylsilane in hydrocarbon solvent (Glass Free), National Diagnostics

N,N-Dimethylformamide (DMF), anhydrous, 99.8%, Aldrich

Dithiothreitol, DL (DTT), ≥98%, Aldrich

Ethanol, 200 proof (EtOH), EMD Chemicals

Ethyl ether (Et₂O), Fisher

Ethidium bromide, 10 mg/ml (EtBr), Promega

Formamide, Ambion

Glycerol, Sigma

Methanol (MeOH), HPLC grade, J.T. Baker

5-Methoxysalicylic acid (MSA). Acros Organics

Potassium phosphate, monobasic (KH₂PO₄), Sigma

Potassium phosphate buffer, 0.1 M, pH 7.5, Sigma

Phenol:chloroform:isoamyl alcohol, 25:24:1, pH 6.6, Ambion

Pyridine, anhydrous (Py), Aldrich

RNase-away, Molecular Bioproducts

Salicyl phosphorochlorodite, Sigma Aldrich

Sodium dodecyl sulfate, 20% solution (SDS), Ambion

Sodium hydroxide, 1 N solution, Fisher

N,N,N',N'-Tetramethylethylenediamine (TEMED), molecular grade, Molecular Bioproducts

Tributylamine, anhydrous (TBA), Aldrich

Triethylamine (TEA), Glen Research

Triethylammonium acetate (TEAA), HPLC grade, Glen Research

Tris(hydroxymethyl)aminomethane (Tris base), Thomas Scientific

Urea, RNase and DNase free, Promega

Xylene cyanol FF (XC), electrophoresis purity reagent, Bio-Rad

Yeast extract, Thomas Scientific

2.2.2 Buffers

RNase-free, sterile buffer solutions were used exclusively for all experiments described in this work. In this section, the commercially available solutions that were used are listed alphabetically by name and accompanied by abbreviation, concentration,

and source. Commercially available solutions were used when possible to ensure lack of contamination by ribonucleases.

Ethylenediaminetetraacetic acid, 0.5 M (EDTA), disodium salt, Ambion

Magnesium acetate, 1M, Optimize

Magnesium chloride, 1M (MgCl₂), Ambion

Potassium acetate, 3M, Ambion

Potassium chloride, 2M (KCl), Ambion

Sodium chloride, 5 M, Ambion

Tris-borate-EDTA, 10X (10X TBE), electrophoresis grade, Sigma

Tris-HCL, 1 M, pH 7.0 and pH 8.0, Ambion

Water, deionized, purified by Hydro filtration system and available on tap

Water, DEPC-treated, Ambion

Water, HPLC grade, Fisher

Water, RNase-Free, Ambion

Self-made stock solutions of buffers were prepared using deionized water or RNase-free water. They were stored at room temperature on the benchtop, except where noted otherwise. In this section they are listed by application.

Annealing

Buffer used for annealing RNA and DNA: 1X solution (100 mM potassium acetate, 50 mM magnesium acetate, 30 mM Tris, pH 7) made by diluting 5X stock solution (500 mM potassium acetate, 250 mM magnesium acetate, 150 mM Tris, pH 7)

Chromatography: All buffers were filtered through 0.2 μ m filters

Ammonium bicarbonate, 400 mM (63.25 g ammonium bicarbonate solid in 2.0 L of deionized water)

Ammonium bicarbonate, 5 mM (25 ml of 400 mM ammonium bicarbonate in 2.0 L of deionized water)

TEAA, 50 mM (50 mL of 2.0 M TEAA stock solution in 2.0 L of deionized, filtered water)

TEAB, 1M Stock (101.1 g TEA in 1 L of deionized, filtered water, bubbled with carbon dioxide for 15-20 minutes until pH was ~ 7; stored at 4°C)

Circular dichroism

Buffer used for CD experiments: 5X solution (250 mM MgCl₂, 25 mM Tris-HCl, pH 7, and 750 mM KCl) stored at room temperature. 1x solution was prepared by diluting stock solutions of the components with RNase-free water (1 M MgCl₂, 1 M Tris-HCl, pH 7, and 2 M KCl). Caution: Tris is a bad buffer at pH <8.

Gel Electrophoresis

20% Ammonium persulfate solution: (2 grams of ammonium persulfate solid in RNase-free water), stored at 4°C.

Gel Loading Solution: 2X solution (95% formamide, 12.5 mM EDTA, 0.01% Bromophenol blue, 0.01% xylene cyanol, RNase-free water), stored at 4°C

Denaturing PAGE 20% stock solution, 7M Urea (500 mL 40% Acrylamide stock (19:1), 100 mL 10X TBE, 424.2 g Urea, QS to 1 L with deionized water), stored in covered bottles and stored in the dark

PAGE dilution solution, 7 M Urea (100 mL 10X TBE, 424.2 g Urea, QS to 1 L with deionized water)

1X Tris-borate-EDTA (TBE) running buffer (1:10 dilution of 10X TBE)

Lipophilicity Experiments:

Potassium phosphate buffer stock solution, 1.0 M (68.1 potassium phosphate solid in 500 mL RNase-free water)

Octanol-saturated potassium phosphate buffer (100 mL of 1.0 M potassium phosphate buffer with a sufficient quantity of 1-octanol was shaken vigorously at room temperature for 24 hours and allowed to stand long enough for phase separation)

Potassium-saturated octanol buffer (100 mL of 1-octanol with a sufficient quantity of potassium phosphate buffer, shaken vigorously at room temperature for 24 hours and allowed to stand long enough for phase separation)

Thermal Stability Experiments

Buffer used for thermal melting experiments: 1X solution (0.1 M potassium phosphate) prepared by diluting 10X stock solution (1.0 M potassium phosphate), pH 7.4. 1.0 M potassium phosphate was made by dissolving 136.09 grams potassium phosphate in RNase-free water.

2.2.3 Enzymes and Kits

The commercially available enzymes used during this project were obtained in ribonuclease-free (RNase-free) and deoxyribonuclease-free (DNase-free) storage buffers and were accompanied by commercially available RNase and DNase free reaction buffers. These enzymes were kept at -20°C in a freezer that was used exclusively for RNase free samples.

Annealing and Enzymatic Extension of Double-stranded DNA: DNA templates (39 nt) and DNA promoters (18 nt) were obtained commercially from Integrated DNA Technologies and Operon. The template and promoter were annealed in 1X annealing buffer by raising the temperature to 90°C for 5 minutes and cooling slowly on the benchtop for an hour.

Extension of annealed, partially double-stranded DNA templates was performed using Klenow Fragment, exonuclease-minus (Promega). This enzyme has a 5'→3' polymerase activity, but lacks any endonuclease activity. The concentration was 10 units/μL, where one unit is defined as the amount of enzyme that incorporates ten

nanomoles of total deoxyribonucleotides into TCA-insoluble material in 30 minutes at 37°C in 67 mM potassium phosphate (pH 7.4 at 25°C), 6.7mM MgCl₂, 1 mM DTT, 50 µg/ml activated calf thymus DNA, and 33 µM dATP, dCTP, dGTP and dTTP (a mix of unlabeled and NTP dTTP). The enzyme was stored in the following buffer: 50 mM Tris-HCl, pH 7.5 at 25°C, 1 mM DTT, 0.1 mM EDTA, and 50% (v/v) glycerol. The 10X reaction buffer was composed of 500 mM Tris-HCl, pH 7.2 at 25°C, 100 mM MgSO₄, and 1 mM DTT.

Enzymatic Synthesis of Normal and Boranophosphate-modified RNA: Transcription of single stranded RNA from double stranded DNA templates was performed using T7 RNA Polymerase. Two kits were employed over the course of this project for RNA transcription. The Ampliscribe T7 High Yield 50 Reaction Transcription kit (Epicentre) contained Ampliscribe T7 Enzyme solution, Ampliscribe 10X reaction buffer, 100 mM ATP, CTP, GTP, and UTP, 100 mM DTT, RNase-free water, control template DNA, and RNase-free DNase 1 (1 U/µL). The Ribomax Large Scale RNA Production System – T7 contained T7 RNA Polymerase Enzyme Mix (RNA polymerase, recombinant RNasin® Ribonuclease Inhibitor, and recombinant inorganic pyrophosphatase), 5X transcription buffer, 100 mM ATP, CTP, GTP, and UTP, linear control DNA (1mg/mL), RQ1 RNase-free DNase (1 U/µL), 3 M sodium acetate, and RNase-free water. Each Ribomax kit contained the components necessary for ten reactions.

Enzymatic Synthesis of 2'F modified RNA and 2'F + α -P-boranotriphosphate modified

RNA: Transcription of single stranded RNA containing both the boranophosphate modification and the 2'F modification was initially performed using a mutant T7 RNA Polymerase with a single Y639F point mutation. The synthesis was performed with the Durascribe T7 25 Reaction Transcription kit, which contained Durascribe 10X Reaction Buffer, 50 mM ATP and GTP, 50 mM 2'F-dCTP and 2'F-dUTP, 100 mM DTT, sterile, deionized water, DuraScript RNA Control DNA Template (0.5 μ g/ μ L), and RNase-free DNase 1 (1 U/ μ L).

Enzymatic Ligation of Single Stranded RNA: Ligations of normal and modified

RNA were carried out using T4 RNA ligase 1 (ssRNA) purified from *E. coli* strain ER2497 containing the plasmid pRF-E35 (New England Biolabs). The concentration was 20 U/ μ L, where one unit was defined as the amount of enzyme required to convert 1 nanomole of 5'-phosphoryl termini in 5'-[³²P] rA20 to a phosphatase-resistant form in a total reaction volume of 50 μ L in 30 minutes at 37°C in 1X reaction buffer. The 10X reaction buffer was composed of 500 mM Tris-HCl pH 7.8 at 25 °C, 100 mM MgCl₂, 10 mM ATP, and 100 mM DTT.

Dephosphorylation of Single Stranded RNA: Alkaline phosphatase from two sources

was used to remove the phosphate groups from the 5' ends of RNA samples. Shrimp alkaline phosphatase (SAP) from Shrimp (*P. borealis*) was used for dephosphorylation of RNA that preceded labeling of RNA with [³²P] ATP and T4 polynucleotide kinase. SAP

(1 U/ μ L, Promega) was received in storage buffer containing 25 mM Tris-HCl, pH 7.6 at 4°C, 1 mM MgCl₂, 0.1 mM ZnCl₂, and 50% glycerol. One unit of SAP was defined as the amount of enzyme required to catalyze the hydrolysis of 1 μ mole of 4-nitrophenyl phosphate per minute at 37°C in 1 M diethanolamine, 10.9 mM 4-nitrophenyl phosphate, 0.5 mM MgCl₂, and pH 9.8. The SAP 10X reaction buffer was composed of 500 mM Tris-HCl, pH 9.0 at 37°C and 100 mM MgCl₂. The reaction was incubated at 37°C for 15 minutes and then heat inactivated at 65°C for 15 minutes.

The second phosphatase used in this work was Antarctic phosphatase (AP) was used to dephosphorylate single stranded RNA to prevent unwanted ligations during the T4 RNA ligase reaction (New England Biolabs). Antarctic phosphatase from an *E. coli* strain that carried the TAB5 AP gene was supplied in 10 mM Tris-HCl, pH 7.4, 1 mM MgCl₂, 1 mM DTT, and 50% glycerol. The AP 10X buffer contained 500 mM Bis Tris-propane pH 6.0 at 25°C, 10 mM MgCl₂, and 0.1 mM ZnCl₂. AP removes the triphosphate group from the 5' end of oligonucleotides. The AP concentration was 5 U/ μ L, where one unit is the amount of enzyme that will dephosphorylate 1 μ g of pUC19 vector DNA cut with HindIII (5' protruding ends), EcoRV (blunt ends), or Pst I (5' recessed ends) in 30 minutes at 37°C. The company defines dephosphorylation is defined as > 95% inhibition of re-circularization in a self-ligation reaction and is measured by transformation into *E. coli*.

Radioactive Labeling of Single Stranded RNA: T4 Polynucleotide Kinase (PNK) (Promega) was used to label the 5' ends of single stranded RNA with ^{32}P immediately following dephosphorylation by shrimp alkaline phosphatase. T4 Polynucleotide Kinase (PNK, 5-10 U/ μL) purified from *E. coli* cells expressing a recombinant clone was supplied in storage buffer containing 20 mM Tris-HCl pH 7.5, 25 mM KCl, 2 mM DTT, 0.1 mM EDTA, 0.1 μM ATP, and 50% (v/v) glycerol. One unit was defined as the amount of PNK required to catalyze the transfer of 1 nanomole of phosphate from [γ - ^{32}P] ATP to the 5'-OH end of a polynucleotide in 30 minutes at 37°C in 40 mM Tris-HCl pH 7.5, 10 mM DTT, 0.1 mM [γ - ^{32}P] ATP, and 0.5 $\mu\text{g}/\mu\text{L}$ 5'-OH polynucleotide end concentration. The 10X PNK exchange reaction buffer supplied with the enzyme contained 500 mM imidazole-HCl pH 6.6, 100 mM MgCl_2 , 50 mM DTT, 1 mM spermidine, and 1 mM EDTA.

Nucleases: Ribonuclease A (RNase A) was obtained from Calbiochem (EMD Biosciences) and was used for nuclease stability assays of modified RNA. The lyophilized solid was dissolved in deionized water to yield a solution with a concentration of eight units per microliter. One unit was defined as the amount of enzyme that will catalyze the hydrolysis of RNA to yield "a first-order velocity constant equal to 1 at 25°C, pH 5.0" according to the manufacturer.

Exonuclease T (Exo T) was obtained from New England Biolabs. Exo T was overexpressed and purified as a C-terminal fusion to maltose-binding protein (MBP).

MBP is removed by Factor Xa cleavage and Exonuclease T is then purified. It has an additional amino acid on the N-terminus and a Phe instead of a Met. Exo T was provided at a concentration of five units per microliter and stored in 10 mM Tris-HCl, 50 mM KCl, 1 mM DTT, 0.1 mM EDTA, 200 µg/ml BSA, and 50% glycerol at pH 7.4 at 25°C. One unit was defined as the amount of enzyme required to produce 0.1 nanomole of TCA-soluble DNA from 1 nanomole of [³H]-labeled polythymidine in a total reaction volume of 100 µl in 30 minutes at 25°C in 1X reaction buffer with 1 nanomole [³H]-labeled polythymidine DNA. The 10X reaction buffer contained 200 mM Tris-acetate, 500 mM potassium acetate, 100 mM magnesium acetate, 1 mM DTT at pH 7.9 at 25°C

2.2.4 Nucleosides, Nucleotides, and Nucleic Acids

The nucleosides, nucleotides, and oligonucleotides used for this project are listed herein, along with abbreviations, source, molecular weight, and extinction coefficient. All samples were stored at -20°C in an RNase-free freezer.

Standards: Natural nucleosides and nucleotides were purchased from commercial sources at >99% purity and were stored as solids. They were used as reference samples for both HPLC and ESI-MS.

Adenosine (A), AMP, ADP, and ATP: Sodium salt, Acros Organics. $\epsilon_{259} = 15,400$

Cytidine (C), CMP, CDP, and CTP: Sodium salt, Acros Organics. $\epsilon_{271} = 9,000$

Guanosine (G), GMP, GDP, and GTP: Sodium salt, Acros Organics. $\epsilon_{253} = 13,700$

Uridine (U), UMP, UDP, and UTP: Sodium salt, Acros Organics. $\epsilon_{262} = 10,000$

Nucleotides: Natural deoxyribonucleotides and ribonucleotides that were used for incorporation into oligonucleotides by DNA and RNA polymerases were commercially available and were stored as aliquots in nuclease-free water to prevent degradation due to frequent freeze/thaw cycles. The concentration of each was 100 mM and the aliquots were 15 μ L.

Adenosine 5'-[γ -³²P] triphosphate ([γ -³²P] ATP), sodium salt, 3.3 μ M solution in 10 mM tricine buffer, 3000 Ci/mmol, 10 mCi/mL, Perkin Elmer. Stored as EasyTide™ stock solution at 4°C. EasyTide™ solutions allow for easy visibility of the radioactive nucleotide by the addition of green dye to the stock solution.

2'-Deoxyribonucleoside 5'-triphosphate mix (dNTP, N = A, C, G, or T), >98% by HPLC, sodium salt, 10 mM per NTP (40 mM overall) in nuclease-free water (Promega). These stock solutions were stored in 10 μ L aliquots at -20°C.

Ribonucleotide 5'-triphosphate (NTP, N = A, C, G, or U), >99% by HPLC, sodium salt, 100 mM solution in water, Promega. Stored in 15 μ L aliquots at -20°C

Ribonucleotide 5'-(α -P-borano)triphosphate (NTP α B, N = A, C, G, or U), >99% by HPLC, stored lyophilized. Triphosphates with boranophosphate (BP) modification were synthesized chemically as described in Chapter 3 in the lab by Laura Moussa, Marcus Cheek, and Dr. S. Nadeem Hashmi. The BP monophosphates and BP diphosphates were byproducts of the chemical synthesis.

2'-Fluoro-2'-deoxynucleotide 5'-triphosphate (2'F NTP, N = C or U), >99% by HPLC, 50 mM in nuclease-free water, stored in 15 μ L aliquots at -20°C. Triphosphates with 2'F modification were synthesized chemically as described in Chapter 3 in the lab by Laura Moussa and Marcus Cheek. The 2'F monophosphates and 2'F diphosphates were byproducts of the chemical synthesis.

Table 2-1. Nucleoside, nucleotide monophosphate, nucleotide diphosphate, and nucleotide triphosphate molecular weights. The molecular weight of each compound with no counter ion was determined using ChemOffice (Cambridge Software).

Adenine	MW (g)	Cytosine	MW (g)	Guanine	MW (g)	Uracil	MW (g)
A	267.24	C	243.22	G	283.09	U	244.20
AMP	347.22	CMP	323.20	GMP	362.21	UMP	308.18
ADP	427.20	CDP	403.18	GDP	441.01	UDP	388.16
ATP	507.18	CTP	483.16	GTP	521.16	UTP	467.97
AMPB	344.05	CMPB	320.20	GMPB	360.09	UMPB	305.01
ADP α B	424.03	CDP α B	400.00	GDP α B	439.05	UDP α B	384.99
ATP α B	504.01	CTP α B	479.98	GTP α B	518.01	UTP α B	464.97
		2'F CMP	325.20			2'F UMP	310.18
		2'F CDP	405.18			2'F UDP	390.16
		2'F CTP	485.16			2'F UTP	469.97

Nucleic acids: The nucleic acids used in this work were from several sources. The sequences, sources, purification, molecular weights, and molar absorptivities (ϵ_{260}) are listed in Table 2-2.

DNA templates were purchased in micromolar quantities from commercial sources and were obtained as desalted, lyophilized powders. Upon arrival, they were stored at -20°C. Prior to use, they were dissolved in deionized water to a concentration of 100 μ M, using UV to determine the concentration and purity. 100 μ M single-stranded

DNA templates (2 μL) were annealed to a 100 μM single stranded T7 DNA promoter (2 μL) in 1X annealing buffer (10 μL final volume). This partially double-stranded DNA (10 μL) was then incubated with Klenow ExoMinus fragment DNA polymerase (2 μL) and dNTP mix (2 μL) in 1X Klenow buffer at 37°C for 30 minutes (20 μL final volume) to yield fully double-stranded DNA template. This double stranded template was then aliquoted and stored at -20°C for future use. DNA templates that were purchased as duplexes were dissolved in deionized water to a concentration of 100 μM , aliquoted in 10 μL aliquots, and stored at -20°C for future use.

DNA standards were synthesized using an ABI DNA synthesizer located in the laboratory of Dr. Rudy Juliano, Department of Pharmacology, UNC-CH. The standards were purified using C-18 Sep-Paks cartridges (Waters) to remove the DMT protecting groups and the purity was determined by HPLC. Purity was determined using gradient elution of the oligonucleotide. Protected DNA standards were stored at 4°C for up to three weeks and deprotected standards were stored in aliquots at -20°C.

The RNA sequences used in this work were produced by enzymatic transcription (see General Methodology section). After purification, they were stored at -20°C in an RNase-free freezer. During experiments, RNA samples were kept on ice at all times to prevent degradation.

Table: 2-2. DNA and RNA sequences with source, purity, molecular weight, and molar extinction coefficient (ϵ_{\max}). S denotes the sense, or passenger, strand of the siRNA and AS denotes the antisense, or guide, strand of the siRNA. For DNA duplexes, T denotes the template strand and C denotes the complement strand. The ϵ_{260} was determined using an online calculator that utilized the nearest-neighbor method for calculation of the molar absorptivity.

DNA	Sequence (5'→3')	Source	Purity	MW (g)	ϵ_{260} (L • mmole ⁻¹ • cm ⁻¹)
<i>DNA Sequences</i>					
HPV 16+24+G S Temp DNA	AAGAGAGATCAGTTGTCTCT GCTATAGTGAGTCGTATTA	Operon	Desalt	12075.8	391.1
HPV 16+24+G AS Temp DNA	AACCAGAGACAACCTGATCTC TCTATAGTGAGTCGTATTA	Operon	Desalt	11973.8	391.8
HPV 16+24+G S Control Temp DNA	AAGAGAGATATCGGTTCTCT GCTATAGTGACTCGTATTA	Operon	Desalt	12035.8	390.4
HPV 16+24+G AS Control Temp DNA	AACCAGAGAACCGATATCTC TCTATAGTGAGTCGTATTA	Operon	Desalt	11973.8	394.0
T7 Promoter DNA	TAATACGACTCACTATAG	Operon	Desalt	5466.6	182.5
HPV 16+24 S Duplex	C:TAATACGACTCAACTATAC CAGAGACAACCTGATCTCTTT T:AAAGAGATCAGTTGTCTCC TGGTATAGTGAGTCGTATTA	IDT	Desalt	23351.3	387.7

Table 2-2 continued

DNA	Sequence (5'→3')	Source	Purity	MW	£260
HPV 16+24 AS Duplex	C:TAATACGACTCACTATAA GAGATCAGTTGTCTCTGGTT T:ATTATGCTGAGTGATATTC TCTAGTCAACAGAGACCAA	IDT	Desalt	23351.3	384.6
Luc S Temp	ATTCGAAGTACTCAGCGTAA GTATAGTGAGTCGTATTA	Operon	Desalt	11755.6	390.5
Luc AS Temp	AACUUACGCUGAGUACUUC GAAGTGAGTCGTATTA	Operon	Desalt	12010.8	388.4
Ligase Duplex	C:TAATACGACTCACTATAG GGAGATCACC T:GGTGATCTCCCTATAGTGA GTCGTATTA	IDT	Desalt	17175.3	275.0
dT 10	TTTTTTTTTT	Operon	Desalt	2980	81.6
dT 20	TTTTTTTTTTTTTTTTTTTT	Operon	Desalt	6022	162.6
dT 25	TTTTTTTTTTTTTTTTTTTTTT TT	Operon	Desalt	7543	203.1
<i>RNA Sequences</i>					
HPV 16+24 S	CAGAGACAACUGAUCUCUCUU	Enz Txn		6617.2	204.6
HPV 16+24 AS	AGAGAUCAGUUGUCUCUGGUU	Enz Txn		6691.2	212.7
HPV 16+24+G S	GCAGAGACAACUGAUCUCUCUU	Enz Txn		6962.4	214.8
HPV 16+24+G AS	GAGAGAUCAGUUGUCUCUGGUU	Enz Txn		7036.4	222.5
HPV 16+24+G S Control	GCAGAGAACCGAUUAUCUCUCUU	Enz Txn		6962.4	217.2
HPV 16+24+G AS Control	GAGAGAUUAUCGGUUCUCUGGUU	Enz Txn		7036.4	223.3
Luc S	CUUACGCUGAGUACUUCGAUU	Enz Txn		6611.2	203.7
Luc AS	UCGAAGUACUCAGCGUAAGUU	Enz Txn		6697.2	214.7
Ligase	GGGAGAUCACC	Enz Txn		3528.2	111.0

2.3 General Methodology

2.3.1 Concentration determination of nucleic acids

The concentrations of modified single nucleotides were determined using the maximum absorbance wavelength (λ_{\max}) and molar extinction coefficient (ϵ_{\max}) specific to each nitrogenous base. (Table 2-3)

Table 2-3. Maximum absorbance wavelength (λ_{\max}) and molar extinction coefficient (ϵ_{\max}) for the four nitrogenous bases of RNA (McGilvery 1975)

	Adenine	Cytosine	Guanine	Uracil
λ_{\max} (nm)	259	271	253	262
ϵ_{\max} ($M^{-1}cm^{-1}$)	15,400	9,000	13,700	10,000

The concentrations of the nucleotides were calculated using the Beer-Lambert Law (Equation 2-1), which uses absorbance (A), path length (B), and molar absorptivity (ϵ) to determine concentration (C).

$$A_{\max} = \epsilon_{\max} \times B \times C \quad (\text{Eqn 2-1})$$

Substitution of one of the non-bridging oxygen with a borane group has been shown to have no effect on the UV absorbance properties of the nitrogenous base. (He 2000) The concentrations of both unmodified and modified oligonucleotides were determined in the same way. The λ_{\max} for oligonucleotide absorptivity for each sequence was calculated using the Ambion oligonucleotide extinction coefficient calculation tool. (Ambion 2003) This calculator uses the nearest-neighbor method, which has been

shown to give the most accurate approximation for oligonucleotides sequences less than 100 nucleotides in length (Fasman 1975).

2.3.2 DNA Template Preparation and RNA Transcription

DNA templates that were obtained as single strands were received in micromolar quantities and stored as lyophilized powders. Deionized water was added to the powder to yield a 100 μM DNA stock solution. The DNA template was annealed to a DNA T7 promoter. The annealing reaction contained 2 μL of 100 μM template, 2 μL of 100 μM promoter, 1 μL of 10x annealing buffer (100 mM potassium acetate, 50 mM magnesium acetate, 30 mM Tris, pH 7), and 5 μL DEPC- H_2O . This mixture was vortexed and incubated at 90°C for 5 minutes and allowed to cool slowly on the benchtop. The Klenow extension reaction mixture contained 10 μL of annealed template and primer, 2 μL Klenow DNA polymerase exonuclease minus, 2 μL 10x reaction buffer, 2 μL 10x dNTP mix, and 4 μL DEPC- H_2O . This mixture was vortexed and incubated at 37° C for 30 min. The final product was aliquoted into 0.5 mL RNase-free tubes (10 μg template/tube) and stored at -20°C.

The total reaction volume of the RNA transcription reactions was 100 μL using the Ribomax™ T7 High Yield Transcription Kit. Each transcription was performed using 10 μg of double-stranded DNA template. Then conditions for each type of transcription were optimized as discussed in Chapter 3. For transcription of unmodified RNA, a final concentration of 4 mM of each NTP was used. For transcription of

boranophosphate (BP) RNA, a final concentration of 2 mM of each NTP was used. For transcription of 2'F + boranophosphate RNA (FB), a final concentration of 4 mM of each NTP was used. The 5X buffer provided with the kit was diluted to 1X and 5 µg of double stranded DNA template was used in each reaction (1 copy of DNA should yield 30-40 copies of RNA). Normal RNA incubated at 37°C for 4 hours, BP RNA incubated at 37°C for 6 hours, and FB RNA incubated at 37°C overnight. To end the reaction, 5 µL of RNase-free DNase was added to the reaction mixture, vortexed, and incubated for 15 minutes longer at 37°C. The transcription reaction produced both the full-length product as well as shorter abortive products that were removed by purification.

To remove the enzymes from the transcription reaction mixture, a 1:1 phenol extraction was performed. 100 µL of phenol:chloroform:isoamyl alcohol was added to the 100 µL reaction mix (in 1X transcription buffer) and vortexed for 1 minute. The mixture was then centrifuged at 14,000 rpm for 2 minutes on the Eppendorf MiniSpin centrifuge to separate the aqueous and organic layers. The upper aqueous layer was removed and transferred to a fresh 0.5 ml tube. To the new tube, 100 µL of chloroform was added and the mixture was again vortexed for 1 minute and centrifuged for 2 minutes to separate the layers. The aqueous layer was transferred to a fresh tube where the chloroform step was repeated. After the second chloroform extraction, the aqueous layer was loaded onto an Illustra G-25 Microspin column (GE Healthcare Life Sciences) and spun at 3300 rpm on the Eppendorf MiniSpin for 2 minutes to remove

unincorporated rNTPs and DNA fragments, as well as short abortive products (2-8 nt). The G-25 is optimized to purify oligonucleotides that are longer than 10 nt and shorter than 100 nt and did not appear to absorb either BP or FB RNA.

2.3.3 Agarose Gels

Gel electrophoresis was used to separate species of DNA and RNA based on size in order to assure that annealing had produced the double-stranded species. Agarose gels were used for size separation of double-stranded (ds) oligonucleotides, as agarose gels did not contain any denaturing agents. NuSieve agarose GTG (Lonza) was used, as it has been shown to separate molecules down to 10 base pairs (Simpson 1998). Four percent agarose gels were used to determine the purity of 39 bp ds DNA templates. A 250-mL Pyrex bottle (Pyrex Laboratory Glassware) was cleaned with RNase Away and DNase Away (Molecular Bioproducts) to ensure lack of contamination by nucleases. To this bottle, 2.0 grams of agarose and 50 mL of 1X TBE were added. The agarose was soaked in buffer for 15 minutes to reduce tendency of the solution to foam during heating. The bottle, cap, and solution were weighed and the cap was loosened before being heated in the lab microwave on medium heat for 2 minutes. The solution was swirled to resuspend any gel powder and fragments and then heated further for one minute to bring the solution to a boil. The solution was swirled to mix completely and distilled water was added to obtain the initial weight. The solution was allowed to cool to 50-55°C on the benchtop. The 10 cm wide, 2 cm thick gel was cast, the 10-well, 10 cm

comb was inserted, and the gel was allowed to cool for at least 1 hour. The gels were run at 7 V/cm for 2 hours using an International Biotechnologies horizontal gel rig and a Hoefer power supply. To stain the gels, ethidium bromide (EtBr) at a concentration of 0.5 mg/mL was used. The gel was immersed in the EtBr for 15 minutes and destained in deionized water for 5 minutes and then imaged using the UVP BioImaging System.

2.3.4 Polyacrylamide Gel Electrophoresis (PAGE)

Denaturing polyacrylamide gels were used for separation of RNA species of varying lengths using polyacrylamide gel electrophoresis (PAGE). 40% acrylamide/bisacrylamide (19:1) was mixed with urea and tris-borate-EDTA (TBE) to make the 20% PAGE stock solution. PAGE dilution solution was made using urea and TBE. Both solutions contained 7 M urea. The 20% PAGE stock solution was diluted with PAGE Dilution Solution to obtain specific gel percentages depending on the length of the RNA to be separated (Table 2-4). The oligonucleotides in this project ranged from 5 nt – 39 nt in length. Glass plates were regularly coated with Glass Free (dimethyldichlorosilane) (National Diagnostics) to decrease sticking between the plate and the gel and allow easy release of the gel. For gels containing fluorescent samples, specialized plates were used to ensure good readings.

Table 2-4. PAGE gel percentages and corresponding ranges of separation. The faster moving dye (Bromophenol blue) shows the lower base pair limit and the slower moving dye (xylene cyanol) shows the upper base pair limit. (Simpson 1998)

Percentage	Bromophenol Blue	Xylene Cyanol
3.5%	100	460
5%	65	260
8%	45	160
12%	20	70
20%	12	45

Two sizes of polyacrylamide gels were cast, Hoefer and sequencing gels. Hoefer polyacrylamide gels were cast using the Hoefer 2-Gel Caster (Hoefer Scientific). These gels were shorter and thicker than normal sequencing gels. They were easier to use for gels that were stained with ethidium bromide and were also easier to prepare, but did not achieve the resolution of sequencing gels. To cast the Hoefer gels, matching plates were cleaned thoroughly with water and 200-proof ethanol and the plate sandwich was formed using 0.75 mm spacers. The gel solution was prepared and a syringe was used to pour the gel into the sandwich. Gel solution consisted of 30 mL of PAGE solution (20% PAGE Stock Solution plus the appropriate amount of Dilution Solution), 70 μ L 10% ammonium persulfate (APS), and 35 μ L TEMED.

Sequencing gels were cast using plate sets consisting of one short plate (19.5 cm wide x 33.5 cm long) and one long plate (19.5 cm wide x 36.5 cm long). Plates were cleaned thoroughly with water and 200-proof ethanol and the plate sandwich was

formed using 0.35 mm spacers and binder clips. First, a quick-setting plug (2 mL PAGE solution, 10 μ L 10% APS, 5 μ L TEMED) was poured at the underside of the sandwich to create a bottom. Then the separating gel solution was made and a 25 mL syringe and a 22-gauge needle were used to pour the gel between the plates. A 0.4 mm 16-well comb was used to create 15 μ L wells.

All gels were allowed to set for at least 1 hour prior to running. Gels that set overnight were stored wrapped in Saran wrap at room temperature. The gels were set into the rigs and the wells were rinsed three times. Samples were loaded in 1X gel loading buffer using flat-tipped gel loading pipets. Twenty percent polyacrylamide/7 M urea Hoefer-sized gels were run for 2 hours at 400-500 V in 1X TBE running buffer and 15% polyacrylamide/7 M urea Hoefer-sized gels were run for 2 hours at 300 V in 1X TBE running buffer. Sequencing gels were pre-run for 2 hours at 30 W and were run for 2 hours at 30 W using 1X TBE running buffer.

Gels that were stained using 0.5 mg/mL ethidium bromide were immersed for 15 minutes in the ethidium bromide solution and then destained using deionized water for 5 minutes. Gels that contained fluorescent samples were left in the plate sandwich and imaged using the Typhoon phosphoimager. Gels that contained radioactive samples were removed from the plate sandwich, wrapped tightly in Saran wrap, and were exposed to a low-energy storage phosphor screen overnight in a light-tight screen cassette (Molecular Dynamics) at 4°C to prevent sample diffusion.

3. Synthesis and Purification of Normal and Chemically Modified Nucleotides and Oligonucleotides

3.1 Introduction

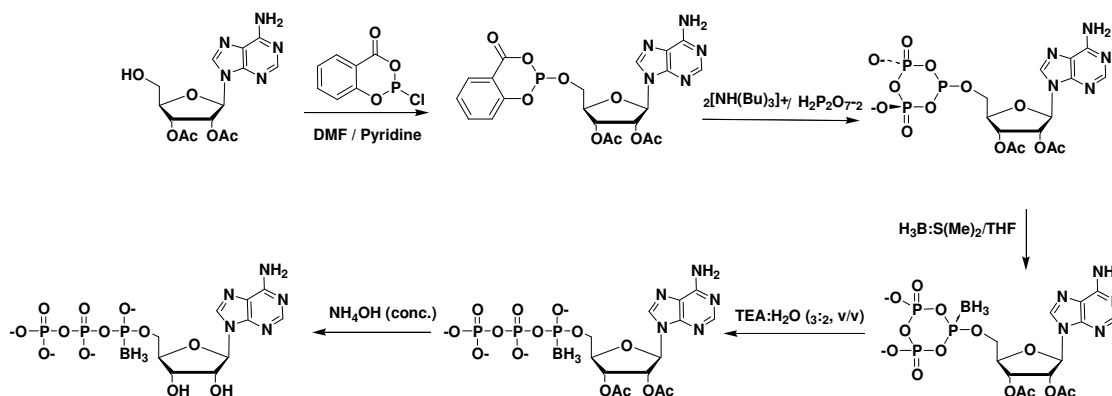
In this chapter, the synthesis of chemically modified triphosphates and the synthesis of normal and chemically modified oligonucleotides will be explored. The biophysical properties and *in vitro* utility and potency of these oligonucleotides will be investigated in later chapters.

3.1.1 Synthesis of modified nucleotide triphosphates

Modification of nucleotide triphosphates imparts unique properties to the molecules. There were two types of chemically modified triphosphates used in this work: 1) α -P-boranoribonucleotide triphosphates (NTP α Bs) and 2) 2'-fluoro-2'-deoxyribonucleotide triphosphates (2'F NTPs).

The Shaw group first reported the chemical synthesis of an NTP α B using the phosphoramidite approach in 1992 (Tomasz, et al. 1992). The boranophosphate group (BP) is isoionic and isoelectronic with oxygen in unmodified triphosphates (PO) and with sulfur in the phosphorothioates (PS) (Porter, et al. 1997). The first synthesis of 2'F UTP was described in 1964, followed by 2'F CTP (Codington, et al. 1964). The 2' fluoro group has similar electronegativity to the hydroxyl group, but has a van der Waals radius that is more similar to hydrogen (Williams, et al. 1991).

The synthetic methods for both modified triphosphates used in this dissertation were based on the salicyl phosphorochlorodite (Sal-p-Cl) approach developed by Ludwig and Eckstein for the synthesis of phosphorothioates (Ludwig and Eckstein 1989). As illustrated in Scheme 3-1, this technique was adapted for the synthesis of 2'-deoxyribonucleotides 5'-(α -P-borano)triphosphates by the Shaw lab, and the reaction produces two diastereomers, *Rp* and *Sp* (Kryzyzanowska, et al. 1998, He, et al. 1998). In this work, the Sal-p-Cl approach was used to produce *Rp* and *Sp* nucleotide (α -P-borano)triphosphates of all four RNA bases (NTP α Bs) and reverse phase high performance liquid chromatography was used to purify the *Rp*-NTP α Bs for use in the synthesis of boranophosphate RNA (BP-RNA) (He 1998, He 2000).



Scheme 3-1. Sal-P-chloride approach to chemical synthesis of adenosine 5'-(α -P-borano) triphosphate. This method can be used to synthesize all four nucleotide triphosphates and produces two diastereomers, *Rp* and *Sp*.

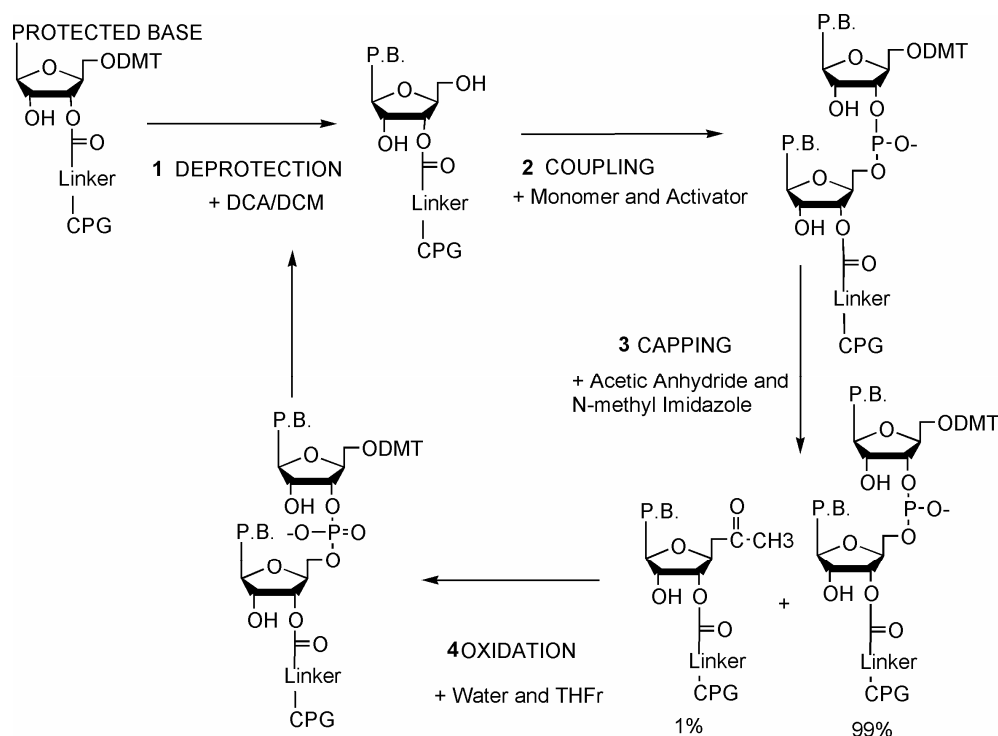
3.1.2 Synthesis of modified oligonucleotides

Synthetic oligonucleotides are increasingly popular therapeutic agents against human viruses and cancers. There are two routes for the synthesis of natural

oligonucleotides and modified boranophosphate oligonucleotides (BP-ON), chemical synthesis and enzymatic synthesis.

3.1.2.1 Chemical synthesis of oligonucleotides

Chemical synthesis of oligonucleotides begins with a protected nucleotide tethered to a solid support, usually controlled pore glass (CPG) (Behlke and Devor 2005). Modern methods make use of phosphoramidite monomers with 5' dimethoxytrityl (DMT) protection groups and use tetrazole to catalyze the coupling reaction, resulting in elongated oligonucleotide chains. The synthesis proceeds in four steps: 1) detritylation of monomer attached to CPG using dichloroacetic acid; 2) coupling of the CPG-monomer to the next desired DMT-protected monomer using tetrazole as an activator to create a tetrazolyl phosphoramidite intermediate, which then reacts with the newly exposed 5' OH group of the CPG-monomer to form a 5' → 3' phosphite linkage; 3) capping of any exposed/unreacted 5' hydroxyl groups via acetylation to prevent base deletions due to coupling failure; 4) oxidation of the labile phosphite group to a pentavalent phosphate group (Sinha 1993; Behlke and Devor 2005). (Figure 3-1) After cleavage of the oligonucleotide from the solid support and deprotection of the bases, this method yields oligonucleotides that are not stereoregular (if modified) and that lack a 5' phosphate (Manoharan 2007).



Scheme 3-2. Chemical synthesis of oligonucleotides. There are four steps for chemical synthesis. 1) Deprotection: removal of DMT group from the 5' positions on the sugar using acidic conditions. 2) Coupling: Addition of the next monomer in the sequence to the deprotected monomer via the formation of a 3'→5' internucleoside phosphite linkage. 3) Capping: Addition of acetic anhydride and N-methyl imidazole to block any unreacted 5' OH groups. 4) Oxidation: Conversion to pentavalent phosphodiester linkage using water. (Sinha 1993; Behlke 2005)

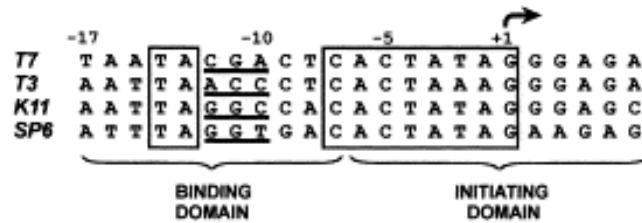
3.1.2.2 Enzymatic Synthesis of oligonucleotides

The obvious alternative to chemical synthesis is enzymatic synthesis. A major advantage of the boranophosphate modification is the ability of the *Rp* stereoisomer of the BP-NTP to be recognized by wild type DNA and RNA polymerases (Li, et al. 1995; Sergueev, et al. 1997; Wan and Shaw 2005). T7 RNA polymerase (T7 RNA pol) has been

used in this project to synthesize enzymatically stereoregular BP-oligonucleotides of various lengths.

T7 RNA pol is a 100-kDa DNA-dependent RNA polymerase that uses double-stranded DNA templates that contain a specific promoter sequence to transcribe natural RNA. (Sousa and Mukherjee 2003) Upon recognition of the T7 consensus sequence, initiation of transcription proceeds from the +1 position, as shown in Figure 3-1 (A). (Kochetkov, et al. 1998) Each polymerase is extremely sensitive to its specific promoter; the T7 RNA polymerase cannot even recognize the T3 polymerase promoter, despite the fact that the sequences only differ in the -10 to -12 positions. (Chamberlin, et al. 1970; McGinness and Joyce 2002) During the initiation phase, the polymerase can fall off of the DNA template, resulting in short, abortive products that are 2-8 nucleotides long. (Gurevich, et al. 1991) The initiation of transcription is followed by elongation, during which the enzyme translocates down the DNA template while unwinding the DNA duplex and processively elongates the RNA transcript. Transcription ends with termination phase of the transcript. (Steitz 2004) The three phases of RNA transcription are shown in Figure 3-1 (B).

(A)



(B)

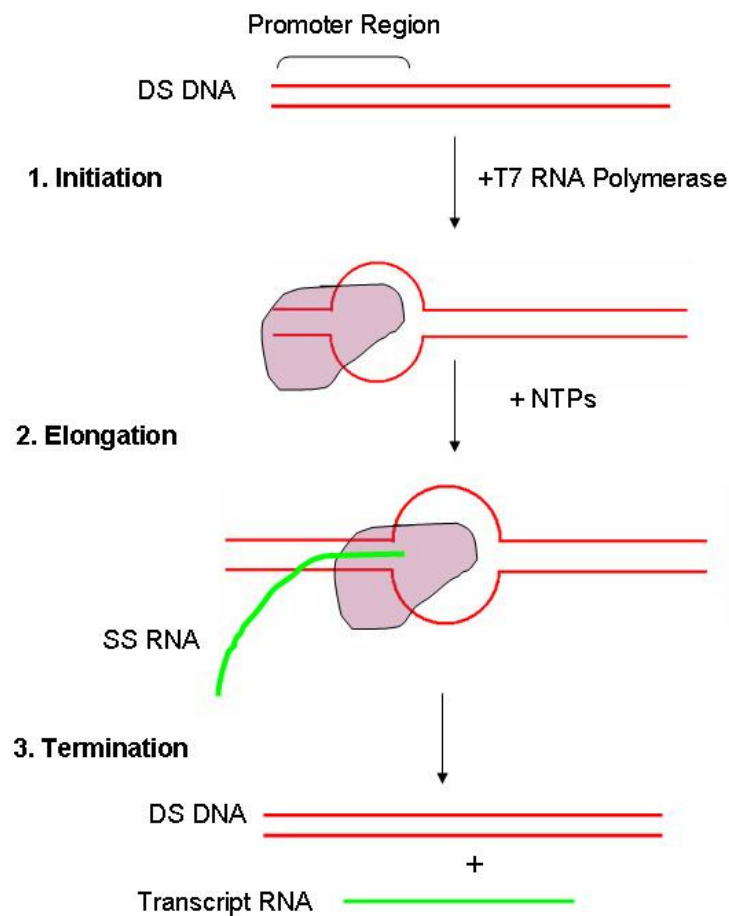


Figure 3-1. T7 RNA Polymerase. **A)** Consensus sequences (promoter regions) for common RNA polymerases. Figure from reference. (Kochetkov 1998) **B)** Transcription begins with an initiation phase. After the polymerase is securely attached to the DNA template, the elongation phase begins. The termination phase ends transcription. Figure from reference (Alberts 2002)

The structure of the T7 RNA pol is homologous to other oligonucleotide polymerases, with palm, fingers, and thumb domains. The thumb domain acts to stabilize the transcription complex and maintain processivity during elongation of the transcript. The palm domain houses the active site of the polymerase and contains the most catalytically relevant residues. The fingers domain makes contact with the DNA template strand downstream of the templating base and is thought to play a role in transcription fidelity. (Sousa and Mukherjee 2003) A ribbon diagram of the T7 RNA pol structure is shown in Figure 3-2.

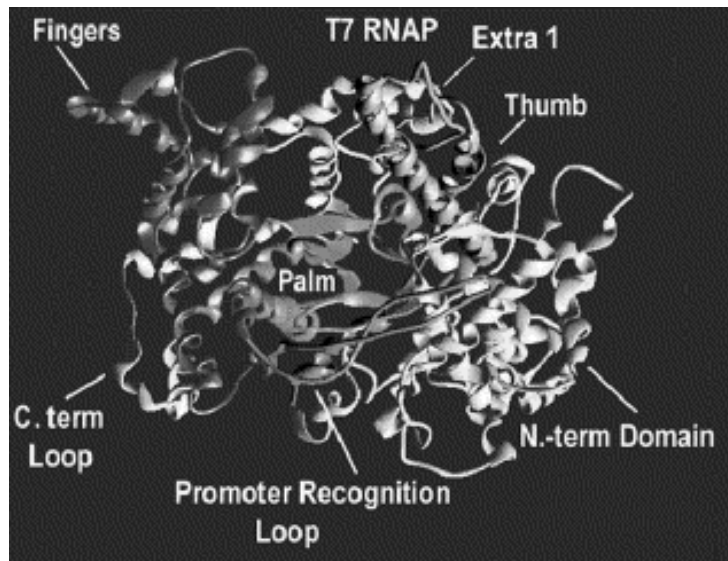


Figure 3-2. A ribbon diagram showing the overall structure of T7 RNA polymerase. The dark gray structures show the fingers, palm and thumb domains that are homologous to structures in other polymerases. (Sousa 2003)

There are several advantages to using polymerases to synthesize RNA; 1) high yield, 2) ease of use, and 3) stereospecificity of modified nucleotides, and 4) relatively low cost. One copy of DNA template typically yields 30-40 copies of RNA transcript

during a 15-minute incubation (McGinness and Joyce 2002). Commercial kits are available that are optimized to yield unmodified siRNA in high yield, usually 2-5 mg per 1 mL of reaction mixture (Promega 2006). However, while it has been shown that T7 RNA pol can accept NTP α Bs as substrates and incorporate them into RNA, it has also been noted that for shorter transcripts (<1000 bp) the borane modification causes a reduction in yield (Wan and Shaw 2005). Therefore, it remained to optimize the enzymatic synthesis of short 21mer boranophosphate siRNA for the maximum possible yield.

3.2 Synthesis of NTP α B Modified and 2' F Modified Triphosphates

3.2.1 Experimental Procedures

NTP α B: The starting materials for the syntheses of NTP α B analogs were 2',3'-diacetylated bases, including adenosine, cytidine, uridine, and guanosine, as the reaction did not require base protection. These starting materials, obtained commercially from ChemGenes, are shown in Figure 3-1. (He 2000) The BP-NTP reactions were performed on a 0.5-mmol scale as a one-pot reaction.

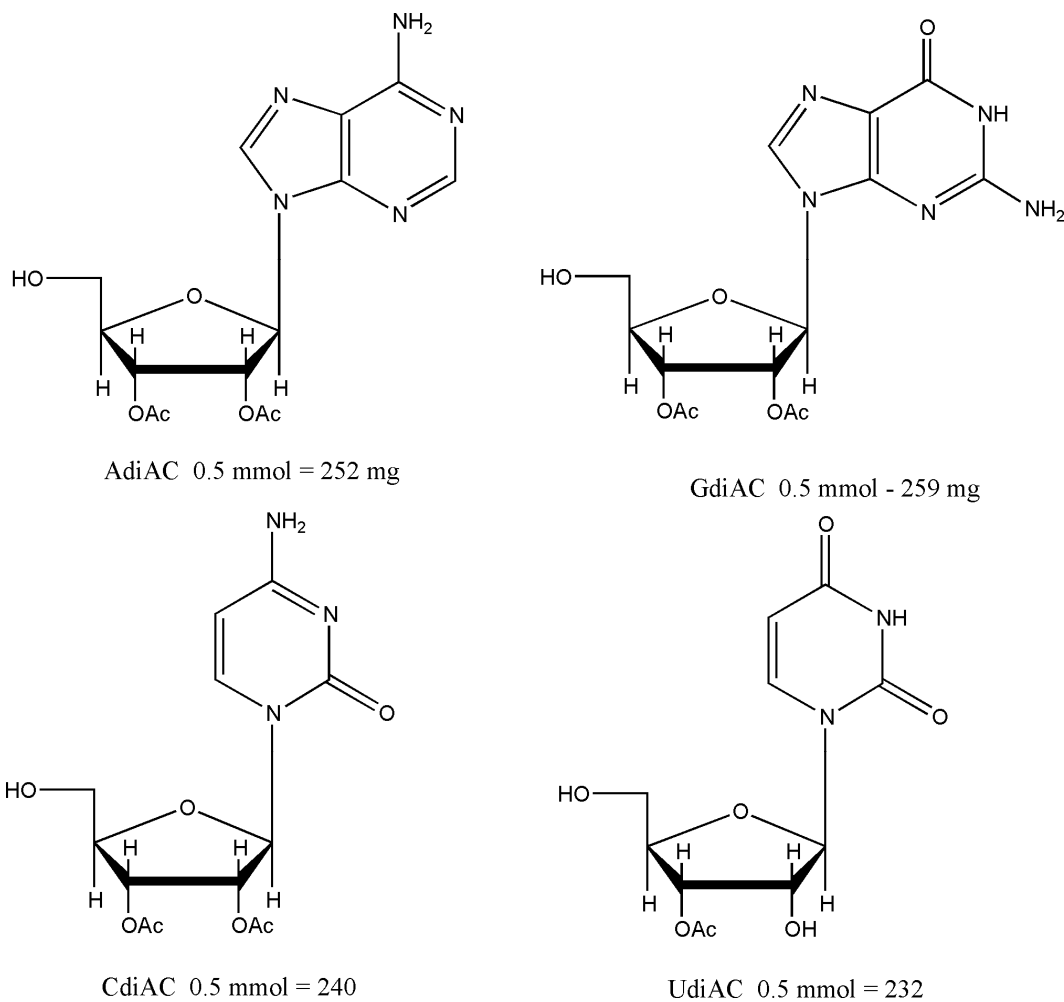


Figure 3-3. Starting materials for the chemical syntheses of NTP α Bs. 1: 2',3'-diacetylated adenosine. 2: 2',3'-diacetylated guanosine. 3: 2',3'-diacetylated cytosine, 4: 2',3'-diacetylated uridine The expected yield for a 0.5 mmol reaction is given in milligrams beneath each reagent.

The starting materials, protected nucleosides (0.5 mmol), was weighed and dried overnight under vacuum at 45-50°C. To begin, the starting material was dissolved in pyridine anhydrous (0.2 mL) and DMF anhydrous (1.0 mL). Under argon, 202.54 mg of salicylphosphochloridate was dissolved in 1.0 mL dichloromethane to make a 1.0 M Sal-p-Cl solution, which was then added to the starting material (1.1 equivalents). After ten

minutes, tributylamine (0.45 mL, 4 eq) and 0.5 M tributylammonium pyrophosphate in DMF anhydrous (1.5 mL) was added (1.5 eq). After twenty minutes, the boronating agent borane dimethyl sulfide complex ($\text{BH}_3\text{:SMe}_2$, 2 mL, 8.0 eq) was added and the reaction was stirred for 30 minutes. A mixture of 3:2 TEA: H_2O (5 mL) was added to the reaction vessel and stirred for two hours. Finally, an excess of concentrated ammonium hydroxide (~10 mL) was added to the vessel and allowed to stir overnight at room temperature.

The next morning, the contents of the reaction vessel were evaporated on a rotovap at 50°C and then reconstituted with deionized water to approximately 10 mL. Following reconstitution, the reaction was extracted once with an equal volume of diethyl ether and the aqueous layer (~10 mL) was removed and concentrated on the rotovap down to 2-3 mL. This volume was subjected to ion-exchange chromatography on a hand-packed column, as described in Section 2.1, composed of QA-52 cellulose (HCO_3^-) with a linear concentration gradient of 5 mM and 400 mM ammonium bicarbonate buffer, pH 9.6. Based on UV absorbance, the desired fractions were collected (desired fraction eluted at $R_t \approx 90$ minutes), evaporated using the rotovap, and lyophilized. The structure, purity, and homogeneity of the product was determined using ^{31}P NMR, ^1H NMR, and ESI-MS. The product was then subjected to stereoisomer purification using reverse phase high performance liquid chromatography (HPLC). The instrument is described in section 2.1 and the experiments in Chapter 3.

2'F NTP: The syntheses of 2'-fluoro-2'-deoxycytidine 5'-triphosphate and 2'-fluoro-2'-deoxyuridine 5'-triphosphate were performed following the Sal-p-Cl methodology. Again, the hydroxyl group on the sugar moiety was acyl-protected and the base did not require any protection. The starting materials for the 2''fluoro NTP analog synthesis are shown in Figure 3-4.

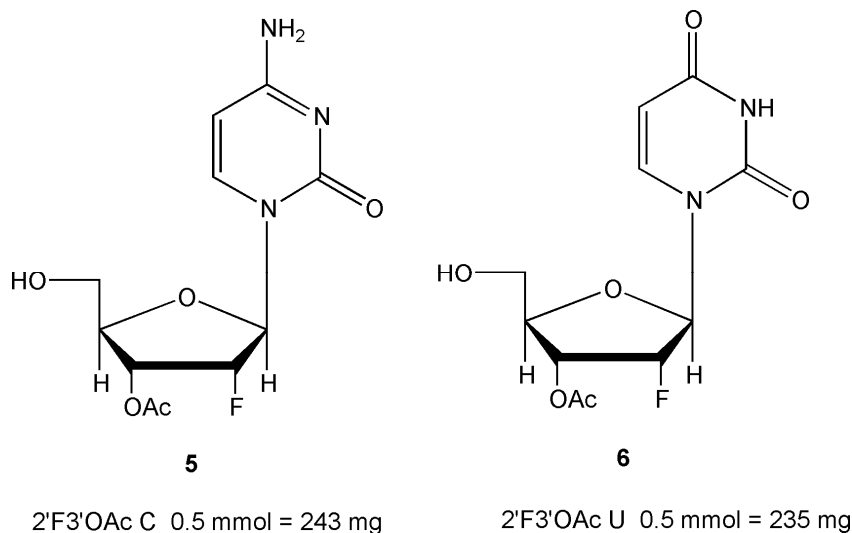


Figure 3-4. Starting protected nucleosides for syntheses of 2'F modified triphosphates. 5: 2'-fluoro-3'-acetylated cytosine. 6: 2'-fluoro-3'-acetylated uridine. The expected yield for a 0.5 mmol reaction is given in milligrams beneath the reagent.

The starting materials, 2'-fluoro-3'-acetylated nucleosides (0.5 mmol), was weighed and dried overnight under vacuum at 45-50°. The next morning, it was dissolved in pyridine anhydrous (0.2 mL) and DMF anhydrous (1.0 mL) and 1.0 M Sal-p-Cl (1.0 mL, 1.1 eq) was added. After stirring for 10 minutes, tributylamine (0.45 mL, 4 eq) and 0.5 M tributylammoniumpyrophosphate (1.5 mL, 1.5 eq) were added at the same time and rate. After stirring for 20 minutes, four equivalents of tert-butyl peroxide (5.5

M) were added over 30 minutes. The reaction was allowed to stir for another 30 minutes and then 5.0 mL of 3:2 TEA:H₂O were added. After stirring for 2 hours, an excess of ammonium hydroxide was added and the reaction was stirred at room temperature overnight.

The next morning the contents of the reaction vessel were evaporated, reconstituted with approximately 10 mL of deionized water, and extracted once with an equal volume of diethyl ether. The aqueous layer was removed, concentrated on the rotovap to 2-3 mL, and loaded onto the QA-52 ion-exchange column with a linear concentration gradient of 5 mM and 400 mM ammonium bicarbonate. Based on UV absorption, the desired fractions were collected, evaporated, and lyophilized. Further purification was done using reverse phase HPLC.

3.2.2 Results and Discussion

Nucleoside (α -P-borano)-triphosphates were prepared using the Sal-p-Cl approach. The final products of the four syntheses are shown in Figure 3-5.

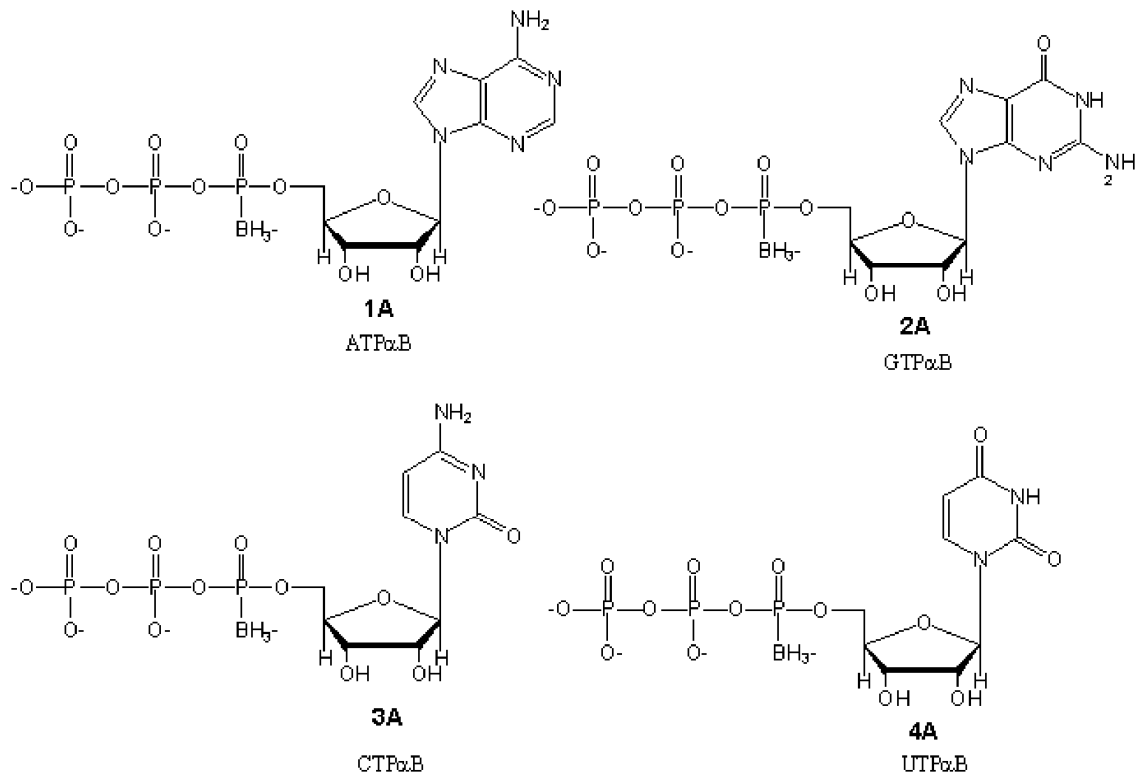


Figure 3-5. The four rNTP α Bs. 1A: ATP α B, 2A: GTP α B, 3A: CTP α B, and 4A: UTP α B are the final products for the synthesis of ribonucleotides modified on the α -phosphorous with the borane moiety.

After separation of the triphosphate from reaction impurities using ion-exchange chromatography, the yields were determined. The yield of the NTP α B syntheses was first calculated by weight and ranged from 20%-40%, which is comparable to the yields found previously (He, et al. 1998; Kryzyzanowska, et al. 1998). However, the yields of the NTP α B syntheses as calculated using the UV absorbance and Beer's Law, ranged from 13% to 20%. (Table 3-1) It is possible that salts accumulated during ion exchange are responsible for the discrepancy in yields. For accurate measurement of yield, all further yields were determined by UV absorbance.

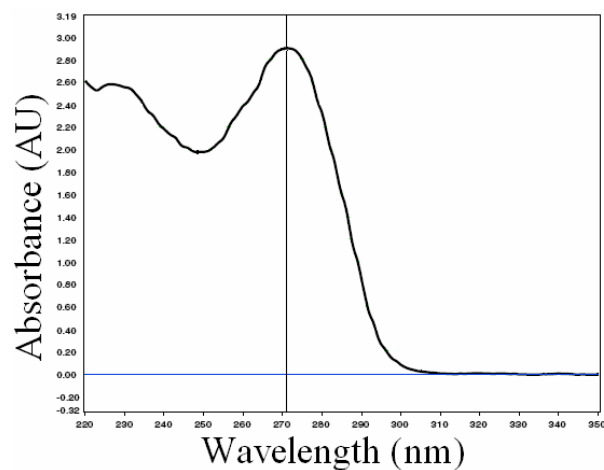
Table 3-1. Yields of NTP α B syntheses by weight and by UV absorbance.

NTP	Yield by weight	Yield by UV
ATP α B	63.0 mg (25%)	15%
CTP α B	48.0 mg (20%)	13%
GTP α B	59.6 mg (23%)	15%
UTP α B	93.0 mg (40%)	20%

The NTP α B modified triphosphates were characterized using UV, ESI-MS and ^{31}P and ^1H NMR. Due to the fact that the chromophore (base) is unmodified, the UV spectra of NTP α B analogs are unchanged with respect to natural triphosphates. A representative UV spectrum is shown in Figure 3-6 A, with the UV spectra of all four NTP α B shown in Appendix I. The concentration of the eluent after ion-exchange chromatography was calculated using Beer's Law (Eqn 2-1) and the measured absorbance was used to determine the yield of each reaction.

A representative spectrum from the ESI-MS characterization is shown in Figure 3-6 B. Due to fragmentation during measurement, there are three major peaks, representing the boranomonomphosphate (319.9 m/z), boranodiphosphate (398.8 m/z), and boranotriphosphate (479.8 m/z), which are comparable to the molecular weights given in Table 2-1.

(A)



(B)

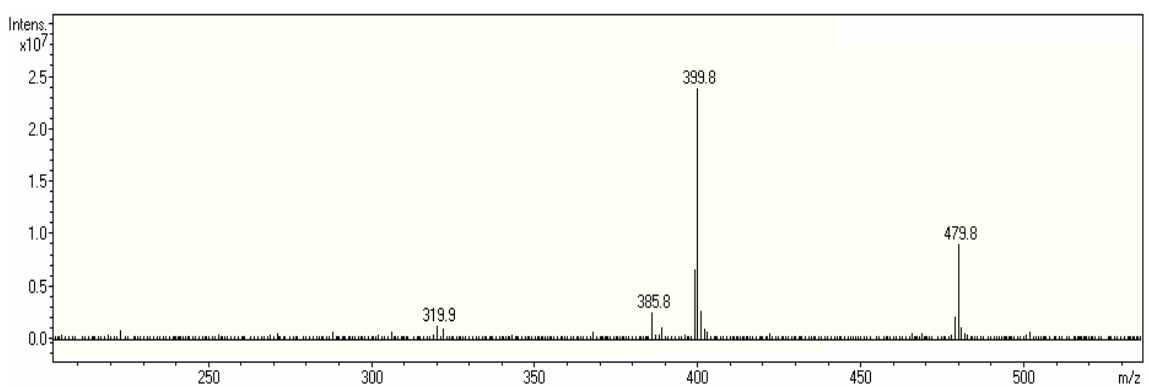
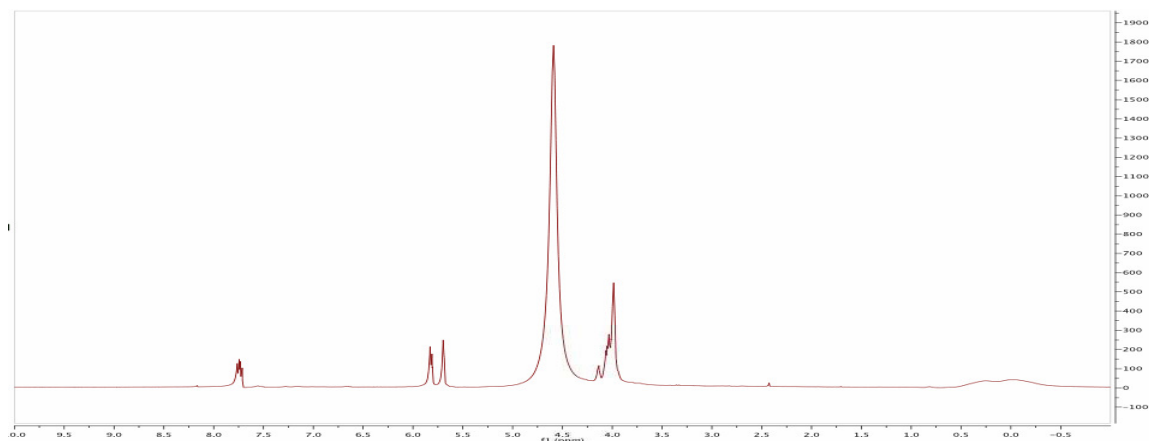


Figure 3-6. Characterization by UV and ESI-MS of the final products of NTP α B synthesis. **(A)** Representative UV spectra of CTP α B where absorbance is measured at 271 nm to determine concentration **(B)** Representative mass spectrometry profile for CTP α B showing peaks for the triphosphate (479.8), diphosphate (399.8), monophosphate (319.9), and a small amount of impurity (385.8).

The proton NMR spectra (Fig 3-7 A) and ³¹P NMR spectra (Fig 3-7 B) are in accordance with previous data (He 2000). The ¹H NMR spectra peaks were assigned as follows: δ = 7.75 (m, 1H, H-6), 5.80 (d, 1H, H-5), 5.4 (d, 1H, H-1'), 4.23 (m, 1H, H-3'), 4.10,

(A)



(B)

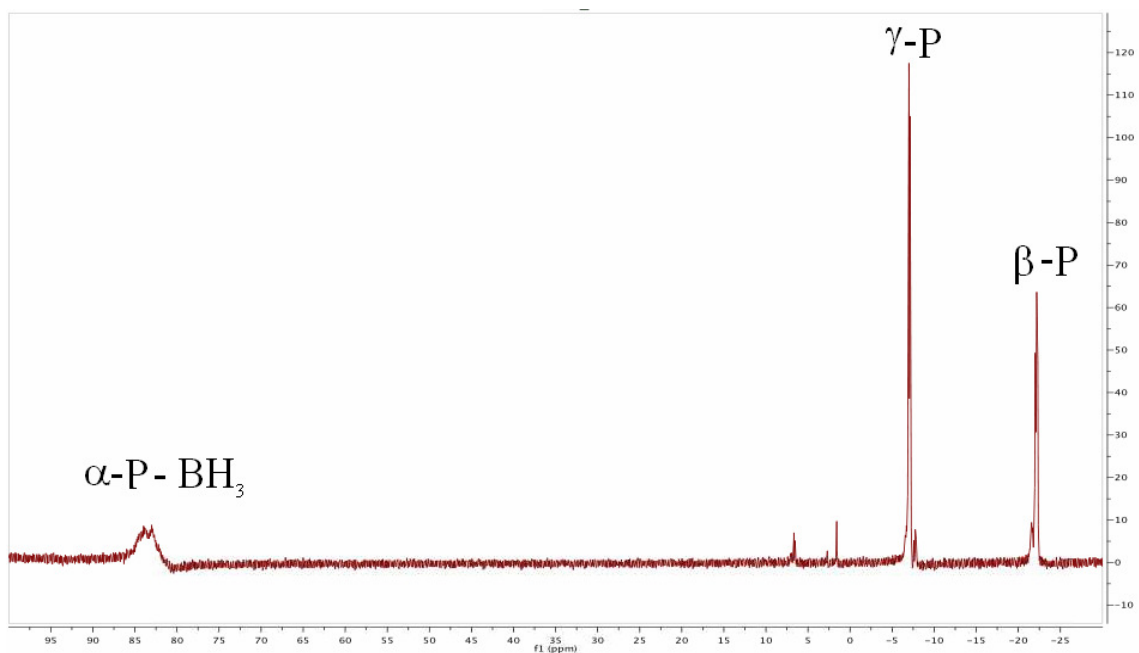


Figure 3-7. Characterization by NMR of final products from NTP α B synthesis. **(A)** Representative ¹H NMR profile for CTP α B in D₂O. **(B)** Representative ³¹P NMR profile for CTP α B in D₂O with the three phosphates identified.

4.00 (2m, 3H, H-4', H-5'), 0.50 to -0.3 (2br, 3H, BH₃). The ³¹P NMR spectrum contains three peaks: δ = 83.05 (br, 1P, α-P), -7.30 (m, 1P, γ-P), -22.05 (m, 1P, β-P). These data are in agreement with previous studies (Li, et al. 1996). The UV, ESI-MS, and ¹H and ³¹P NMR spectra for all four nucleoside (α-P-borano)triphosphate final products can be found in Appendix I.

2'F NTPs were also synthesized using the Sal-P-Cl method and characterized by the same methods as above. Only the pyrimidines were synthesized as 2'F analogs (CTP and UTP). The yield for 2'F CTP was 20% by weight and 10% by UV. The yield for 2'F UTP was 36 % by weight and 21% by UV. The final products for the 2'F NTP syntheses are shown in Figure 3-8.

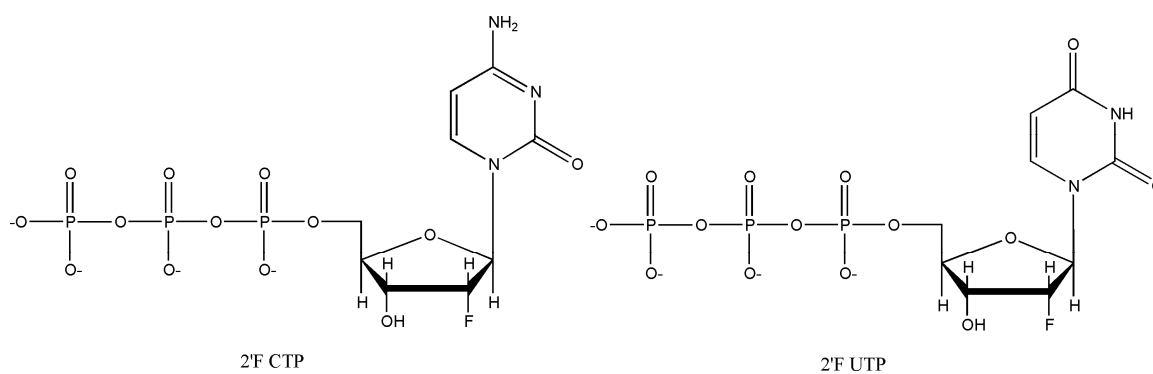
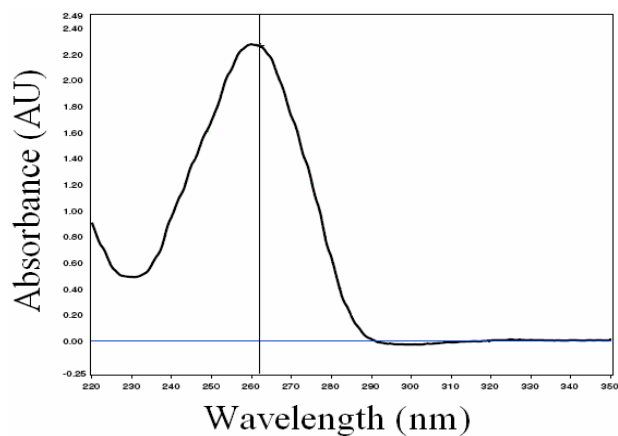


Figure 3-8. 2'F NTPs. The final products for the 2'F NTP syntheses are 5A: 2'F CTP and 6A: 2'F UTP

The modification of the 2' position did not have an affect on the absorption maximum of the UV spectra of the modified nucleotides. (Figure 3-9 A) The ESI mass

(A)



(B)

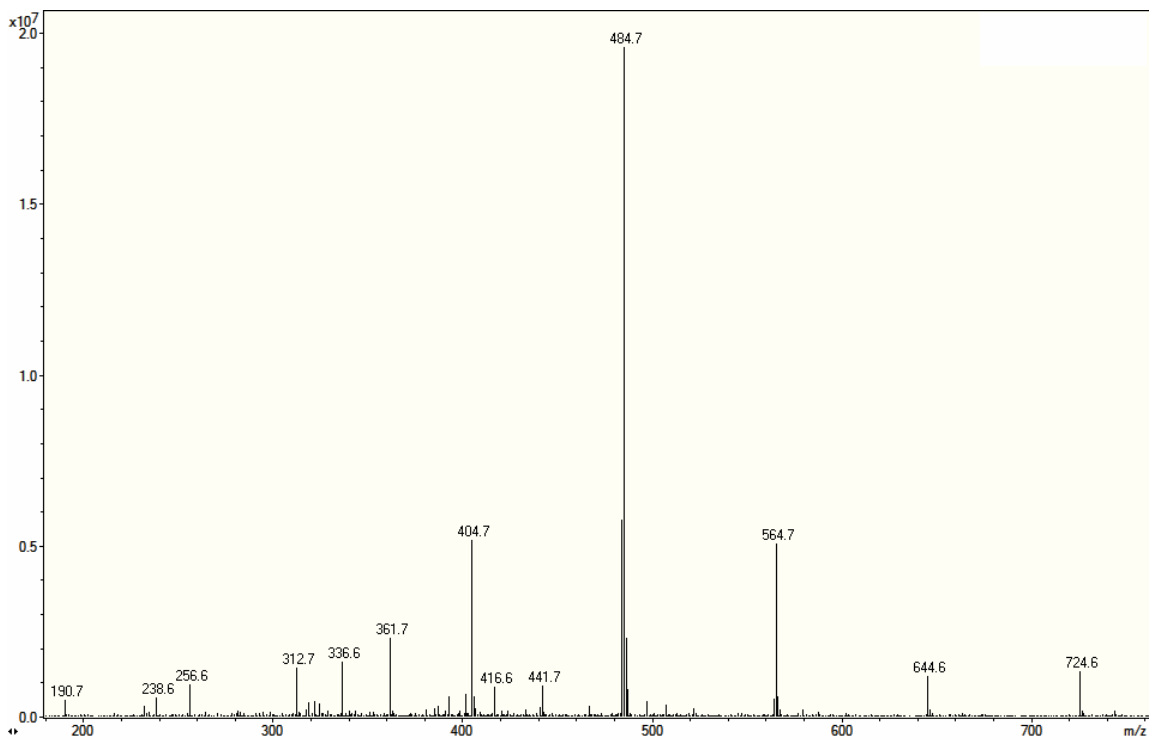


Figure 3-9. Characterization by UV and ESI-MS of the final products of 2'F NTP synthesis. (A) Representative UV spectra of 2'F UTP where absorbance is measured at 271 nm to determine concentration (B) Representative mass spectrometry profile for 2'F UTP showing peaks for the triphosphate (484.6) and diphosphate (404.86).

spectrometry spectra for each 2'F NTP showed three peaks corresponding to the 2'F NMP, 2'F NDP, and 2'F NTP. (Figure 3-9 B)

The 2'F NTPs were also characterized by ^1H NMR (Figure 3-10 A) and ^{31}P NMR (Figure 3-10 B). The spectra are in accordance with literature data (Huang 1994). The ^{31}P NMR shows peaks at 2.2 ppm ($\gamma\text{-P}$), -9.8 ppm ($\alpha\text{-P}$), and -21.0 ppm ($\beta\text{-P}$). (Appendix I)

Overall, the work in this section has demonstrated the synthesis of modified nucleoside triphosphate in sufficient yield for synthesis of boranophosphate RNA. The final products were characterized by UV, mass spectrometry, and NMR to determine yield, structure, and purity.

3.3 Purification of NTP α B and 2'F-NTP Modified Triphosphates

3.3.1 Experimental Procedures

NTP α B: The one-pot synthesis of NTP α Bs produces two stereoisomers, *Rp* and *Sp*. Purification of the stereoisomers was carried out by ion-pairing chromatography using the Waters Preparative HPLC fitted with a Varian reverse phase preparative column (PrepPak), as described in Chapter 2. Samples consisted of 10-20 mg of the modified NTP dissolved in 1-2 mL of filtered, deionized water. Prior to loading the sample onto the column, it was filtered using a Microcon YM-30 Centrifugal Filter Unit (Millipore) with an Ultracel-YMTM filter and a nominal molecular weight limit of 30 kDa to remove any large particles that might clog the column. The compounds were

separated using isocratic elution, where the mobile phase consisted of methanol and 50 mM TEAA. The fractions corresponding to all the desired peaks were collected, analyzed, and pooled. The organic phase was removed on a Rotovap and the remaining liquid was frozen on liquid nitrogen or dry ice and then lyophilized three times to remove buffer components.

Following purification, the collected fraction was analyzed using the Varian HPLC fitted with an analytical column (DeltaPak). For each base, standards were run under the same conditions for calibration and proper peak identification. The standards consisted of the nucleoside, the nucleoside monophosphate, the nucleoside diphosphate, and the nucleoside triphosphate (all unmodified).

2'F NTP: The one-pot syntheses of *2'F CTP* and *2'F UTP* do not produce stereoisomers, but do require purification from by-products of the reaction. Both *2'F CTP* and *2'F UTP* were purified using the PrepPak C-18 column on the Waters HPLC with an isocratic method of 94% 50 mM TEAA and 6% methanol with a flow rate of 6 mL/min. Each injection was approximately 10-20 mg of the lyophilized sample after ion exchange chromatography that was reconstituted with deionized water and then filtered using a Microcon YM-30 centrifugation unit to remove any particulates that could clog the column. The desired *Rp* and *Sp* boranotriphosphate peaks were identified using the UV absorbance, collected and the organic phase was removed on a Rotovap. The remaining liquid was frozen on liquid nitrogen or dry ice and then lyophilized

repeatedly to remove buffer components. The final product was characterized as pure using analytical HPLC and run on LC-MS.

3.3.2 Results and Discussion

Replacement of the non-bridging oxygen with the BH_3 group introduces a chiral center at the α -phosphorous, resulting in 2 diastereomers, *Rp* and *Sp*. The Shaw lab has consistently used stereoisomerically pure $\text{NTP}\alpha\text{B}$ samples are required for biological applications, due to the fact that the *Rp* stereoisomer is preferred by DNA polymerase (Porter, et al. 1997) and RNA polymerase (Wang and Shaw 2005). Therefore, after synthesis, purification of $\text{NTP}\alpha\text{B}$ s must be done using reverse phase a high performance liquid chromatography (HPLC) to separate the sample into *Rp* and *Sp* stereoisomers (Kryzyzanowska, et al. 1998). The assignment of the stereochemistry of the two stereoisomers, based on NMR data (He, et al. 1998) is shown in Figure 3-10.

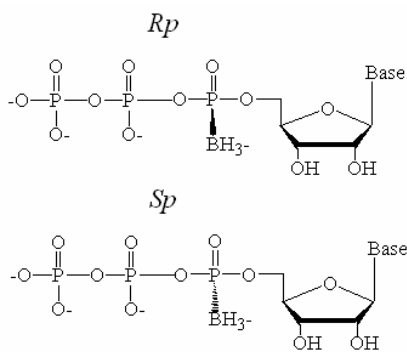


Figure 3-10. *Rp* and *Sp* stereoisomers that result from the introduction of the chiral center by substitution of a non-bridging oxygen with a borane group (Wan 2005)

Analytical scale purifications (<1 mg) of NTP α Bs have been done previously, but there has not yet been preparative scale separation of the stereoisomers of each of the four rNTP α Bs (N=A, C, G, U), which is required if they are to be produced in sufficient quantity for biological applications. The conditions for preparative scale separation can differ greatly from the analytical scale separations, due to differences in column dimensions, especially the internal diameter (ID) of the column. (Horvath, et al. 1967) A column with a smaller ID will show increased detection sensitivity and separation selectivity versus a column with a larger ID. Many different separation conditions were tested to ensure the best separation of the stereoisomers, including varying the composition of the mobile phase, the flow rate, and the elution gradient.

The aqueous solvents that were tested in this work included 0.05 M TEAA, 0.1 M TEAA, and 0.1 M TEAB. Overall, it was determined that 0.05 M triethylammonium acetate (TEAA) and 0.1 M triethylammonium bicarbonate (TEAB) were equally good for separation; however, TEAB required extra steps for preparation, as described in Chapter 2, and careful monitoring of the pH, due to the fact that as the CO₂ degases from the solvent, the pH increases, which is dangerous for the column. Therefore, 0.05 M TEAA was used for all separations of nucleotides. The organic solvents tested included methanol and acetonitrile. Acetonitrile is a stronger eluent than methanol, requiring a lower percentage for separation, and therefore it is harder to manipulate the conditions for good separation of the stereoisomers (Han 1989). Methanol is easier to manipulate

when creating the separating conditions, but there is some concern that any formaldehyde impurities in the methanol might react with a borano moiety and lead to increased cleavage of the BH₃ group, resulting in an unmodified NTP. However, this effect was not seen when the separated NTP α Bs were run under analytical conditions, perhaps because the exposure to methanol was limited to the duration of the run. (Figure 3-13) Therefore, methanol was the organic solvent of choice for separations.

The flow rate can directly influence the separation, as flow rate is directly related to the molecular diffusion, and therefore to peak broadening (Horvath, et al. 1967). Since peak broadening decreases the separation efficiency, higher flow rates (6 ml/min vs 1 ml/min) were used for separations to ensure sharp peaks and base-line separation. (Table 3-2)

The percentage of organic solvent was also varied for each NTP α B to get the best separation of the stereoisomers. The purification conditions varied depending on the nitrogenous base (Table 3-1). The stereoisomers were identified based on previous work that showed that the *Rp* stereoisomer was the faster eluting isomer (He 1998). Each peak in the spectra was analyzed using LC-MS to ensure its identity.

Table 3-2. Optimal preparative scale purification conditions for the four NTP α Bs. All purifications were done using isocratic conditions on a PrepPak C-18 column. Approximately 10 mg was loaded for each run.

NTPαB	Buffer	Flow Rate	<i>R_p</i> Rt	<i>S_p</i> Rt
ATP α B	92% 0.05 M TEAA 8% MeOH	6 mL/min	35.0 min	54.2 min
CTP α B	94% 0.05 M TEAA 6% MeOH	4 mL/min	18.5 min	38.0-42.0 min
GTP α B	92% 0.05 M TEAA 8% MeOH	6 mL/min	14.5 min	22.0 min
UTP α B	89% 0.05 M TEAA 11% MeOH	6 mL/min	39.0 min	69.0-79.0 min

Representative spectra of the preparative scale separations of the four NTP α Bs are shown in Figure 3-11. The spectra are characterized by a tall, skinny peak for the *R_p* stereoisomer and a short, wide peak for the *S_p* stereoisomer. For preparative scale separations, collection of the peak did not begin until the absorbance reached 100 mAU to ensure that the peak would be entirely free of impurities. A representative peak of the stereoisomerically pure *R_p*-ATP α B is shown in Figure 3-12.

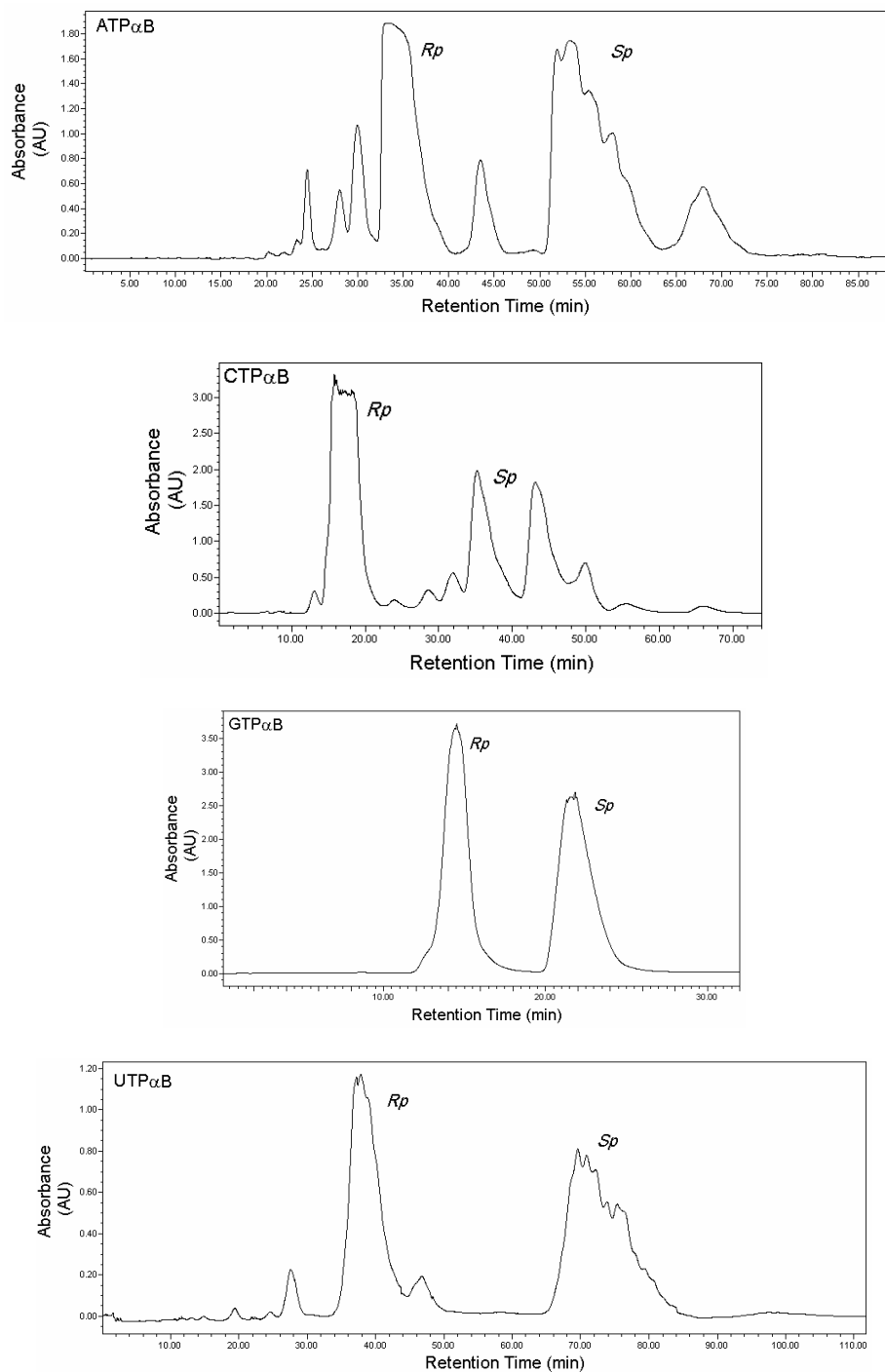


Figure 3-11. Separation profiles of the four NTPαB stereoisomers, where time is plotted versus absorbance. The separation conditions and retention times of the *Rp* and *Sp* isomers are given in Table 3-2.

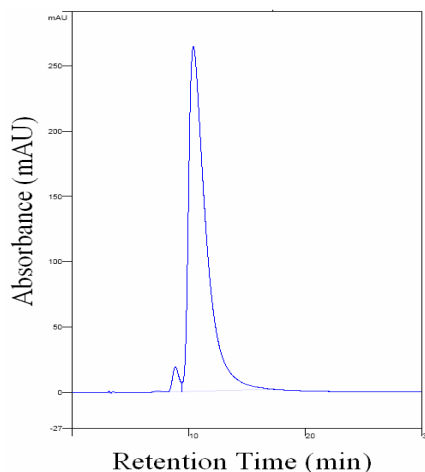


Figure 3-12. Representative analytical RP-HPLC spectra. *Rp*-ATP α B is shown to be >99% pure after stereoisomer separation.

The preparative scale purification of the 2'F CTP and 2'F UTP analogs did not require optimization, as there were no stereoisomers. Approximately 10 mg of each sample were loaded onto the preparative column and run with 92% 0.05 M TEAA and 8% methanol, at a flow rate of 6 mL/min. A representative analytical spectrum of the purified final product of 2'F UTP synthesis (Rt = 43 min) with a small diphosphate impurity (Rt = 30 min) is shown in Figure 3-13.

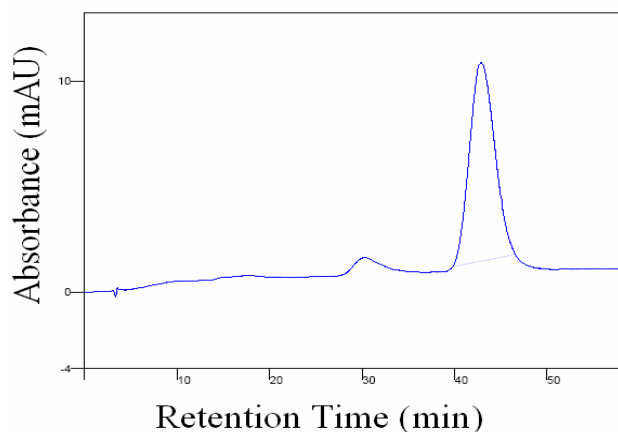


Figure 3-13. Analytical spectra of 2'F UTP. The purified product (>98%) is shown on analytical HPLC under conditions of 92% TEAA and 8% methanol.

For both samples, the purity is greater than 95% (determined by peak integration on analytical HPLC). The identity of the purified peak after prep scale separation was determined by analytical HPLC and LC-MS. The LC-MS analysis confirmed that the collected peak had the correct molecular weight, allowing positive identification of the modified triphosphate. Analytical HPLC allowed determination of the modified triphosphate stereoisomer purity at acceptable levels (in this case, greater than 95%).

3.4 Enzymatic Synthesis of Normal and Chemically Modified Ribonucleic Acids

3.4.1. Experimental Procedures

Short 21mer RNA was required for use in RNA silencing. These short ribooligonucleotides are termed **siRNA**. The enzymatic synthesis of normal and boranophosphate siRNA was performed using wild-type (wt) T7 RNA polymerase. The

transcription reactions were performed using Ribomax™ High Yield Transcription kit (Promega), which was deemed superior to the Ampliscribe kit (Epicentre). The Ribomax kit is optimized to make long, unmodified RNA. In this work, it was utilized to make modified siRNA, and so the reaction parameters had to be optimized. The amount of DNA template, the concentration of the NTPs, and the time of incubation were varied to determine the optimal conditions for transcriptions of siRNA that included boranophosphate modified nucleotides. The recommended amount of DNA template for the normal transcription reaction is 5-10 µg. For the template used in this work, this is approximately 200-400 pmol. Transcriptions to obtain normal, unmodified RNA were performed using 5 µg, 7.5 µg and 10 µg of DNA template.

The concentration of NTPs recommended in the literature for synthesis of normal mRNA is 7.5 mM (Gurevich 1991). However, previous work with modified NTPs has shown good yields with lower concentrations. Therefore, NTP concentrations of 2 mM, 4 mM, and 8 mM were tested in transcription reactions. The recommended time for normal transcription to incubate at 37°C is four hours. Again, the literature suggests that other modified NTPs showed greater yield when transcribed for longer periods of time (Kawasaki 1993, Sousa 2003). Therefore, the incubation times that were tested here were 4 hours, 6, hours, and overnight (12-14 hours) incubations.

Transcriptions that included 2'F NTP analogs were initially performed with the Durascribe kit from Epicentre that contains a mutant polymerase for facilitated

incorporation. However, preliminary experiments showed very little difference in the yield of the reactions and therefore it was decided to use the wt T7 polymerase from Promega due to its much lower cost. The six sequences that were studied are shown in Table 3-3.

Table 3-3. HPV 16+24 AS sequence 21mer RNA transcripts were used for comparison of yield under different conditions. Modifications are shown in color. Blue nucleotides are boranophosphate modified and red nucleotides are 2'-fluoro modified. Enzymatically transcribed RNA may contain additional bases on the 3' end.

Name	Mod	# Mod (%)	Sequence (5'→3')
N AS	None	0 (0)	AGA GAU CAG UUG UCU CUG GUU
1B AS	GTP α B	6 (29)	AGA GAU CAG UUG UCU CUG GUU
2B AS	CTP α B, GTP α B	9 (43)	AGA GAU CAG UUG UCU CUG GUU
3B AS	CTP α B, GTP α B, UTP α B	17 (81)	AGA GAU CAG UUG UCU CUG GUU
4B AS	ATP α B, CTP α B, GTP α B, UTP α B	21 (100)	AGA GAU CAG UUG UCU CUG GUU
FB AS	2'F CTP, GTP α B, 2'F UTP	18 (86)	AGA GAU CAG UUG UCU CUG GUU

For each sequence studied, three 60 μ L stock solutions were made, containing 10 μ g of DNA (~400 pmol) template in RNase-free water for the 16+24 antisense (AS) sequence. The first NTP stock solution contained a final NTP concentration of 2 mM in RNase-free water, the second had a final NTP concentration of 4 mM, and the third had a final NTP concentration of 8 mM. These are representative of typical NTP concentrations use by RNA polymerases. The three stock solutions were each aliquoted

into three fresh, 500 μL polypropylene tubes that contained 20 μL of the NTP stock. The first aliquot was incubated for 4 hours, the second aliquot was incubated for 6 hours, and the third aliquot was aliquoted overnight (approximately 12 hours). At the end of the incubation, DNase was added to each of the 9 tubes and further incubated for 20 minutes. The RNA transcripts were phenol extracted, microcolumn purified, and YM-3 filtered, as described in Chapter 2. The concentration of the final product was determined by the UV absorbance at 260 nm.

The typical yield of normal 21mer transcription with a final volume of 100 μL is approximately 15 nmoles. The typical yield of boranophosphate modified 21mer transcription with a final volume of 100 μL and with 5 GTP α B modifications is approximately 5-7 nanomoles. The yield was calculated in two ways, percent of maximum (% max) and "mole per mole". The % max yield was calculated by determining the yield in moles of the [NTP] = 8 mM overnight incubation for each of the six sequences and setting that value as the maximum amount of RNA transcript that could be produced (Y_{max}). Then the yield in moles for each of the six reactions under the different reaction conditions was determined (Y_n). The values were substituted into Eqn 3-1.

$$\% \text{ max} = \frac{Y_n}{Y_{\text{max}}} \times 100 \quad \text{Eqn 3-1}$$

The mole per mole yield allowed the determination of the efficiency of the reaction. The moles of RNA were divided by the combined moles of all the NTPs present in the reaction mixture.

Matrix assisted laser desorption/ionization mass spectrometry (MALDI-MS) was used to characterize the mass distribution of the normal and GTP α B modified siRNA HPV 16+24+G sequences (5' GAGAGAUCAGUUGUCUCUGGUU 3'). This sequence will be further discussed in Chapter 7.1. The sample was admixed in a 5:1 ratio of matrix:sample. The matrix used was 5-methoxysalicylic acid (MSA) and the sample/matrix mix was spotted on gold sample plates for MALDI-MS analysis by the Voyager-DE PRO Biospectrometry Workstation.

3.4.2 Results and Discussion

In this section, three types of siRNA were enzymatically transcribed. Firstly, normal, unmodified siRNA was transcribed to use as a comparison for all experiments. Secondly, boranophosphate siRNA was transcribed, and for the first time, the enzymatic synthesis of a fully BP modified siRNA has been described. Finally, fluoro/borano siRNA containing 2'F pyrimidines and GTP α B has been enzymatically synthesized for the first time.

In this project, T7 enzymatic transcription of boranophosphate modified RNA was used to create 21 and 22 nt siRNA. RNA with the HPV 16+24+G AS (22 nt) sequence will be discussed later in this dissertation (Chapter 7.1). This sequence was used in

siRNA silencing in cells and was first synthesized under the manufacturer's recommended reaction conditions. MALDI-MS was used to characterize the final product in the case of the normal and singly (GTP α B) borano-modified sequence. (Figure 3-14) The use of a new matrix, 5-methoxysalicylic acid, allowed the collection of MALDI-MS spectra with higher intensities and better signal to noise ratios than previously reported. (Wan 2005) This matrix had recently been shown to improve the spectral resolution of single-stranded oligonucleotides. (Distler and Allison 2001) As seen in Figure 3-14, peaks for the fully extended normal and GTP α B-modified RNA were seen, as well as peaks that represented the N+1 sequence and peaks representing the sequence with an adsorbed cation (sodium or triethylamine). Further improvements in the resolution may possibly be gleaned from desalting the samples to remove the triethylamine that is residual from the HPLC purification and by the addition of spermine into the matrix.

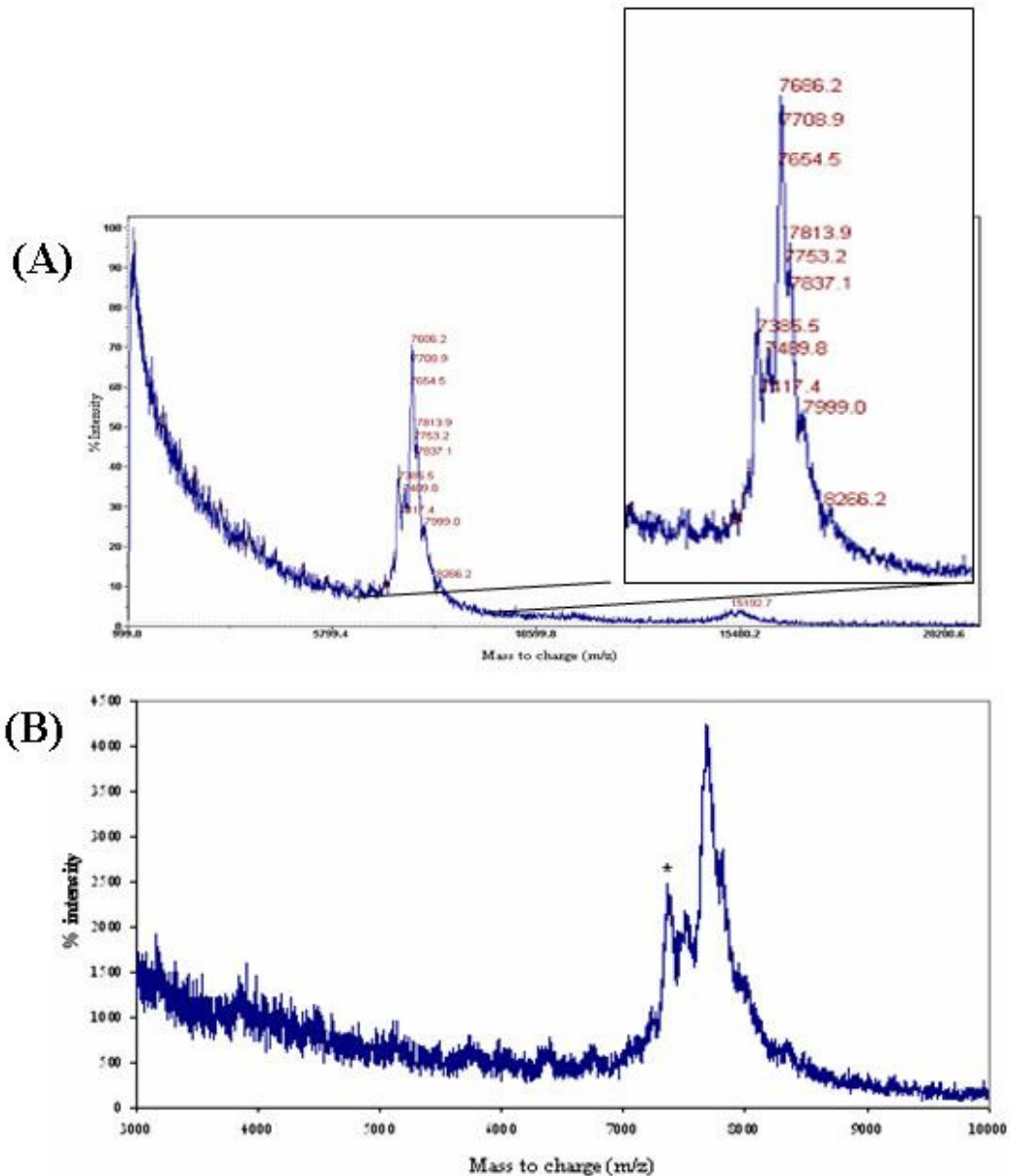


Figure 3-14. MALDI-MS of enzymatically synthesized normal siRNA and boranophosphate siRNA using *Rp*-GTP α B. Spectra were collected on gold sample plates using samples mixed with 5-MSA as a matrix. (A) MALDI of normal unmodified HPV 16+24+G sequences. The largest peak corresponds to the N+1 sequence and the shoulder that precedes it corresponds to the N sequence. Also present are peaks that correspond to N + Na⁺ and N + TEA⁺ (B) MALDI of GTP α B modified HPV 16+24+G sequence. The peak marked with an (*) is the molecular weight of the fully extended product, 1B, (~7022 m/z) and the adjoining peaks correspond to the 1B + Na⁺ and 1B + TEA⁺.

It was previously shown that T7 RNA polymerase is sensitive to the concentration of both the DNA template and the nucleotide triphosphates, and that the yield of the reaction can be influenced by the incubation time (Melton, et al. 1984; Gurevich, et al. 1991). For example, it was shown that increasing the concentration of NTPs over the range of 0→4 mM in the reaction mixture increased the yield, but not linearly. After a certain point, increasing NTP concentration did not result in increased yield. Although the reaction conditions have been optimized for unmodified triphosphates, it remained to optimize the conditions for the transcription reaction with NPT α Bs, and with NTP α B + 2'F NTPs. These siRNA transcripts were synthesized using the HPV 16+24 AS sequence (21 nt), which targets the E6/E7 mRNA transcript in cells that are infected with human papillomavirus (Chapter 7.1). (Table 3-3)

The first variable that was tested was the DNA concentration. It has been shown that when using linearized plasmid DNA, each copy of DNA yields 30-40 copies of RNA. However, the studies that have been previously done have used longer mRNA transcripts (>1000 nt) and therefore it remained to determine the effect of DNA template concentration for shorter, 21 nt siRNA transcripts. By comparing the average yields with the amount of DNA template, it was found that for normal RNA transcribed from the HPV 16+24 sequences, the average number of copies of RNA transcribed per copy of DNA was 28. Under the same conditions, the average number of copies of BP-modified RNA containing GTP α B modifications was 26. For both normal and modified RNA

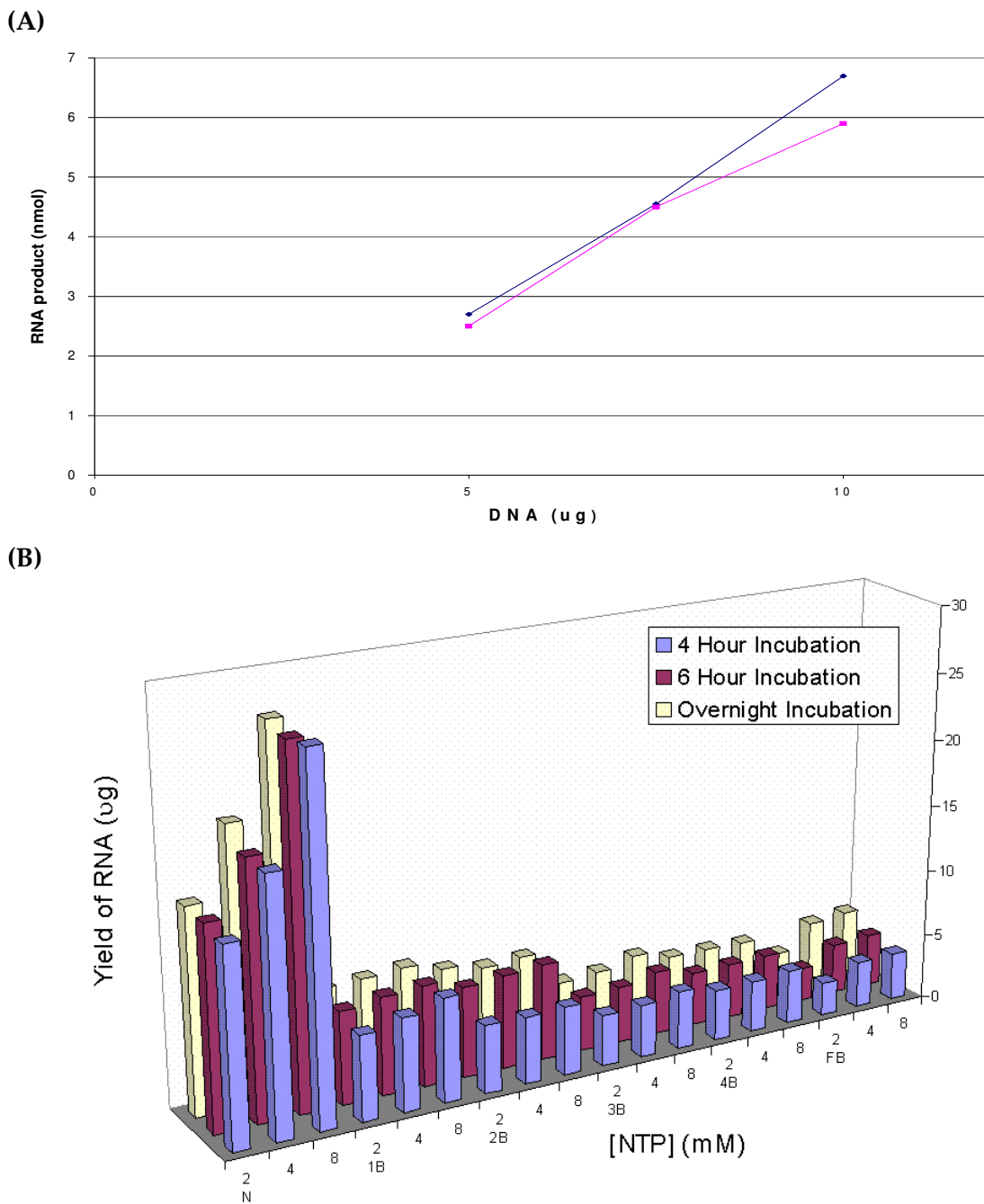


Figure 3-15. Yield comparisons of 21mer normal and boranophosphate modified RNA
(A) Yield of RNA with different amounts of DNA template in the transcription reaction. Blue = normal RNA and pink = GTP α B modified RNA. **(B)** Yield of RNA at different NTP concentrations and with different incubation times, as determined by UV.

there was a direct relationship between the amount in μg of DNA (between $5\mu\text{g}$ and $10\mu\text{g}$) and the amount in nanomoles of RNA produced. (Figure 3-15 A) For all further experiments, $10\mu\text{g}$ of DNA template was used to maximize yield.

Changing both the NTP concentration and the time of incubation can increase the yield up to a point. (Figure 3-15 B) However, due to the time and expense of preparing modified NTPs, the yield should be maximized in terms of NTP α B input. The "mole per mole" yield is the amount of RNA transcript that is produced divided by the amount of NTPs that were present in the reaction mixture, allowing the determination of the yield in terms of efficiency. Previously, work that was done to maximize the yield of long (>200 nt) RNA transcripts showed that for wt T7 RNA pol, RNA production increased linearly up to a concentration of 4 mM . However, the protocol that accompanied the RiboMax kit recommended a final NTP concentration of 7.5 mM . Therefore, final NTP concentrations of 2 mM , 4 mM , and 8 mM were test for each of the modified sequences. For the unmodified RNA transcript (normal), the % max was highest after four hours of incubation when using the 8 mM NTP. For the α -P-borano or $2'\text{F}$ NTP modified sequences, different conditions maximized the yield of the RNA transcript. The transcription reactions containing only boranophosphate modified NTPs had a % max that was highest when 2 mM of each NTP was used. Also, the maximum yield was attained when the reaction was incubated for 6 hours. The transcription reactions that contained both NTP α Bs and $2'\text{F}$ NTPs had a % max that was

highest when 4 mM of each NTP was used and the maximum yield was attained when the reaction was incubated overnight.

A plot of incubation time versus RNA yield shows a hyperbolic curve, with the yield increasing linearly until it reaches a maximum synthesis yield. This trend can be seen in Figure 3-15b. It was previously shown for normal RNA that the greater the NTP, template, or polymerase concentration, the earlier the maximum synthesis yield is reached. (Gurevich, et al. 1991) Therefore, the increase in yield of unmodified siRNA with increasing NTP concentration is in accordance with previous data. However, the modified siRNA does not show the same trend, and the mole per mole yield decreased sharply with increasing NTP concentration. This might be ascribed to the difference in kinetic parameters for T7 RNA pol in the presence of NTP α B. It has been shown that incorporation efficiency of NTP α Bs is approximately 2-fold higher than those of the corresponding NTPs (Wan and Shaw 2005; Wan 2005), Therefore, the maximum synthesis yield can be reached using a lower concentration of NTPs. The increased incubation time from 4 hours to 6 hours increases the yield without impacting the efficiency of the reaction. The incorporation efficiency of wt T7 RNA pol for the 2'F NTPs is lower than the both the corresponding NTPs and NTP α Bs. Therefore, an increase in both NTP concentration and incubation time is required to get the maximum percent yield while maintaining the mole per mole efficiency of the reaction.

3.5 Purification of Enzymatically Synthesized Normal and Chemically Modified Oligonucleotides

3.5.1 Experimental Procedures

There were several techniques utilized for purification of modified oligonucleotides. First, DNase was added to the transcription reaction to hydrolyze the DNA template. Second, phenol extraction was performed to remove the RNA polymerase and DNase enzymes. An equal volume of phenol:chloroform:isoamyl alcohol (25:24:1) was added to the reaction mixture and vortexed at high speed for 1 minute. The sample was subjected to high-speed centrifugation to separate the layers and the aqueous layer (top) was removed to a fresh tube. Third, to remove the phenol, the transcription mixture was extracted with chloroform two times. Phenol absorbs in the same UV range as oligonucleotides; therefore it is very important for accurate concentration calculations to ensure that RNA samples are not contaminated with phenol. The $A_{260}:A_{280}$ ratio can be used as one indication of the purity of the RNA. A ratio of 2.0 generally indicates pure RNA free of DNA and protein contamination (Davidson 1976). Another indication of purity is the $A_{260}:A_{230}$ ratio; again, a ratio close to 2.0 indicates pure RNA that is free of contamination by proteins, chaotropic salts, and phenol (Davidson 1976). An equal volume of chloroform was added to the transcription reaction and vortexed for one minute, followed by high-speed centrifugation.

Finally, the aqueous layer was removed and applied to a G-25 Illustra Microspin column. The liquid that was collected at the end of filtration was applied to an YM-3

filtration unit at 14,000 rpm for 15 minutes. The filtrate was discarded and the desired fraction was collected by flipping the filtering unit upside down into a fresh tube and further centrifuging at 6000 rpm for two minutes. Five μ L of the final solution was mixed with an equal volume of gel loading solution and the RNA was separated by size and quantified on a 20% PAGE/7 M urea gel run at 30 W for 2 hours. Gels were run at room temperature. The GeneRuler DNA Ladder, Ultra Low Range size markers (Fermentas) were used as standards to determine band sizes.

An attempt was also made to use reverse phase HPLC for the purification of the oligonucleotide sequences. Method development was done using chemically synthesized DNA dT polynucleotides from 5 nt to 30 nt long because they were easy to obtain and were of exact length, unlike transcribed RNA which may contain additional bases on the 3' end. The DNA was synthesized using the ABI DNA Synthesizer in the lab of Dr. Rudy Juliano at UNC-CH. DMT-protected deoxyribonucleotide phosphoramidites were purchased from Glen Research and amidite coupling calculations were used to determine the amount of phosphoramidite to dissolve in acetonitrile. After synthesis, the standards were deprotected using Sep-Paks and were stored at -20°C. Literature suggested HPLC separation gradients using acetonitrile and 0.1 M TEAA for separation of DNA and RNA. The starting and ending percentage of acetonitrile was varied to ensure maximum possible separation.

3.5.2 Results and Discussion

Previous work with RNA oligonucleotides in the Shaw lab has been done with PAGE gel-purified oligonucleotides. This has been to ensure that there are no unincorporated nucleotides or short abortive products left in the transcription reaction mixture. However, there are several disadvantages to gel purification, namely significant decrease in yield (Fasman 1975). Especially in the case of the boranophosphate modified RNA, it has been proposed that gel purification reduces the yield due to degradation of the BP-RNA at the high temperatures that reached during PAGE electrophoresis (60-70°C) (Wan 2005). Further, gel purification is time-consuming, and includes many steps, the pre-electrophoresis, sample electrophoresis, band excision from the gel, and overnight elution from the gel slice into buffer, purification to remove all acrylamide out of the final product, concentration, and then quantification. In this section, a different method of purification was pursued that would 1) remove phenol contamination, 2) remove unincorporated nucleotides, and 3) remove aborted products.

At first, HPLC purification of the short oligonucleotides was attempted using the Varian Prostar HPLC with photo diode array (PDA) detector. Polythymidine standards with lengths of 5, 10, 15, 20, and 30 nucleotides were chemically synthesized by the Shaw lab using the ABI synthesizer and deprotected using C-18 Sep-Paks. These standards were separated on a Waters reverse phase C-18 column using numerous

acetonitrile gradients in an effort to create a linear relationship between oligonucleotide length and retention time (Rt). This has been done previously to good effect using the “DMT-on” method, where chemically synthesized oligonucleotides are separated before deprotection to make use of the hydrophobic DMT group for efficient separation of species of different lengths (Gilar, et al. 2002). However, enzymatically synthesized RNA does not have DMT groups, so it was necessary to attempt to separate the dT standards after deprotection. Despite the application of many separation conditions, efficient separation of the standards could not be achieved using the Delta-Pak C-18 reverse phase column. A graph of the retention times from the best set of separating conditions is shown in Figure 3-16.

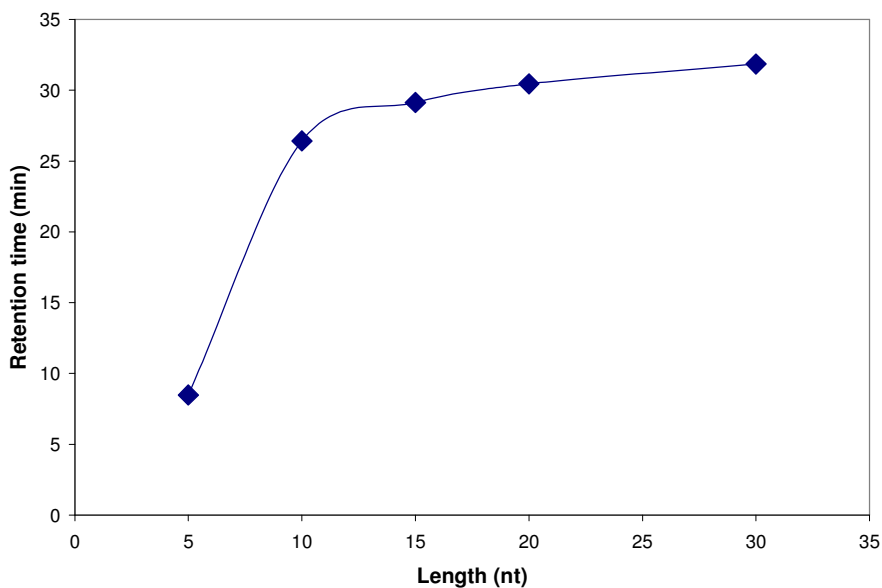


Figure 3-16. Retention times of dT standards (5, 10, 15, 20, 30 nt) on reverse phase HPLC column. The aqueous solvent was 0.1 M TEAA and the organic solvent was acetonitrile. The gradient ran from 10% ACN to 18% ACN over 65 minutes with a flow rate of 1.0 ml/min.

Clearly, while this set of conditions can separate a 5mer from a 15mer or 30mer, the difference in retention time between a 20mer and a 25mer would be impossible to differentiate. Although the standards could not be separated from each other using the above HPLC system, it may be possible in the future to utilize specialized columns, such as the Xterra© Oligonucleotide column (Waters) for separating oligonucleotides in order to achieve HPLC purification.

After the attempt with HPLC to purify DNA based on size, another purification method was investigated that combined phenol extraction, microcolumn purification, and microfiltration. The first step of the purification involved a phenol extraction. This step was necessary to remove the transcription enzymes from the reaction mixture. However, phenol absorbs in the same range as do oligonucleotides, so phenol contamination should be avoided if accurate concentration calculations based on the UV absorbances are to be done (Roig, et al. 2003). Therefore, to completely remove the phenol contamination, it was determined that the reaction solution must be extracted twice with chloroform, as recommended in the Short Protocols In molecular Biology. Chloroform extraction was followed by purification using a G-25 Illustra Microspin column (GE Life Sciences). This column has the ability to perform buffer exchange. Analysis of this method showed that greater than 98% of the phenol is removed from the final product. To remove both the unincorporated nucleotides and the abortive transcripts, a YM-3 filtration membrane was used. This membrane has a nominal

molecular weight cutoff at 3000 daltons. Since abortive transcripts occur at the 2-8 positions, they have molecular weights that are below 3000 daltons and should pass through the membrane during centrifugation. A comparison of unpurified radiolabeled RNA and purified radiolabeled RNA on 20% PAGE/ 7 M urea is shown in Figure 3-17. The RNA was detected by overnight exposure to a low energy phosphor screen and was imaged using the Typhoon, as described in Chapter 2. The size was determined in comparison to GeneRuler DNA Ladder Ultra Low Range size markers. To ensure that the running temperature of the PAGE electrophoresis did not result in degradation of the RNA sample, it may be helpful to perform electrophoresis at 4°C by placing the gel rig in the cold room. However, this may increase the run time. HPLC purification remains the most desirable method of purification and it is recommended that different columns are tried in order to optimize the purification.

Together the above procedures ensured that more than 98% of the phenol was removed from the sample to allow for accurate concentration determination. Also, this method successfully removed the majority of the aborted transcripts from the reaction mixture without considerable decreases in the yield. Abortive products occur because the T7 RNA polymerase, during the initiation phase, can fall off the DNA template, resulting in short (2-8 nt) abortive RNA transcripts. In order to properly characterize the secondary structure, short products must be removed from the reaction mixture to ensure that the structure is a fully formed helix.

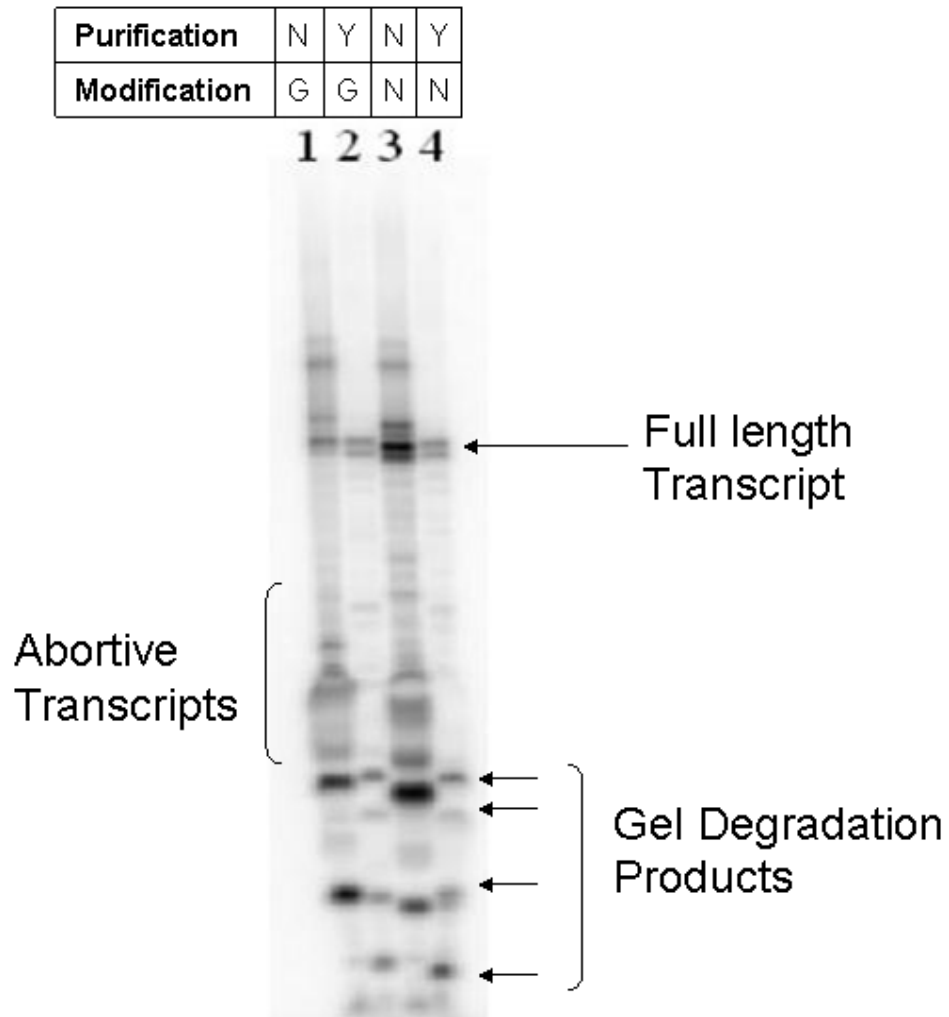
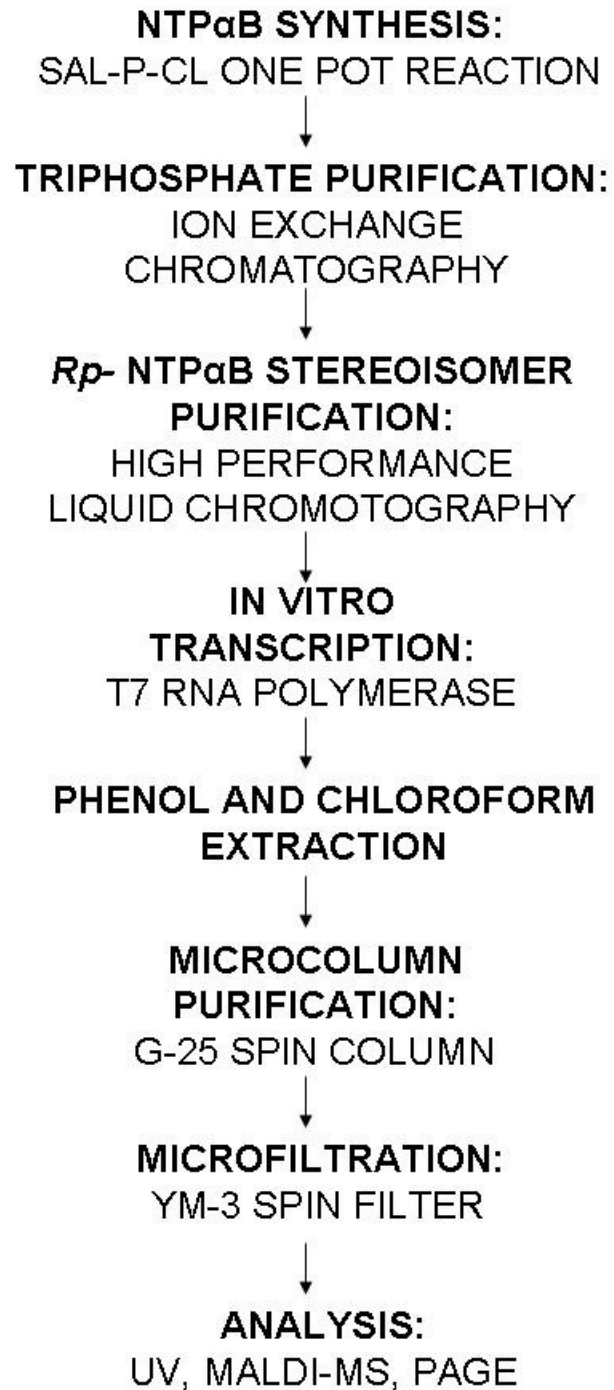


Figure 3-17. 20% PAGE/7M Urea Analysis of enzymatically transcribed, radiolabeled unpurified and purified 21mer HPV 16+24 AS RNA. Lane 1 contains BP-RNA modified with GTP α B prior to purification. Lane 2 contains the same sample after purification. Lane 3 contains unmodified RNA prior to purification. Lane 4 contains the same sample after purification. The bands towards the bottom of the gel in the purified sample lanes can be considered degradation products due to PAGE analysis.

3.5 Chapter Summary

The work that has been presented in Chapter 3 represents studies on the synthesis of modified ribonucleotides and their use in enzymatic synthesis of modified oligonucleotides. The flow chart on the following page outlines the experiments that were performed in this chapter. The NTP α B (N=A,C,G,U) and 2'F nucleotide triphosphates were synthesized using a Sal-p-Cl approach. The conditions required for preparative scale HPLC purification of the *Rp* and *Sp* isomers of boranophosphate NTPs were described for each nucleotide. The enzymatic synthesis of 21mer siRNA containing normal, boranophosphate, 2'fluoro, and fluoro/borano nucleotides was described using wild type T7 RNA polymerase. The optimization of the conditions for maximum yield and efficiency of siRNA transcription reactions incorporating different amounts of modified NTPs were determined and were used for the syntheses of the modified siRNA used in later chapters. The purification of these siRNAs was discussed using HPLC and microcolumn/filtration purification. The use of the siRNAs produced in this chapter is presented in the next several chapters in order to elucidate the effect of the modifications on the hybridization affinity, nuclease stability, and lipophilicity of modified siRNA.

BORANOPHOSPHATE siRNA SYNTHETIC SCHEME



4. Investigations of modified siRNA duplex in regards to secondary structure

4.1 Background Overview

It has been well established that the structure of nucleic acids plays a significant role in efficacy of RNA therapeutics (Reynolds, et al. 2004; Rana 2007). The RNA induced silencing complex (RISC), is a programmable endonuclease that is loaded with the antisense strand of the siRNA. Therefore, secondary structure may play a role in proper loading of RISC (Preall and Sontheimer 2005). It was previously shown that the secondary structure is a major determinant in the success of gene silencing using siRNA. This is partly based on the sequence of the siRNA, especially the G-C content, where it has been shown that lower G-C content of the siRNA guide strand correlates with better silencing (Elbashir, et al. 2001; Harborth, et al. 2003; Haley and Zamore 2004). Also, the mRNA target sequence often has secondary structure that can hinder the effect of RNAi. In fact, it has been shown that there is a linear correlation between siRNA efficacy and the local free energy of the target region (Schramm and Ramsey 2005). Therefore, in this work, siRNA sequences were chosen whose complementary target mRNA had been shown in the literature to be amenable to RNAi silencing.

Two features of modified siRNA were studied in this chapter: melting temperature and circular dichroism. The melting temperature (T_m) of a double stranded nucleic acid can be used to characterize the affinity and specificity the siRNA

has for its complementary target. Upon target recognition and binding, the siRNA/mRNA duplex is presumed to form a helix. The most important factors in the formation of a helix are the affinity and specificity that an siRNA has for its complement. Therefore, determination of the T_m of modified duplexes is a good way to determine the effect of the modification upon secondary structure.

It has been shown that for the RISC mechanism to function properly, the siRNA guide strand must form an A-form helix with the target mRNA (Chiu and Rana 2002; Chiu and Rana 2003; Heale, et al. 2005). Therefore, the type of helix that formed between modified siRNAs and their complements were studied in this chapter in order to determine the effect of the modification on the type of helix that formed. Circular dichroism (CD) can be used to gauge the type of helix formed.

Overall, the work presented in this chapter gives a comprehensive and systemic analysis of the effects of the boranophosphate modification and the combined boranophosphate/2'fluoro modifications on the secondary structure and duplex stability of siRNA.

4.2 Thermal stability of modified RNA duplexes

4.2.1. Introduction

Two types of base-base interactions occur in the double helix: hydrogen bonding of the bases that occurs within the plane of the bases (Figure 4-1 A), and base stacking that occurs perpendicular to the plane of the bases. (Figure 4-1 B)

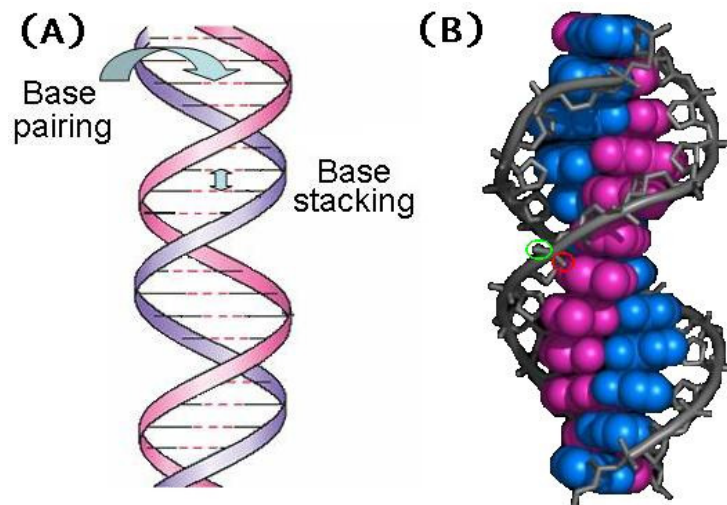


Figure 4-1. Base interactions in oligonucleotide duplexes. **(A)** Two types of base interactions stabilize the double helix. Base pairing occurs in the plane of the bases and base stacking occurs perpendicular to the plane of the bases. **(B)** Modifications on the α -phosphorous can occur in the R_p position (green circle) or S_p position (red circle). Figure adapted from ref. (ScienceDaily 2005)

Helices are stabilized by base stacking; therefore measurement of the melting temperature (T_m) gives insight to the stability of the duplex (Saenger 1984). Base stacking that occurs when single strands form the duplex results in decreases in the UV absorption at 260 nm; consequently monitoring the UV spectrum is one way to measure the secondary structure of oligonucleotides. Increasing the temperature of a solution of

oligonucleotides will cause a subsequent increase in the UV absorption as the duplex is denatured into separate single strands; this effect is known as hyperchromicity. (Figure 4-2) The melting temperature is defined as the midpoint of the dissociation of the helix (Saenger 1984; Mathews, et al. 2000).

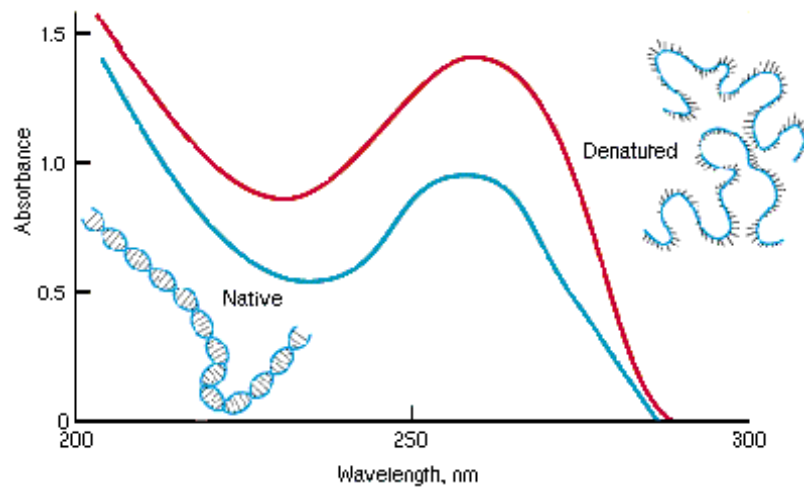


Figure 4-2. Hyperchromicity. Denatured, single stranded oligonucleotides have an increased UV absorbance as opposed to native, double stranded oligonucleotides. Native DNA becomes denatured as temperature is increased, and renatured as the oligonucleotide is slowly cooled. Figure adapted from reference. (Mathews 2000)

The trend of stability of oligonucleotides duplexes has shown that RNA:RNA duplexes are the most stable, then RNA:DNA duplexes, followed by DNA:DNA duplexes (Ponnuswamy and Gromhia 1994). Also, chain length and GC/AT ratio can affect the duplex stability. An increase in either of these variables will increase the T_m . (Saenger 1984) It has been shown that chemical modification can affect the thermal stability of the RNA:RNA duplex that is formed between the siRNA and its complement (Manoharan 1999). This can be attributed to the secondary structure. Substituents on

the phosphorus can point toward the center of the duplex (*Rp* boranophosphate linkages) or can point away from the center of the duplex (*Sp* boranophosphate linkages), depending on the stereochemistry of the linkage. (Figure 4-1 B) Enzymatically transcribed boranophosphate RNA is stereoregular, consisting of *Sp* boranophosphate linkages (formed from *Rp* NTP α B stereoisomers).

Previous work from the Shaw lab has shown that when a single boranophosphate linkage was introduced into a DNA:DNA duplex, there was very little destabilization of the duplex. (Li, et al. 1996; Wang 2004) It was also shown that partially modifying the antisense strand of an RNA:RNA duplex increased the melting temperature of the duplex. (Wan 2005) In this section, the effect of partially and fully modifying the RNA of the antisense strand or both strands of an RNA duplex will be investigated, as well as the effect on duplex thermal stability when the boranophosphate modification is mixed with the 2'F modification.

4.2.2. Experimental Procedures

The siRNAs that were used in this chapter were prepared enzymatically. The sequence used was the HPV 16+24 AS RNA sequence (Table 2-2). Double stranded DNA templates containing a T7 promoter for transcription of both the sense and antisense RNAs were purchased commercially and used as the template for the transcription reactions. During the transcription reactions, different modified NTPs were substituted for the unmodified analog to create boranophosphate RNA that was

modified as shown in Table 4-1. The reactions were carried out under the conditions determined in Chapter 3 in order to maximize the yield and the concentrations were determined by UV absorbance at 260 nm.. The single stranded RNA transcripts were purified by phenol extraction, microcolumn purification, and YM-3 filtration, as described in Chapter 3. All RNAs were run on 20% polyacrylamide denaturing gel to ensure that products were full-length.

For thermal melting experiments, 400 picomoles each of sense (S) and antisense (AS) RNA were mixed with 10X thermal stability buffer (1 M potassium phosphate) to result in a final concentration of 2.2 μM in 0.1 M potassium phosphate. 180 μL of this solution was placed in a Varian 80 μL quartz cuvette and capped to prevent evaporation of the sample during heating. Another cuvette was filled with 180 μL of 1X thermal stability buffer to act as a background. The cells were placed in the thermostable multicell holding block of the Varian Cary 500 spectrometer.

The Cary WinUV software was used to develop the thermal stability method. The parameters of the method included an annealing cycle followed by three rounds of denaturation/renaturation. For the annealing cycle, the cells were heated from 20°C to 98°C at a speed of 30°C per minute. The block stayed at 98°C for 30 seconds and was then cooled back to 20°C at a speed of 3°C per minutes. During the annealing cycle, no data was collected. Data was collected during the denaturation and renaturation cycles.

Table 4-1. Modified RNA sequences used for the melting temperature and circular dichroism experiments. All sequences are based on the 16+24 sequences (Table 2-2). Borano modifications are shown in blue and 2'-fluoro modifications are shown in red. S denotes the sense strand and AS denotes the antisense stand.

Name	Mod	# Mod (%)	Sequence (5'→3')
N S	None	0 (0)	CCA GAG ACA ACU GAU CUC UUU
N AS	None	0 (0)	AGA GAU CAG UUG UCU CUG GUU
1B S	GTP α B	3 (14)	CCA GAG ACA ACU GAU CUC UUU
1B AS	GTP α B	6 (24)	AGA GAU CAG UUG UCU CUG GUU
2B S	CTP α B, GTP α B	9 (43)	CCA GAG ACA ACU GAU CUC UUU
2B AS	CTP α B, GTP α B	9 (43)	AGA GAU CAG UUG UCU CUG GUU
3B S	CTP α B, GTP α B, UTP α B	16 (76)	CCA GAG ACA ACU GAU CUC UUU
3B AS	CTP α B, GTP α B, UTP α B	17 (81)	AGA GAU CAG UUG UCU CUG GUU
4B S	ATP α B, CTP α B, GTP α B, UTP α B	21 (100)	CCA GAG ACA ACU GAU CUC UUU
4B AS	ATP α B, CTP α B, GTP α B, UTP α B	21 (100)	AGA GAU CAG UUG UCU CUG GUU
F S	2'F CTP, 2'F UTP	12 (57)	CCA GAG ACA ACU GAU CUC UUU
F AS	2'F CTP, 2'F UTP	11 (52)	AGA GAU CAG UUG UCU CUG GUU
FB S	2'F CTP, GTP α B, 2'F UTP	15 (71)	CCA GAG ACA ACU GAU CUC UUU
FB AS	2'F CTP, GTP α B, 2'F UTP	18 (86)	AGA GAU CAG UUG UCU CUG GUU

The denaturation cycle began at 20°C and ended at 98°C, at a speed of 0.4°C/min. The renaturation cycle returned the temperature to 20°C at a rate of 0.4°C per minute.

The melting curves were analyzed using the WinUV Thermal Software and the T_m was calculated for each duplex, using the derivative method or the hyperchromicity method. To determine the T_m of the sample by the derivative method, the first derivative of the data was taken and the maximum of the derivative curve was assigned as the T_m value. To determine the T_m of the sample by the hypochromicity method, the software scans the melting curve to determine the temperature at which 50% of the duplex has dissociated. This was done by defining the lower limit, where the strands were associated and upper limit, where the strands were dissociated, on the thermal melting curve and determining the midpoint. (Figure 4-3)

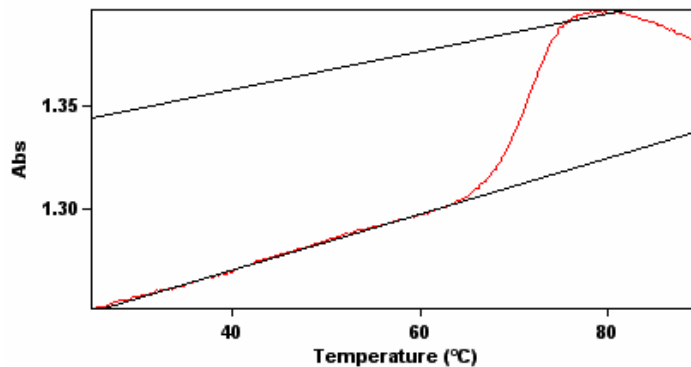


Figure 4-3. Lower and upper limits for hyperchromicity calculations of T_m . The lower limit is the duplex in its associated state and the upper limit is duplex in its associated state. Once these limits are defined by the user, the software can determine the point where 50% of the duplex is dissociated (T_m).

The hyperchromicity method allows the determination of molecular energetic results such as ΔH , ΔG and ΔS using the van't Hoff equation. First, the equilibrium constant K for the non-self complementary single strand \leftrightarrow duplex transition is determined using Equation 4-1 (Saenger 1984).

$$K = \frac{2(1-\alpha)}{C_t\alpha^2} \quad \text{Eqn 4-1}$$

α is the mole fraction of single strands, as determined by the number of strands in single form divided by the number of total strands. C_t refers to the total concentration of strands (in this case 2.2 μM). The van't Hoff equation can be used to determine ΔH and ΔS from the equilibrium constant (Equation 4-2).

$$\ln K = -\frac{\Delta H^\circ}{RT} + \frac{\Delta S^\circ}{R} \quad \text{Eqn 4-2}$$

The Gibbs free energy of the transition can then be determined using Equation 4-3. The Gibbs free energy is directly related to the binding affinity.

$$\Delta G^\circ = \Delta H^\circ - T\Delta S^\circ \quad \text{Eqn 4-3}$$

4.2.3 Results

In order for gene silencing to occur through the RNAi pathway, the siRNA guide strand must recognize and bind its target molecule in a sequence-specific manner.

Therefore, the thermal stability of the duplex, and the information that it conveys about the structure of the duplex, must be studied for each sequence and modification. The

RNA duplex that is formed by the annealing of the sense and antisense 16+24 RNA strands contains a 19 bp double stranded region flanked on each side by 2 nt 3' overhangs. (Figure 4-3) This sequence was chosen because it has been shown to downregulate human papillomavirus, as discussed in Chapter 7. Both strands were enzymatically synthesized, which means there may have been one or two additional nucleotides on the 3' end. The sense and antisense strand for each duplex studied were modified according to Table 4-1. Each modified antisense sequence was tested in duplexes with either an enzymatically transcribed unmodified sense sequence or a sense sequence containing the same modification(s). Previous work has only focused on duplexes with an unmodified, chemically synthesized sense strand (Wan 2005).



Figure 4-4. HPV 16+24 RNA:RNA duplex. The sense strand is shown above the antisense strand. Both strands were enzymatically synthesized and modified as described in Table 4-1.

Normalized melting curves were obtained for the each duplex, as shown in Figure 4-4. There were two types of RNA:RNA duplexes studied; the first type of RNA:RNA duplex consisted of an unmodified sense strand and a modified antisense strand (hetero duplex). The second type of RNA:RNA duplex consisted of modified sense and antisense strands (homo duplex). Due to the hyperchromic effect, as temperature increases, the absorbance of the RNA should also increase (Saenger 1984). The heteroduplexes all exhibited an increase in absorbance as the temperature increased,

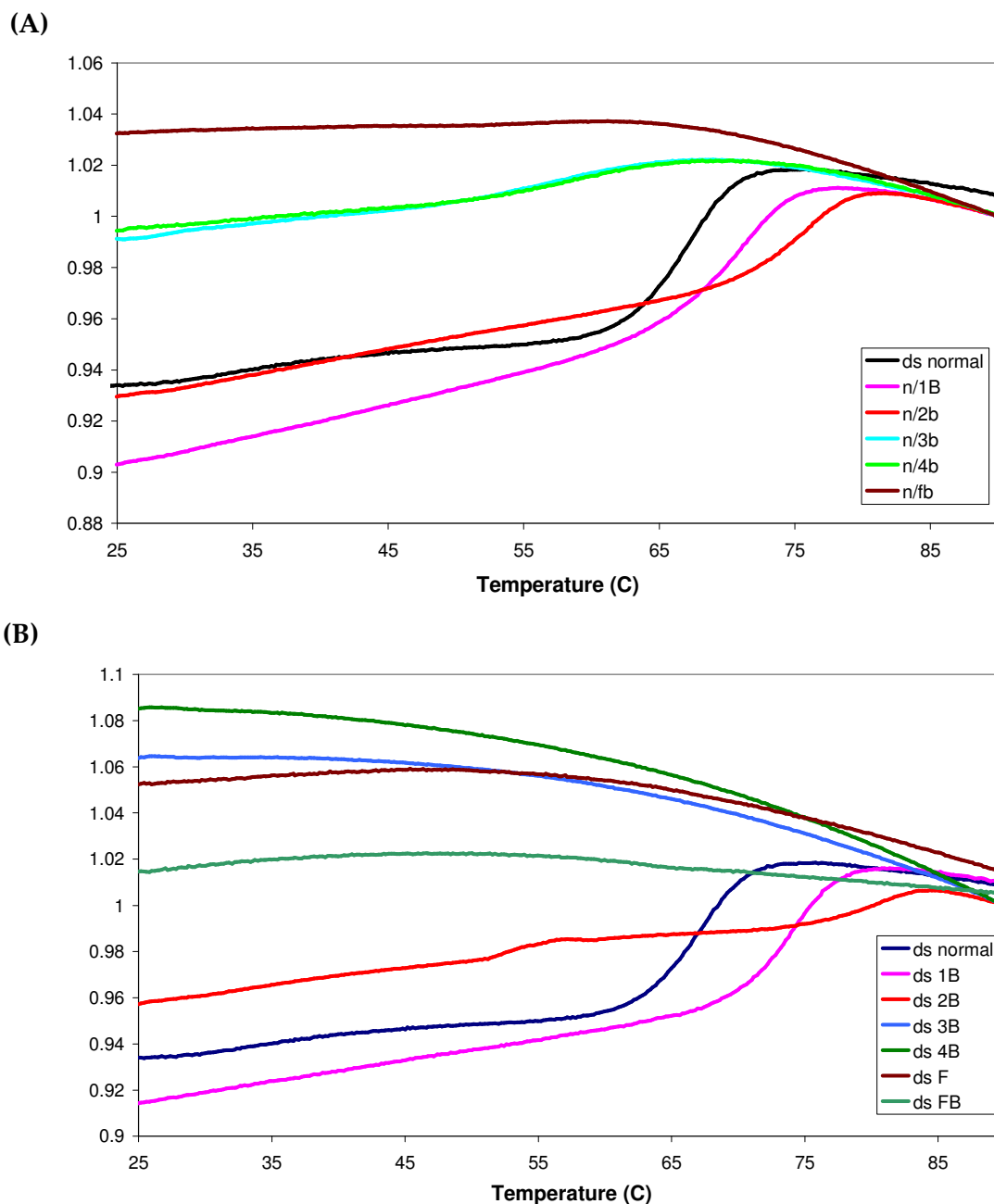


Figure 4-5. Representative melting curves of modified duplexes at a final concentration of $2 \mu\text{M}$ in 0.1 M potassium phosphate, pH 7.4. The absorbance was normalized to 1 at 90°C . **(A)** Hetero duplexes consisting of a normal S strand and a modified AS strand **(B)** Homo duplexes with both S and AS strands modified. The modified strands can be found in Table 4.1

although the more modifications the antisense strand contained, the less dramatic the increase. (Figure 4-5 A) The homoduplexes of siRNA modified with one or two NTP α Bs both exhibited the expected increase in absorbance as the temperature increased. However, the homoduplexes of siRNA modified with three or four NTP α Bs showed an overall decrease in absorbance (hypochromicity) as the temperature increased, suggesting that a duplex was not formed during the annealing step. Analyses of the melting curves were performed as described in the experimental procedures. The melting temperatures and thermodynamic parameters are given in Table 4-2.

Table 4-2. T_m values for the homo- and hetero- duplexes. The T_m 1 value was calculated using the derivative method and the T_m 2 value was calculated using the hyperchromicity method. The thermodynamic parameters were calculated using the van't Hoff equation. Values that were unavailable are marked N/A. All values are the averages of at least three experiments.

	Duplex	T _m (°C) 1	T _m (°C) 2	ΔG _{20°} (kcal/mol)	ΔH (kcal/mol)	ΔS (cal/mole·K)
Homoduplex	Normal	67.72 ± 0.6	66.56	-150.97	-206.9	-582.3
	1B	73.80 ± 0.4	73.55	-163.62	-203.5	-560.9
	2B	80.35 ± 0.2	80.69	-277.57	-341.4	-938.4
	3B	30.75 ± 0.2	N/A	N/A	N/A	N/A
	4B	31.55 ± 0.4	N/A	N/A	N/A	N/A
	F	34.02 ± 0.3	53.81	-135.19	-344.5	-1065
	FB	32.40 ± 0.3	29.51	-49.31	-144.0	-451.1
Heteroduplex	Normal	67.72 ± 0.6	66.56	-150.97	-206.9	-582.3
	NS - 1B AS	71.42 ± 0.6	71.13	-175.59	-230.6	-643.5
	NS – 2BAS	75.54 ± 0.2	75.58	-234.24	-277.3	-767.2
	NS – 3B AS	58.41 ± 0.3	54.78	-62.23	-60.82	-159.5
	NS – 4B AS	59.14 ± 0.5	57.64	-96.52	-134.4	-379.7
	NS –FB AS	49.62 ± 0.5	48.18	-60.62	-76.92	-231.0

Clearly, the modification of one or both strands of the RNA duplex had a dramatic impact on the stability of the duplex, as monitored by the melting temperature. Sample 1B, containing 6 GTPαB modifications on only the antisense strand of the duplex had an increased the melting temperature versus the normal by 3.7 °C (Table 4-4), according to the derivative method. Modification of both strands of the duplex with

GTP α B (3 modifications on the sense strand, 5 modifications on the sense strand) resulted in an increase of 6.7°C (Table 4-3). However, as previewed in the thermal melting curves, increased modification of both strands resulted in an increasingly unstable duplex. Based on the T_m data, the fully borano modified antisense strand appeared not to form a duplex with its fully modified sense strand, and formed a duplex with a relatively low T_m with its unmodified sense strand. The dependence of the T_m on the number of modifications is shown in Tables 4-3 (homoduplex) and 4-4 (heteroduplex).

Table 4-3. Comparison of effect of modification on T_m for homoduplexes. T_m values were calculated using the derivative method. The sequences are given in Table 4-1.

Homoduplex	T _m (°C)	Δ T _m (°C)	# Mod	Δ T _m /mod
Normal	67.72 \pm 0.6	---	0	----
1B (GTP α B)	73.80 \pm 0.4	6.08	8	0.76
2B (CTP α B, GTP α B)	80.35 \pm 0.2	12.63	18	0.70
3B (CTP α , GTP α B, UTP α B)	30.75 \pm 0.2	-36.97	17	-1.12
4B (all NTP α B)	31.55 \pm 0.4	-36.17	42	-0.86
F (2'F CTP, 2'F UTP)	34.02 \pm 0.3	-33.70	23	-1.46
FB (2'F CTP, GTP α B, 2'F UTP)	32.40 \pm 0.3	-35.32	33	-1.07

Table 4-4. Comparison of effect of modification on T_m for heteroduplexes. T_m values were calculated using the derivative method

Heteroduplex	T_m (°C)	ΔT_m (°C)	# Mod	$\Delta T_m/\text{mod}$
Normal	67.72 ± 0.6	---	0	---
1B (GTP α B)	71.42 ± 0.6	3.70	5	0.74
2B (CTP α B, GTP α B)	75.54 ± 0.2	7.80	9	0.87
3B (CTP α , GTP α B, UTP α B)	58.41 ± 0.3	-9.31	17	-0.54
4B (all NTP α B)	59.14 ± 0.5	-8.58	21	-0.41
FB (2'F CTP, GTP α B, 2'F UTP)	49.62 ± 0.5	-18.10	18	-1.00

4.2.4 Discussion

The work contained in this section represents the first characterization of the duplex stability of RNA with increasing amounts of boranophosphate modifications and the first characterization of the duplex stability of fluoro/borano RNA. Previous work had shown that modification of a sequence using UTP α B, CTP α B, and ATP α B + CTP α B increased the melting temperature of heteroduplexes. (Wan 2005) This is consistent with the results found in this section; introducing one or two boranophosphate modifications into the antisense strand of a heteroduplex does increase the melting temperature. Also, it appears that this is not a sequence specific effect, as it has now been seen in all three sequences that have been tested (Wan 2005). However, it appears that further modification of the antisense strand destroys the ability of the RNA to form a classic duplex, especially with a highly modified sense strand as judged by the melting

data. It is the antisense strand that is incorporated into the RISC complex. There are several potential explanations for this finding.

It has been hypothesized that the increase in T_m boranophosphate RNA could be due to the fact that is enzymatically transcribed, and therefore subject to the addition of an extra nucleotide to its 3' end. A dangling 3' end has been shown to increase the T_m of duplexes via base stacking effects; therefore enzymatically transcribed RNA may show an increase in T_m . (Frier, et al. 1983) In this work, the normal duplexes were synthesized enzymatically as a control. If the increase in T_m were due to the dangling 3' end, the effect would also be seen in the normal duplex and there would be no difference in the thermal stability of the normal and boranophosphate modified duplexes.

A second explanation of the increase in T_m is that the boranophosphate modification allows for decreased backbone repulsion between the two strands of the duplex, because of the change in the polarity of the P-BH₃ bond versus the P-O bond. (Summers, et al. 1998) Because the boranophosphate group carries less negative charge than the native phosphate, it was hypothesized that hybridization affinity between the two strands would be increased. Increased hybridization affinity would increase the amount of hyperchromicity. However, it would be expected that if this were the reason for the increase in thermal stability, it would increase the T_m of the fully BP modified duplex to an even greater extent. Since this was not the case, this explanation must be

regarded as not the primary reason for the increase in T_m , although it could still be a factor in the higher stability of the partially modified duplexes.

A third explanation involves the water molecules that are located in the major groove of the A-form RNA. It is thought that the greater thermal stability of RNA duplexes compared to DNA duplexes is due to the fact that the 2' hydroxyl group acts in two ways: 1) it stabilizes the RNA duplex by rigidifying the A-type conformation, and 2) it links backbone and base hydration across the strands (Rozners and Moulder 2004). Since the boranophosphate modification is stereoregular in the *Sp* conformation, the BH_3 moiety points into the major groove, where the difference in its electronegativity compared to the native phosphate could negatively impact its ability to form hydrogen bonds with the water molecules. Although this is enthalpically disfavored, it is entropically favorable. Therefore, the situation could be one where the entropic considerations outweigh the enthalpic considerations up to a certain point of modification; past that point, the positioning of the borane group in the major groove is too enthalpically disruptive to allow stable duplex formation. This means that the decrease in thermal stability would be dependent on the stereochemistry around the chiral phosphorous. This explanation is supported by results reported in the literature that show that stereochemistry of the boranophosphate backbone linkages plays an important role in the ability of the modified oligonucleotide to bind its complement specifically for phosphorothioates, methylphosphonates, and boranophosphate

DNA:RNA duplexes. (Yu 2000; Thivyanathan 2002; Wang 2004) Notably, in the case of methylphosphonates, which have comparable stereochemistry to the boranophosphates but lack a negative charge, the *Sp* linkage on the antisense strand depressed the melting temperatures of the duplex compared to the melting temperature of a duplex containing the same modification oriented in an *Rp* stereochemistry.

To gain a clearer understanding of the thermodynamic factors that influence the duplex stability of boranophosphate modified RNA, the Gibbs free energy (ΔG), enthalpy (ΔH) and entropy (ΔS) were derived using the van't Hoff equation (Eqn 4-2). (Table 4-2) This method assumes a two-state equilibrium, where the duplex is either completely folded or completely denatured. (Mergny 2003) Overall, the Gibbs free energy values that were calculated agreed with the T_m values. The most stable homoduplex was the 2B modified > 1B modified > normal > F modified > FB modified. Compared to the normal duplex, the 1B-modified duplex shows a slightly less favorable ΔH (less negative) and a slightly more favorable ΔS value (less negative), which is in line with the theory that the boranophosphate decreases the enthalpy but makes up for it by increasing entropy by disrupting duplex hydration. However, the ΔH value for the 2B-modified duplex is much more negative (more favorable) than the normal and the value for ΔS is significantly less favorable (more negative) than the normal. Despite its increased stability of the 2B-modified duplex versus the normal, enthalpy-entropy compensation cannot be used as the explanation.

The stability of the heteroduplex was in the order of: 2B modified > 1B modified > normal > 4B modified > 3B modified > FB modified. The 1B and 2B modified heteroduplexes exhibited a more favorable (more negative) ΔH value and a less favorable (more negative) ΔS value. In contrast, the 3B and 4B modified heteroduplexes had less favorable (less negative) ΔH values and more favorable (less negative) ΔS values. Clearly, for this sequence, we must reject the enthalpy-entropy compensation as the sole explanation, but it may play a role, albeit minor, in the overall trend in stability. Again the FB modified duplex showed the least thermal stability.

The 2' fluoro modification has been shown to confer desirable properties to RNA and so it was combined with the boranophosphate modification. The decrease in stability with the 2'F NTP modification was not consistent with results in literature, where most reports show an increase in T_m when 2'F RNA is hybridized with normal RNA. (Manoharan 1999; Blidner 2007) However, there are some reports where it was shown that even one 2' fluoro substitution is reasonably well tolerated, but two 2' fluoro modifications can lower the T_m by over 4°C, due to the adoption of a DNA-like conformation by the 2' fluoro modification. (Williams, et al. 1991) The sequence used for the T_m experiments contained eleven 2' fluoro modifications on the antisense strand and twelve 2' fluoro modifications on the sense strand, which may explain the drastic difference in melting temperatures between the normal and F duplexes. It was hypothesized that the addition of the boranophosphate modification may be able to

increase the T_m of fluoro-modified RNA duplexes due to previous work that showed BP-RNA had an increased T_m compared to normal. This was not the case here, and the 2'F/borano modified RNA duplex (75% modified) exhibited the least duplex stability and the least favorable (least negative) ΔG value, as measured by thermal melting.

It is possible that the 2'F modified RNA is adopting a 2' endo conformation of the sugar, which would lead to a B-form helix and would account for the decrease in duplex stability (RNA:DNA hybrids are less stable than RNA:RNA hybrids). (Figure 4-6)

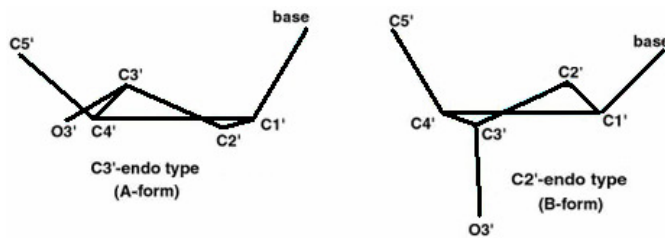


Figure 4-6. C2' endo and C3' endo sugar conformations of DNA and RNA.

Although the adoption of the B-form (C2' endo) conformation is unusual, it has been previously reported in the literature for fluoro modified RNA. (Williams, et al. 1991; Manoharan 1999; Blidner 2007) It is also possible that the boranophosphate modification, when applied to the molecule as a whole, is changing the conformation of the duplex in a maladaptive manner, resulting in a decrease in the ability of the modified siRNA to hybridize to its complementary sequence. It remained to determine the overall conformation of the modified duplexes. In the next section, the secondary structure of single and double stranded modified siRNA homo- and hetero duplexes were investigated using circular dichroism.

4.3 Circular Dichroism

4.3.1. Introduction

Changes in the three dimensional structure of RNA can be monitored using circular dichroism (CD), which studies the differential absorbance of circularly polarized light (Wold 1971). CD can be used to gauge the structure of a double helix because the form of the helix imparts a distinct CD spectra and it has been shown that there is no systematic change in this spectra with base composition (Graetzer and Royce 1971). For instance, it is known that RNA or DNA duplex in an A form helix has a shallow trough at approximately 210 nm and a large peak at approximately 262-264 nm and a B form helix has a trough at 220 nm and a peak at 270 nm with approximately the same magnitude. C form duplexes exhibit a collapsed intensity at the 275 maximum compared to the B form (Saenger 1984; Steely, et al. 1986; Johnson 2000). (Figure 4-3)

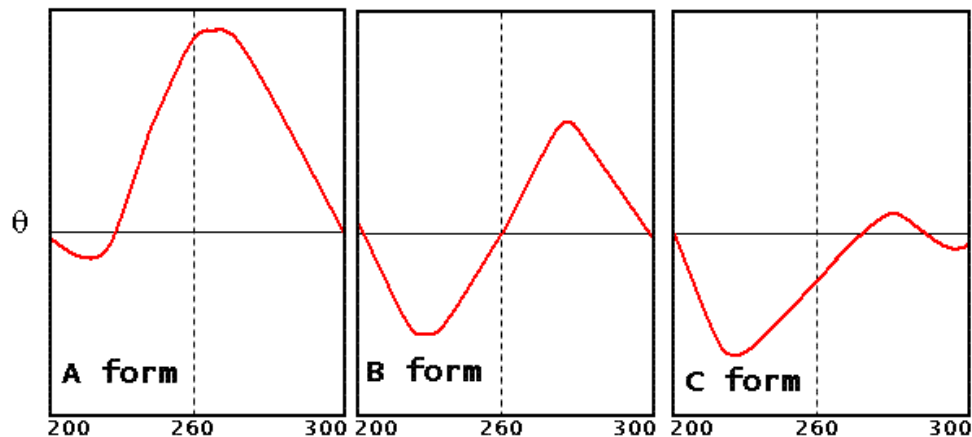


Figure 4-7. Representative CD spectra for three types of helical structures. A form helices are typical of RNA:RNA duplexes and B form helices are typical of DNA:DNA duplexes. Figure redrawn from reference (Saenger 1984).

Circular dichroism has been tremendously useful for studying the interactions between chemically modified oligonucleotides with their target sequences. CD is especially useful in the case of backbone-modified oligonucleotides where the chromophore (base) remain unchanged, because any change in the molar ellipticity (θ) can be attributed primarily to a conformational change in the oligonucleotide or complex, revealing valuable information about the secondary structure (Maurizot 2000).

4.3.2. Experimental Procedures

The RNAs used in the section were synthesized enzymatically. The sequences are shown in Table 4-1. The antisense sequences were used to determine the CD spectra of the single stranded oligonucleotides. The desired duplexes were annealed by dissolving equimolar amounts of the sense and antisense strand in 5X CD buffer (Sect 2.2.2) for a final concentration of 1.5 μ M. Then the solution was subjected to the annealing cycle as described in Sect 4.2.2. Six hundred microliters of this solution was transferred to a 0.8 mL quartz cuvette with a 1 cm path length. CD spectra were collected at 25°C on the Circular Dichroism Spectrometer. The Aviv 202 software was used to set the method parameters. Spectra were collected at 0.5 nm intervals with a 1 second average time from 200 nm to 350 nm. Background spectra were collected on the day of each run, using the same cuvette and averaged. Three scans were performed for each sample, averaged, and the background was subtracted. Spectra were exported to Excel for processing and peak maximum determination.

4.3.3 Results

The CD spectra for the single stranded oligonucleotides, the homoduplexes, and the heteroduplexes were recorded. For the single stranded oligonucleotides, the samples were compared with the CD spectrum of the unmodified sequence, which had a maximum at 267 nm and a minimum at 208, which is indicative of an A-form-like RNA structure. (Figure 4-7) The singly modified 1B RNA, with 6 GTP α B modifications, surprisingly showed a shift in the maximum from 267 nm to 273 nm, indicative of a more B-form like helix, although the minimum did not shift. Both the minimum and the maximum absorbances were reduced in intensity compared to the normal, a fact that is usually attributed to a reduction in base stacking (Berova 2000).

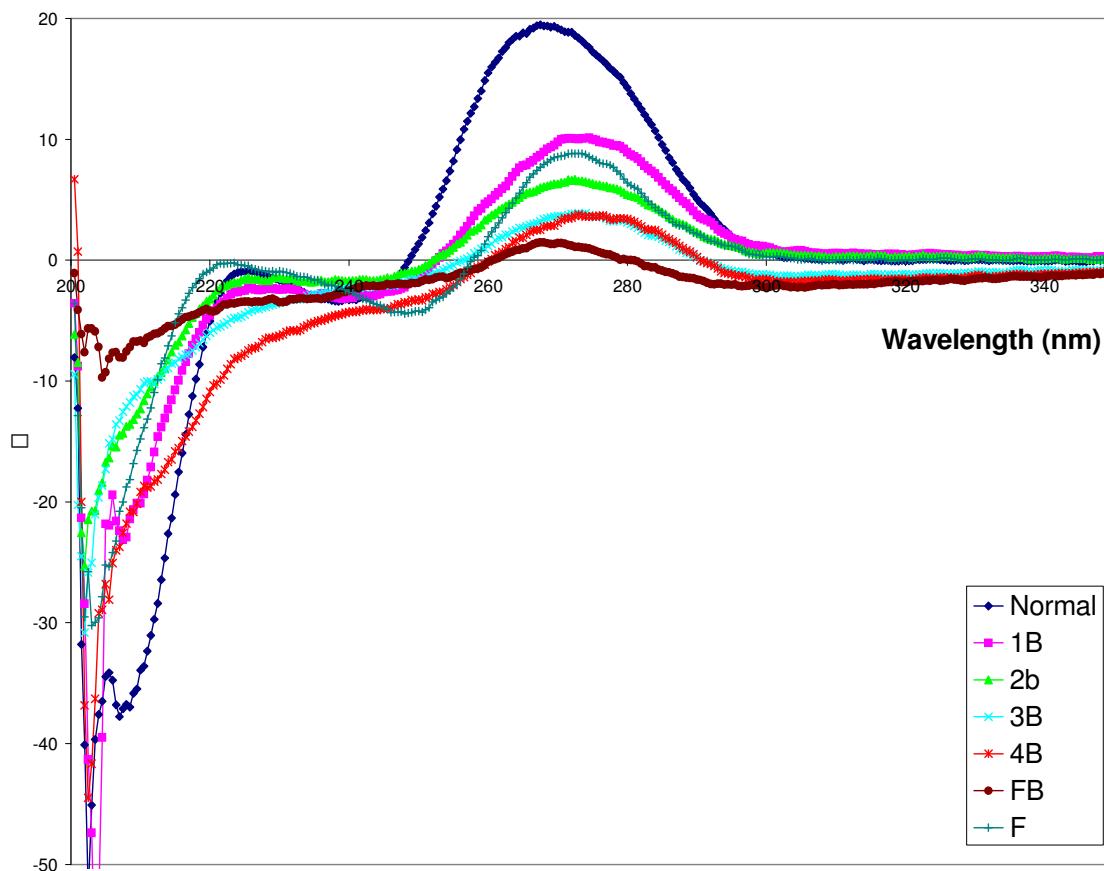


Figure 4-8. CD spectra of single stranded RNAs. The final concentration of the oligonucleotides was 1.5 μM in 1X CD buffer. CD spectra were recorded at 25°C.

The effect on the CD spectra of increasingly amounts of boranophosphate modification of single-stranded RNA followed the same trend. The molar ellipticity maximum wavelengths for the 2B, 3B, and 4B sequences were at 273 nm, 272 nm, and 275 nm, respectively. These sequences also showed a slight shift in their minimum molar ellipticity wavelengths as well, exhibiting a shift to 202 nm. Clearly, modification of the backbone with the boranophosphate has a dramatic impact on the structure of the RNA. Most surprisingly, the 2'fluoro modified RNA showed signs of a more DNA-like

structure, with a maximum absorbance at 272 nm, a well-defined minimum absorbance at 248 nm, and an intercept of 258 nm. The maximum molar ellipticity was smaller than the maximum for the normal RNA, also indicative of a more B-form helix. By contrast, the fluoro/borano modified RNA had a maximum absorbance at 269 nm and a minimum absorbance at in the region of 240 nm.

The effects of the change in structure on both the homoduplex and hetero duplex were also studied. The homoduplexes were annealed and the CD spectra were recorded as shown in Figures 4-8. Analysis of these spectra yield results that are consistent with the data from the single stranded RNAs. The unmodified and 1B homoduplexes are clearly A form helices, with maximum absorbances at 267 nm and 268 nm, respectively, and minimum absorbances at ~ 208 nm. However, the 2B homoduplex has a slightly more shifted maximum absorbance at 271.5 nm. This could be indicative of a shift towards a B form helix. The most modified homo duplexes, 3B and 4B sequences exhibit maximum absorbances of 275 nm, and 276 nm, respectively. This shift implies a more B form helix, however, there is no corresponding shift in the minimum absorbance. Overall, it appears that the trend is more boranophosphate modifications present in this sequence, the more B form helix characteristics are seen.

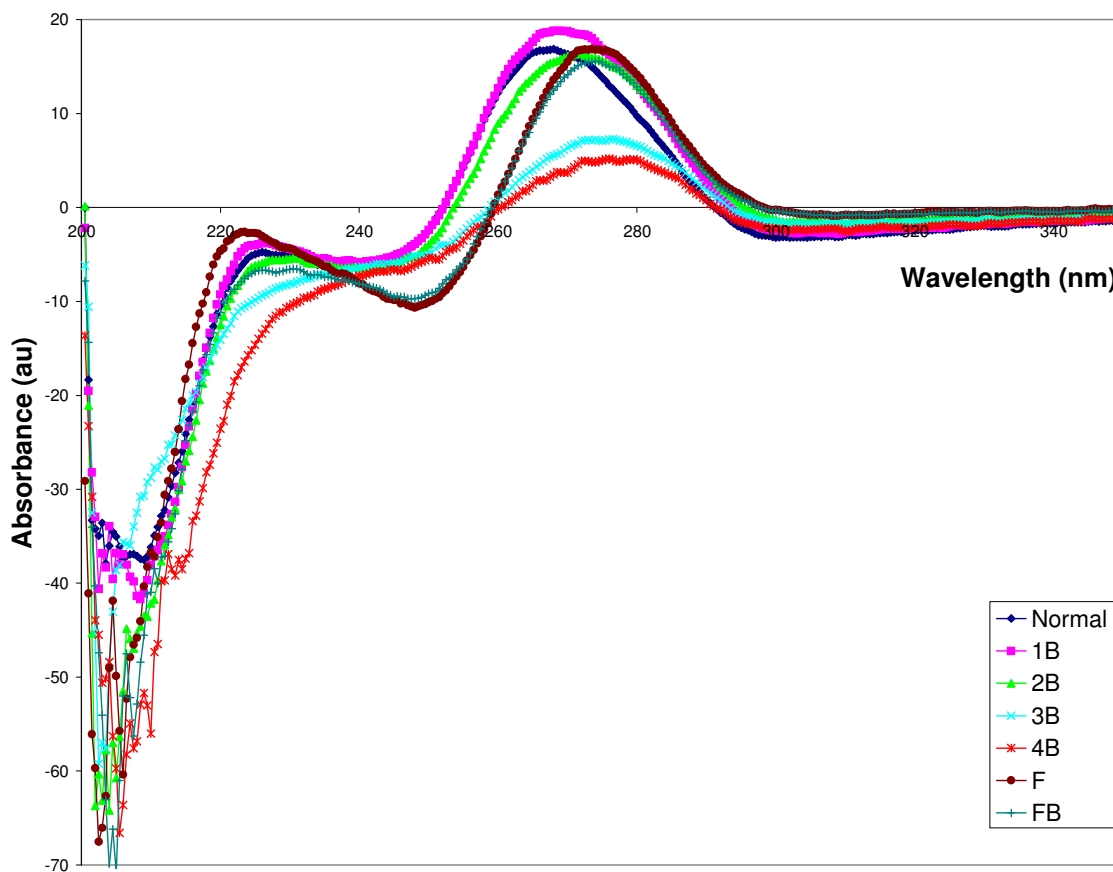


Figure 4-9. CD spectra of homoduplex RNA. The final concentrations of the duplex were 1.5 μM in 1X CD buffer. CD spectra were recorded at 25°C.

For the 2'F modified RNA, both with and without the borano modification, there is a clear shift to a B form helix. The maximum absorbance for the fluoro RNA was at 273.5 nm and for the fluoro/borano RNA was at 275 nm. The minimum absorbance for the F RNA was at 247.5 nm and for the FB RNA was at 248 nm. Both spectra had intercepts on the X-axis at 259 nm. All of these parameters support the conclusion that for the homoduplex, the fluoro modification causes the duplex to adopt a fully B form duplex.

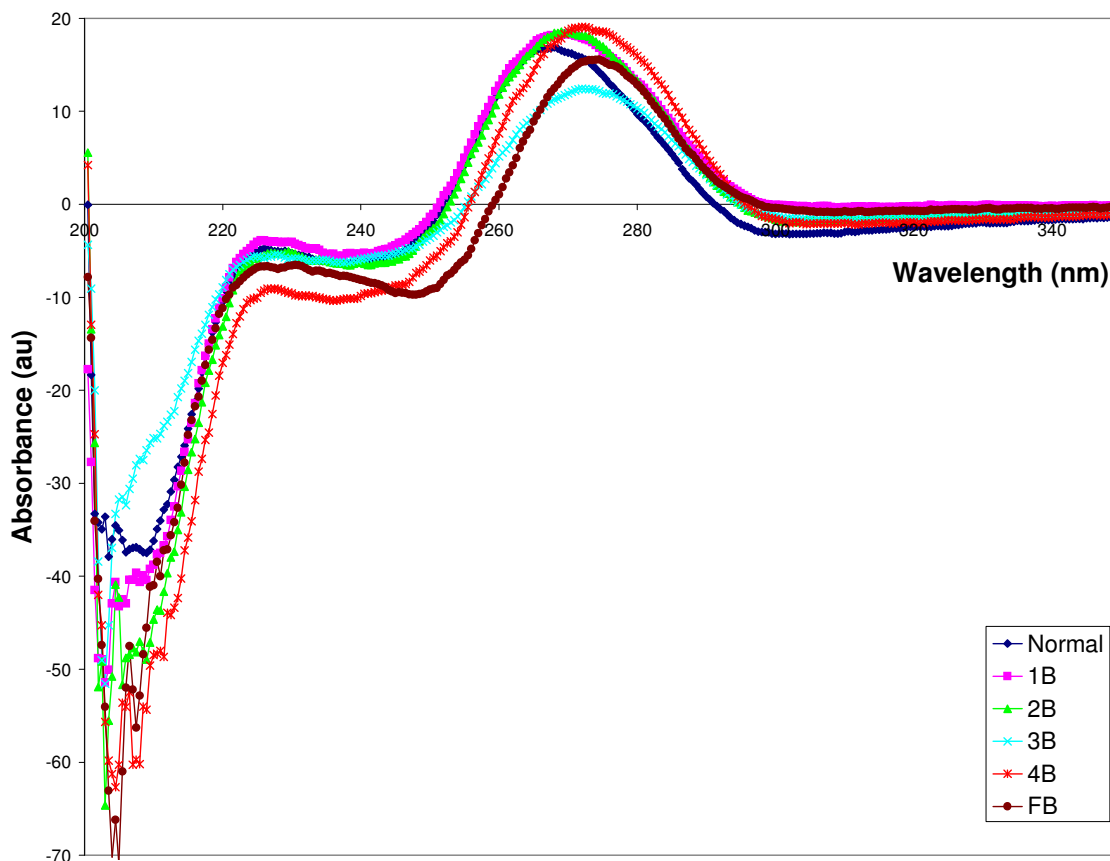


Figure 4-10. CD spectra of heteroduplex RNA. The final concentrations of the duplex were $1.5 \mu\text{M}$ in 1X CD buffer. CD spectra were recorded at 25°C

The heteroduplexes were annealed and the CD spectra recorded is shown in Figure 4-9. The normal, unmodified duplex is included as a comparison, although it is technically a homoduplex.

The heteroduplexes showed the same trends as the homoduplexes, but the extent of the B form shift was reduced, probably due to the fact that only half of the duplex was modified. The 1B-modified duplex had a maximum molar ellipticity at 268 nm and a minimum molar ellipticity at 208 nm. This is comparable to the homoduplex

parameters. The 2B-modified duplex exhibited less B form characteristics than its homoduplex, with a maximum absorbance at 269.5 nm and a minimum absorbance at 208 nm. The 3B modified duplex and 4B modified duplex showed the same trend, although their maximum absorbances were still significantly shifted towards 270 nm. The spectra of the fluoro/borano heteroduplex retained the same CD parameters as its homoduplex, exhibiting totally B-form characteristics despite the fact that only one strand of the duplex was modified.

4.3.4. Discussion

The work contained in this section represents the first characterization of the secondary structure of homoduplex and heteroduplex RNA with increasing amounts of boranophosphate modification, and the first characterization of the secondary structure of the fluoro/borano RNA. The CD spectra of single-stranded unmodified and modified RNA were helpful due to the fact that the trends that were apparent from the parameters recorded therein translated well to the homo- and hetero- duplexes that were the focus of this chapter. Although there were no T_m data to compare them to, the CD spectra of the single strands showed that increasing borano modification appears to shift the secondary structure from RNA-like to DNA-like. This was even more apparent for the 2'fluoro modification. The ability of the CD experiment to give some results about the structure from the single-stranded RNA may be due to secondary structure caused by self-pairing. When RNAstructure software is used to predict the secondary

structure of the single stranded HPV 16+24 AS RNA, there is a short (6n) stem loop near the 5' end. (Figure 4-10) This small double-stranded region may be responsible for the A-form-like and B-form-like attributes of the CD spectra of single stranded RNA.

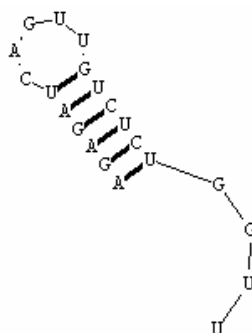


Figure 4-11. Secondary structure of single stranded HPV 16+24 antisense RNA. Structure was predicted using RNAstructure software.

The normal, 1B, and 2B homoduplexes showed the greatest hyperchromicity during the melting experiments. It is proposed that these are the most stable during the T_m measurements. The CD parameters that were recorded confirm that these duplexes exhibit the most A form characteristics of all the sequences that were studied, although there is evidence that the 2B duplex may be shifted towards the B form. The T_m data for the 3B and 4B duplexes indicated that these modifications resulted in helices that were significantly less stable than their less modified counterparts. The CD parameters that were recorded for these duplexes show that there is a distinct shift towards B form helices. This is consistent with literature data that has shown that B form duplexes are less stable than A form duplexes (Saenger 1984). This conclusion was reached for the fluoro and fluoro/borano modified homoduplexes studied in this work, as both

exhibited CD spectra that are clearly B form-like helices and both had T_m 's that were significantly lower than the unmodified RNA. This differs from some previous reports in the literature that have shown that 2'F RNA adopts a fully A form duplex (Kawasaki 1993). The CD spectra of the heteroduplexes again showed the same trends as the single-stranded CD spectra, albeit to a lesser extent than the homoduplexes. The 1B and 2B modified duplexes exhibited the most A form characteristics, in line with the T_m data that showed these duplexes were the most stable. The 3B, 4B, and FB duplexes all exhibited B form characteristics, in line with their lowered T_m values.

4.4 Chapter Summary

Overall, T_m and CD data support the conclusion that while an RNA duplex modified on one or two NTPs show an increased stability, further increasing the amount of boranophosphate modifications of RNA duplexes leads to destabilization, most likely due to a more B form helix versus unmodified RNA. Clearly, introduction of the 2'F modification destabilized the duplex by shifting the duplex to a B form conformation. In this case, it appears that the 2'F modification causes the ribose to adopt a C2'-endo conformation that is native to DNA. This is also supported by the decrease in the intensity of the maximum near 270 nm. It has been shown that this correlates to an increase in the winding angle of the helix. Greater winding angles are characteristic of DNA. (Bloomfield 2000)

Although many different methods exist to predict siRNA sequences that will yield the highest potency signal attenuation, none can predict the effect of boranophosphate modification. (Pei and Tuschl 2006) At the present time, it seems that empirical studies are the best way to determine the thermal stability and secondary structure of a modified duplex. There are surely sequence-dependent effects of chemical modification that will have implications on duplex stability. Furthermore, there may be positional effects of the placement of the modification. Since we do not currently have the ability to site-specifically modify boranophosphate RNA, it is recommended that for any new siRNA sequence, the T_m and CD experiments are undertaken to ensure the ability of the modified siRNA to form a thermodynamically stable duplex with normal RNA. Further studies may be carried out by determining the kinetic parameters from the T_m across a range of duplex concentrations. Also, more information may be determined about the duplexes using CD spectroscopy by investigating the effects of salt and divalent cation concentrations on the duplex by making use of CD titration experiments.

5. Chemical and Biological Properties of Boranophosphate siRNA

The major motivation for chemical modification of RNA is to enhance the properties of RNA for the possibility of therapeutic applications. The major factors that define whether RNA can be used for therapeutic applications are stability and lipophilicity. Stability is required if the siRNA is to persist in biological media long enough to have the desired effect. Lipophilicity is desirable for reasons of delivery; since the siRNA must pass through the cell membrane, an increased lipophilicity of the molecule may ease the passage.

5.1 Chemical Stability of Boranophosphate Modified siRNA

5.1.1 Introduction

Oligonucleotides are subject to both chemical and enzymatic hydrolysis to their composite NTPs. (Manoharan 2007) Ribonucleotides contain a 2' hydroxyl group that makes the polymer vulnerable to cleavage-transesterification and less stable than DNA. (Jenkins Autry and Bashkin 1997) During the hydrolysis, the nucleophilic 2' OH group attacks the adjacent phosphorus, resulting in a cyclic phosphodiester which undergoes hydrolysis to the 3' PO₄ fragment and 5' OH fragment. (Figure 5-1)

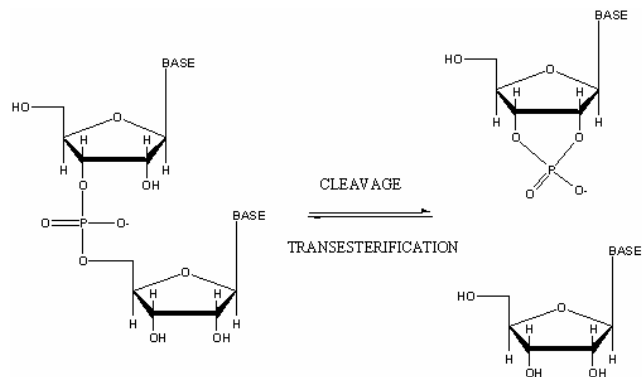


Figure 5-1. Thermodynamic hydrolysis of RNA. The 2'OH group carries out nucleophilic attack on the phosphate group yielding a cyclic phosphodiester and a nucleoside. The cyclic phosphodiester is further hydrolyzed to an NMP.

Previous work done by the Shaw lab has shown that partially modified boranophosphate RNA had comparable stability to normal and phosphorothioate-modified RNA at physiological pH and temperature. (Wan 2005) The first section in this chapter extends that work to increasingly modified boranophosphate RNAs and the new class of modified RNA, the fluoro/borano RNA.

5.1.2 Experimental Procedures

The RNAs used in this section were synthesized enzymatically. Transcription reactions with T7 RNA polymerase were set up using the 16+24 AS DNA template and reaction conditions to produce each modified RNA transcript were set up under the conditions outlined in Chapter 3. Transcripts were dephosphorylated using Antarctic phosphatase and then radioactively labeled by PNK and [γ - 32 P] ATP. This resulted in RNA with a 5' monophosphate radioactive label. The RNAs were purified as described in Chapter 3, by phenol extraction, G-25 microcolumn purification, and YM-3 filtration

to remove unincorporated nucleotides and short transcripts. The sequences are shown in Table 5-1.

Table 5-1. Enzymatically transcribed 21mer RNA used in thermodynamic and enzymatic stability assays, as well as lipophilicity assays. Boranophosphate (NTP α B) modifications are shown in blue and 2'fluoro (2'F NTP) modifications are shown in red.

Name	Mod	# Mod (%)	Sequence
N AS	none	0 (0)	AGA GAU CAG UUG UCU CUG GUU
1B AS	GTP α B	6 (29)	AGA GAU CAG UUG UCU CUG GUU
2B AS	CTP α B, GTP α B	9 (43)	AGA GAU CAG UUG UCU CUG GUU
3B AS	CTP α B, GTP α B, UTP α B	17 (81)	AGA GAU CAG UUG UCU CUG GUU
4B AS	ATP α B, CTP α B, GTP α B, UTP α B	21 (100)	AGA GAU CAG UUG UCU CUG GUU
F AS	2'F CTP, 2'F UTP	11 (52)	AGA GAU CAG UUG UCU CUG GUU
FB AS	2'F CTP, GTP α B, 2'F UTP	18 (86)	AGA GAU CAG UUG UCU CUG GUU

To determine the chemical stability of the boranophosphate and fluoro/borano RNA, a stock solution of each 32 P labeled RNA sequence with 10^5 cpm of radioactivity (approximate 100 picomoles) was made by mixing the RNA and RNase-free water with 10X potassium phosphate buffer, pH 7.4 (1 M). The final concentration of the RNA was approximately 4 μ M in 1X phosphate buffer (0.1 M). The pre-determined time points to measure the chemical hydrolysis were: 0, 3.5, 7.5, 15, 30, 60, 120, 240, 480, 720, and 1440 minutes (24 hours). At each time point, a 3 μ L aliquot of the stock solution was removed

and mixed with an equal volume of gel loading buffer. This mixture was vortexed, spun down, and frozen at -20°C for subsequent PAGE analysis of the amount of chemical hydrolysis. Due to limited quantities of the fluoro modified oligonucleotides, the 15 minutes and 2-hour time points were skipped.

For the stability studies, the time points were run on a single 20% PAGE/ 7M urea denaturing gel for 2 hours at 30W. After electrophoresis, the gel was removed from the plates and transferred to Saran wrap and thoroughly and carefully wrapped. To image the RNA, the wrapped gel was dried with Kimwipes and placed in the exposure cassette, where it was exposed to the phosphorous storage screen overnight. The screen was imaged the next day using the Typhoon Phosphoimager using the phosphor storage mode. The gels were quantified using ImageQuant 5.2 to determine the relative amount of radioactivity in each band. Background correction was done using a square of the same area in the same lane as each band.

5.1.3 Results

Radioactively labeled RNAs with various modifications were enzymatically transcribed and purified in order to test the resistance of each sequence to chemical hydrolysis. Single stranded siRNA with the HPV 16+24 antisense sequences were incubated at 37° C to test their stability to chemical hydrolysis at biological temperatures. Each radiolabeled sequences was incubated for 24 hours in potassium phosphate buffer, pH 7.4, and analyzed on 20% PAGE/ 7M urea gels to determine the

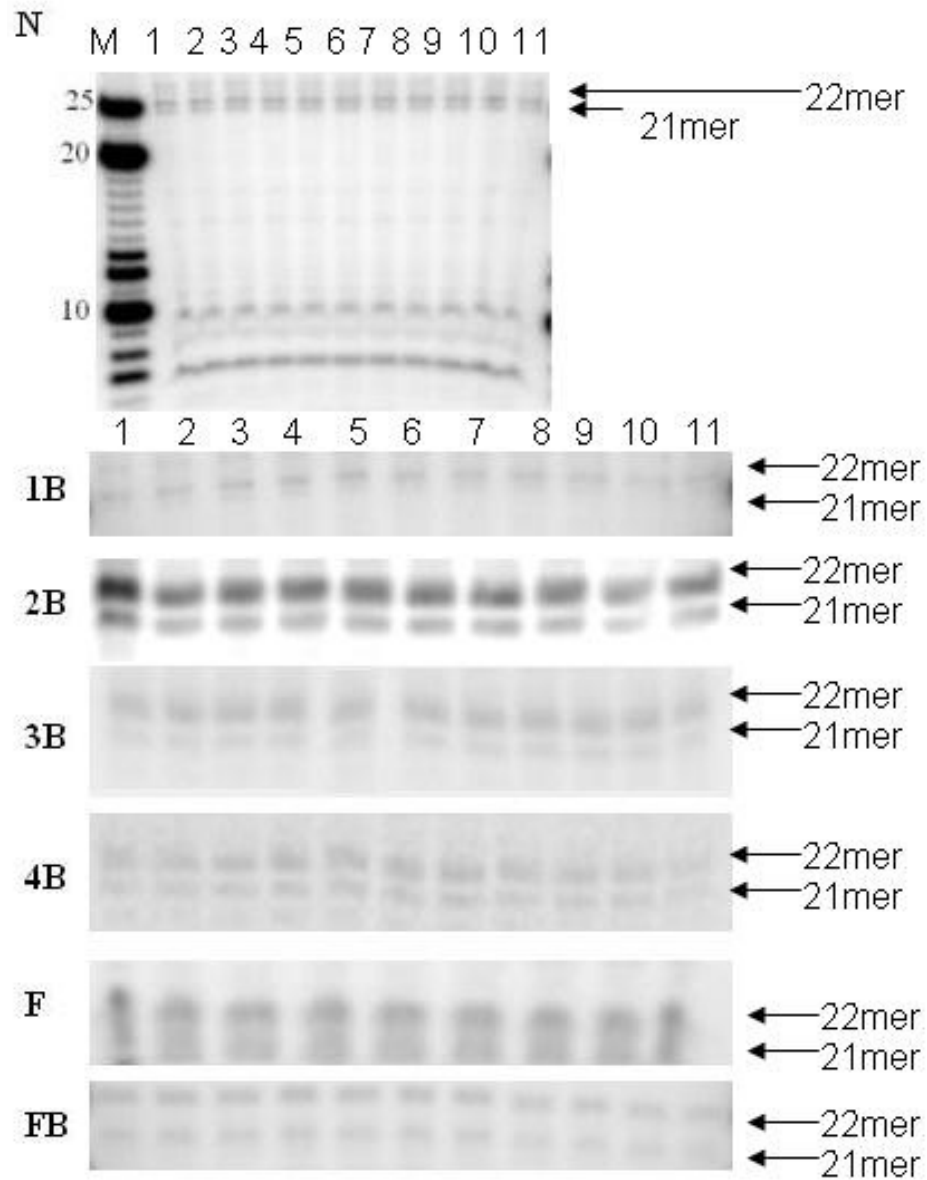


Figure 5-2. 20% PAGE/ 7 M urea analysis of the stability of single stranded siRNA at 37°C and pH 7.4, incubated over 24 hours. Each well was loaded with 3 μ L of 32 P endlabeled sampled and 3 μ L gel loading buffer. The 20% PAGE/7M urea gel was run for 2 hours at 30 W. The lane marked M contains DNA size markers, as labeled. Each numbered well is a time point: 1) 0 min, 2) 3.5 min, 3) 7.5 min, 4) 15 min, 5) 30 min, 6) 1 hr, 7) 2 hr, 8) 4 hr, 9) 8 hr, 10) 12 hr, 11) 24 hr

percentage of full-length transcript that remained. The degradation of the full-length transcripts can be seen in Figure 5-2. In addition to the full-length transcripts, there are shorter products towards the bottom of the gel. These can be regarded as products of degradation due to electrophoresis, as these are present in all lanes, even at time 0, where there should be no degradation of the RNA.

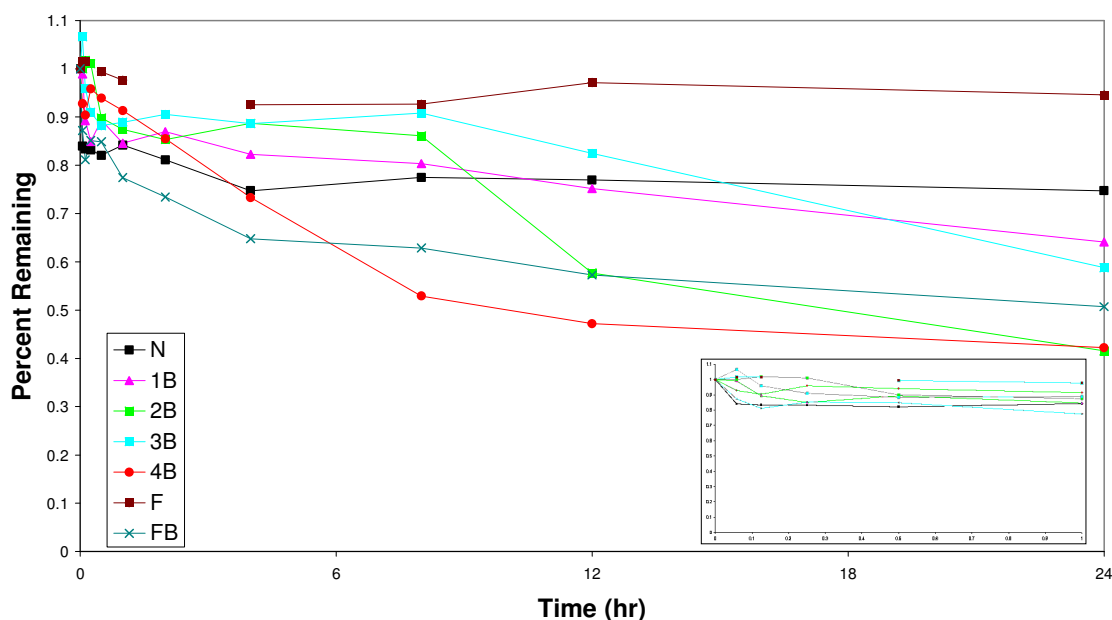


Figure 5-3. Chemical hydrolysis of RNA over 24 hours under physiological temperature and pH. The sample sequences and modifications are shown in Table 5-1. Experiments were done in 0.1 M potassium phosphate buffer using sequences that were radiolabeled on the 5' ends. Results are the averages of at least three hydrolysis experiments. Inset shows the first hour of incubation.

As seen in Figure 5-3, the unmodified RNA AS strand showed little decrease in full-length transcript even after 24 hours, suggesting that it is reasonably stable at biological temperatures. The fluoro modified RNA showed the greatest stability, with

very little degradation. However, boranophosphate modified and fluoro/borano modified RNA did show considerable degradation over the time period that was studied, although there was no statistically significant trend seen as the amount of modification increased.

5.1.4 Discussion

The work in this section represents the first time that increasingly modified boranophosphate and fluoro/borano siRNA has been evaluated for its resistance to chemical hydrolysis under biological conditions of temperature (37°C) and pH (pH 7.4). For all samples, there was some degradation that appeared to be due to the gel electrophoresis, as it was present in all lanes, even at time point 0. Unfortunately, although gel electrophoresis allows single nucleotide resolution of oligonucleotide species, it is performed at high temperatures (~60-70°C) that denature RNA. This degradation may be mitigated by running gels in the cold room (~4°C), but this will prolong the time required for electrophoresis. In this study, the intensity of the band of the full length RNA at time 0 was used to normalize the results. Since this RNA is also subject to electrophoresis, it can be assumed that any degradation in comparison to the time 0 RNA is due to increase in incubation time.

Overall, boranophosphate modified RNA was slightly less stable to chemical hydrolysis than unmodified RNA at 37°C and pH 7.4. There may be different results under different temperature and pH conditions. The extent of modification did not

seem to matter, as there was not a statistically significant trend linking amount of modification to the amount of degradation. One explanation for the increase in degradation is the decrease in electronegativity of the BH₃ group compared to oxygen. The difference in polarization of the P-B bond may increase the vulnerability of the bridging oxygen to nucleophilic attack by increasing the negative charge on the non-bridging oxygen. To determine if it is the case that the borane modification destabilizes the phosphate backbone, it would be necessary to look at the products of the cleavage. This experiment would have to be done using [α -³²P] labeling, in order to accurately track all of the cleavage products. However, the small stability change should not greatly affect the ability of boranophosphate and 2'F/boranophosphate modified siRNA to induce gene silencing through the RNA interference pathway.

5.2 Enzymatic Stability of Boranophosphate Modified siRNA

5.2.1. Introduction

Organisms are constantly under attack from foreign nucleic acids, i.e. viruses. In order for a cell to protect itself against invaders, it produces nucleases to enzymatically degrade foreign DNA and RNA. In order for siRNA to get past host defense and have therapeutic benefits, the siRNAs must be able to withstand degradation by exonucleases and endonucleases that catalyze the hydrolysis of phosphodiester bonds. It has been

shown that certain chemically modified oligonucleotides show increased enzymatic stability. (Chiu and Rana 2003; Zhang, et al. 2006; Manoharan 2007) Previous work in the Shaw lab has looked at the stability of boranophosphate dinucleotides using exonucleases, such as snake venom phosphodiesterase, and endonucleases, such as Ribonuclease A and found that *Sp* boranophosphate linkages are significantly stable to exonucleases and reasonably stable to RNase H. (He 2000; Wan 2005) It has also been shown that modification of siRNA with 2'F NTP imparts significant stability to endonucleases. (Kawasaki, et al. 1993) It was hypothesized that combining the two modifications would yield an siRNA with superior nuclease stability.

5.2.1.1 Ribonuclease A

Ribonuclease A cleaves after pyrimidines and is often used for nuclease digestion assays. (Raines 1998) It is an endonuclease that catalyzes the cleavage of the RNA phosphodiester bond by the mechanism shown in Figure 5-4.

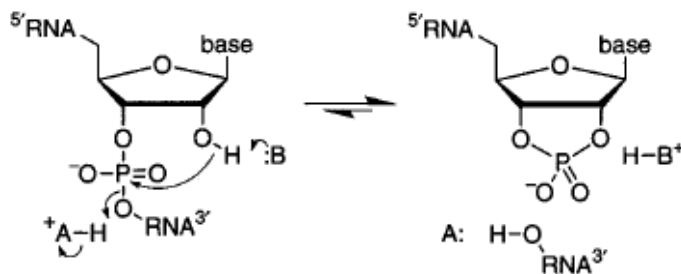


Figure 5-4. Mechanism of RNase A catalyzed cleavage of the phosphodiester bond. “B” represents the histidine 12 residue of the enzyme. Figure adapted from reference. (Raines 1998)

In this section, RNase A is used as a representative endonuclease to probe the nuclease stability of partially and fully modified boranophosphate siRNA and fluoro/borano siRNA.

5.2.1.2 Exonuclease T

Exonuclease T (Exo T) is a 3'→5' exonuclease purified from *E. coli*. (Deutscher 1984; Deutscher 1993) Exo T is a specific single-stranded DNA or RNA nuclease that releases mononucleotides from the 3' end of RNA in divalent cation-dependent reaction. (Deutscher 1993) It belongs to subfamily of exonucleases known as the DEDD family, which share a four amino acid motif and have a common catalytic mechanism involving two divalent cations bound to four acidic residues that form the catalytic center of the enzyme. (Zuo, et al. 2007) In this section, RNase T is used as a representative exonuclease to probe the stability of partially and fully modified siRNA and fluoro/borano siRNA.

5.2.2 Experimental Procedures

The sequences used in this section were enzymatically transcribed and purified as described in Chapter 3. The siRNA that was used to test the nuclease stability was the HPV 16+24 antisense sequence (Table 2-2), and the sequences were modified with NTP α B and 2'F NTP (Table 5-1). The RNAs were dephosphorylated at the 5' end using

Antarctic phosphatase and were radiolabeled on the 5' end using [γ - ^{32}P] ATP and PNK, as described in Chapter 2.

Nuclease stability assays were performed using RNase A and Exo T. The RNase A was obtained from Calbiochem and the assays were done in 1X reaction buffer (10 mM Tris-HCl, 1 mM EDTA, 0.2 M NaCl, pH 7.5). A 50 μL stock solution containing 10 μL of γ - ^{32}P 5' end labeled RNA and 8 units of RNase A was incubated at 37°C. At each time point, 5 μL of the mixture was quenched with an equal amount of 2X gel loading buffer and stored at -20°C for later gel analysis.

The Exo T nuclease was obtained from New England Biolabs and the assays were carried out in 1X reaction buffer (20 mM Tris-acetate, 50 mM potassium acetate, 10 mM magnesium acetate, 1 mM DTT, pH 7.9). A 50 μL stock solution containing 10 μL of γ - ^{32}P 5' end labeled RNA and 5 units of Exo T was incubated at 25°C. At each time point, 5 μL of the mixture was quenched with an equal amount of gel loading buffer and stored at -20°C for later gel analysis. The time points measured were 0, 5, 15, 30, 60, and 120 minutes. The GeneRuler DNA Ladder, Ultra Low Range DNA size markers were used to determine the size of the hydrolysis products.

The 20% acrylamide gel was pre-run for two hours at 30 W for 2 hours and then loaded with the sample and run at 30 W for two hours. Afterwards, the gel was removed from the plate sandwich, wrapped in Saran wrap, and exposed to the low-energy phosphor storage screen overnight at 4°C. The screen was imaged using the

Typhoon phosphoimager. Analysis of the band intensities was measured using ImageQuant 5.2 software and the background was subtracted using a square of equal area in the same lane as the sample. Prior to analysis, no image adjustment was performed. The gel images shown in the Results section have been improved in contrast and brightness to make the bands more visible to the human eye, but this did not interfere with accurate measurement.

5.2.3 Results and Discussion

5.2.3.1. Ribonuclease A

The radiolabeled, modified siRNA sequences were synthesized and tested for their ability to resist enzymatic hydrolysis by RNase A. The amount of full-length transcript at the initial time point was used to normalize the data into the percent of full-length transcript at each time point. (Table 5-2) It was expected that the normal and boranophosphate RNA would be rapidly degraded, while the addition of the 2'F modification would increase the stability of the RNA to exonuclease degradation.

Table 5-2. Kinetics of RNase A digestion of ³²P endlabeled modified HPV 16+24 AS RNA over time. The reaction products were run on 20% PAGE/7 M urea to separate the species by size. The percentage remaining of the radiolabeled full-length transcript as compared to the amount at time 0 is shown. Each data point is the average of three hydrolysis experiments.

Time (min)	N (%)	1B (%)	2B (%)	3B (%)	4B (%)	F (%)	FB (%)
0	100 ± 5	100 ± 3	100 ± 2	100 ± 2	100 ± 4	100 ± 7	100 ± 3
5	3.0 ± 5	10.1 ± 1	11.4 ± 4	10.4 ± 3	10.0 ± 7	108.1 ± 4	103.1 ± 2
15	0.87 ± 4	5.0 ± 2	3.5 ± 2	7.5 ± 5	9.2 ± 2	101.0 ± 3	95.8 ± 3
30	0.59 ± 1	4.3 ± 1	3.2 ± 2	7.2 ± 3	8.3 ± 1	89.2 ± 4	86.1 ± 4
60	0.52 ± 3	3.6 ± 1	2.7 ± 2	7.0 ± 5	8.5 ± 2	75.9 ± 3	82.5 ± 3
120	0.57 ± 4	4.2 ± 2	2.6 ± 1	7.2 ± 4	8.1 ± 3	66.2 ± 2	82.0 ± 4

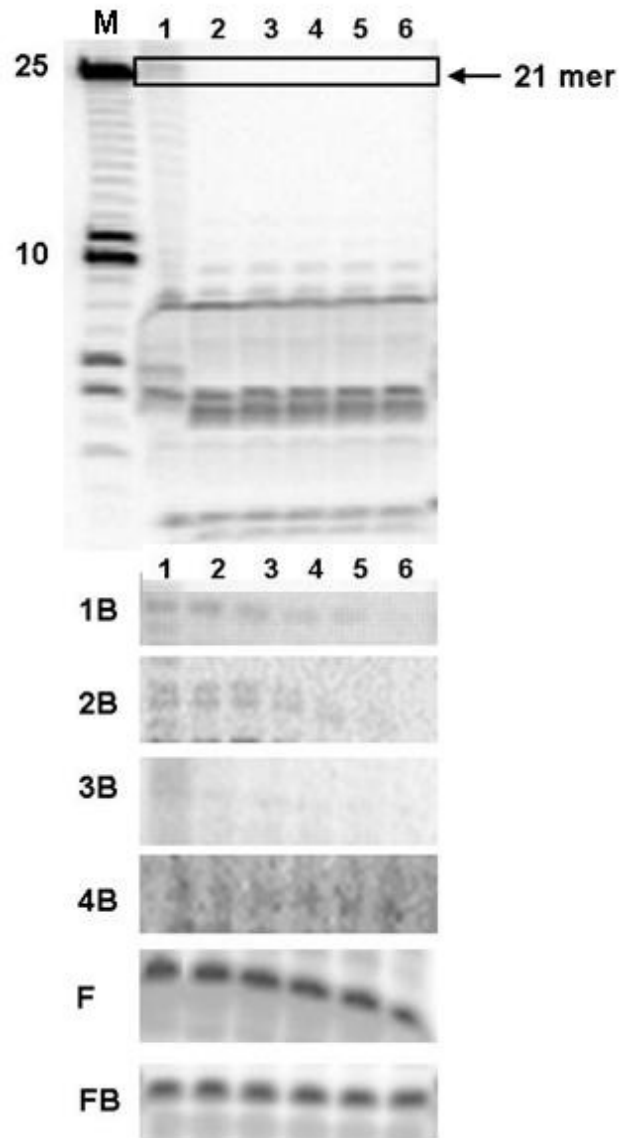


Figure 5-5. 20% PAGE/7 M urea gel analysis of natural and modified RNA stability to RNase A hydrolysis assay. The sequences are given in Table 5-1. Top: The gel of the normal RNA is shown, with the area of interest (21 nt) boxed. Bottom: The area of interest (21 nt) is enlarged for the gels containing modified RNAs. Intensity of the radiolabeled bands was quantified using a Typhoon phosphoimager. After quantification, the images were adjusted to increase visibility of bands for the human eye. The marker lane is denoted as M and the time points are 1) 0 min, 2) 5 min, 3) 15 min, 4) 30 min, 5) 1 hr, 6) 2 hr

An equal amount of radioactively labeled RNA was loaded into each lane.

There did not appear to be any difference in radioactive labeling between unmodified and modified RNA. Normal, unmodified RNA is rapidly degraded by RNase A, which cleaves after C and U (Figures 5-5 and 5-6). Even at the first time point (0 min), directly after the RNase has been added, there is a ladder of degraded products as seen in Figure 5-5, probably caused by short interval before the addition of the quenching solution to the sample aliquot. After ten minutes of incubation with RNase A, there was no full-length unmodified (N) transcript left. Increasing the percent of borano modifications per RNA molecule slightly decreased the degradation while the introduction of the 2'F modification greatly increased the stability.

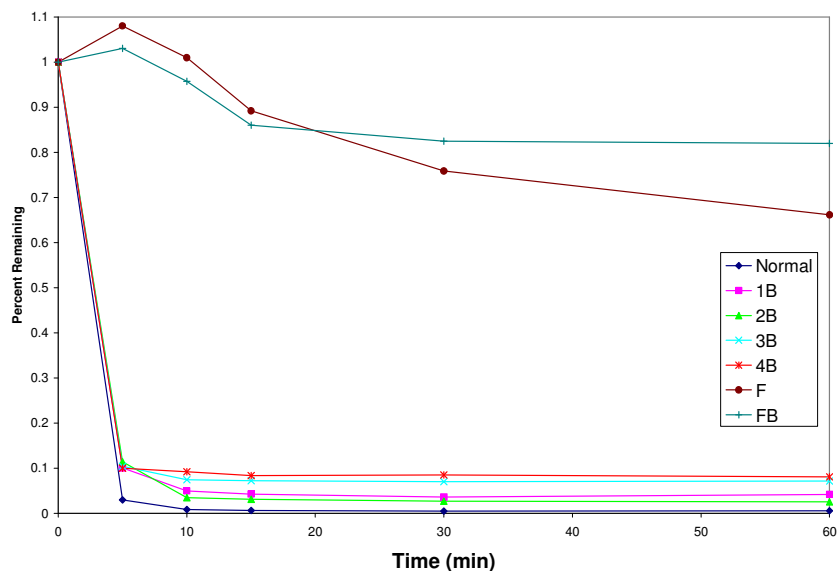


Figure 5-6. Kinetics of natural and modified RNA against RNase A degradation assays. The amount of full-length transcript remaining at each time point for each sample was determined by normalization to time point 0. Each time point is the average of three separate hydrolysis experiments.

There is a difference between the chemical (Fig 5-3) and enzymatic stability (Fig 5-6) of the modified siRNA sequences. Although the borano modification slightly decreased the chemical stability, it slightly increased the stability to the endonuclease. One possible explanation for this difference is the nature of the endonuclease. As shown in Chapter 4, the boranophosphate modification changes the structure of the RNA. It may be that there is a K_m effect, that the endonuclease has a hard time binding the modified siRNA or it may be a K_{cat} effect, after the RNA is bound, the backbone is no longer at the catalytic site of the enzyme. To better understand the mechanics of this stability, it is recommended that a steady-state kinetic analysis be performed with the enzyme. In this manner, the rate of the reaction and the dissociation constant can be determined. However, the amounts of modified RNA required to undertake those experiments are quite large, and will require synthesis of purified siRNA in millimolar quantities

5.2.3.2 Exonuclease T

The same batch of radiolabeled, modified siRNA sequences (Table 5-1) was tested for their ability to resist enzymatic hydrolysis by Exo T. Time points of the incubation of the radiolabeled RNA were analyzed using PAGE electrophoresis. (Figure 5-7) The amount of full-length transcript at the initial time point was used to normalize the data into the percent of full-length transcript at each time point. (Table 5-3)

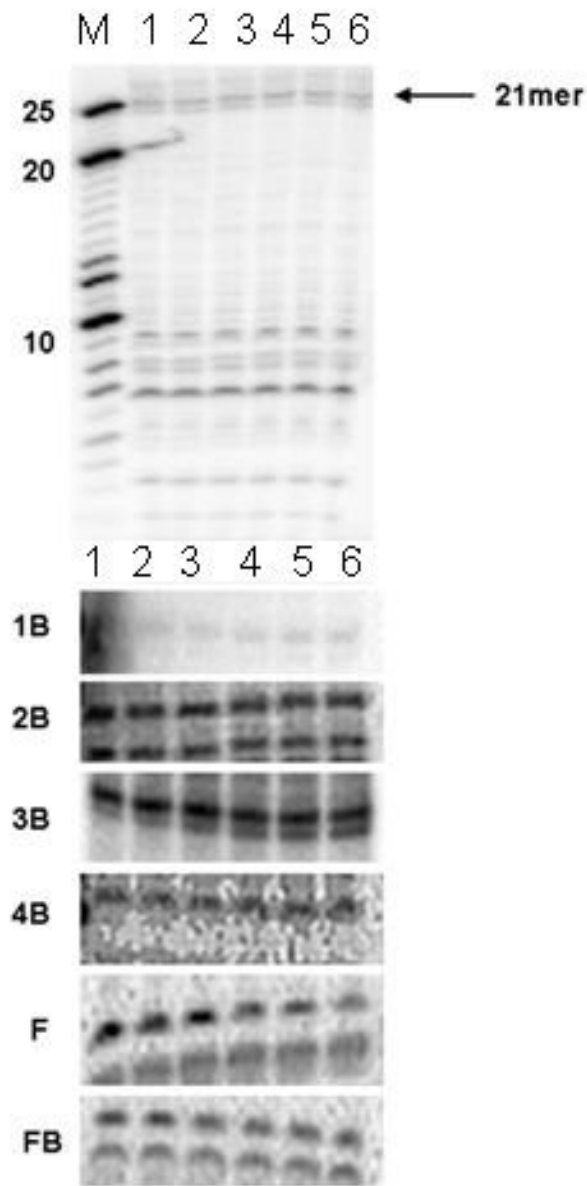


Figure 5-7. . 20% PAGE/7 M urea gel analysis of natural and modified RNA stability to Exonuclease T hydrolysis assay. The sequences are given in Table 5-1. Top: The gel of the normal RNA is shown, with the area of interest (21 nt) boxed. Bottom: The area of interest (21 nt) is enlarged for the gels containing modified RNAs. Intensity of the radiolabeled bands was quantified using a Typhoon phosphoimager. After quantification, the images were adjusted to increase visibility of bands for the human eye. The marker lane is denoted as M and the time points are 1) 0 min, 2) 5 min, 3) 15 min, 4) 30 min, 5) 1 hr, 6) 2 hr

Table 5-3. Kinetics of Exo T (5 U/ μ L) digestion of natural and modified RNA over time. The sequences are given in Table 5-1. The percentage remaining of the full-length transcript as compared to the amount at time 0 is shown. Each data point is the average of three hydrolysis experiments.

Time (min)	N (%)	1B (%)	2B (%)	3B (%)	4B (%)	F (%)	FB (%)
0	100	100	100	100	100	100	100
5	82.5 \pm 8	87.2 \pm 5	84.2 \pm 6	93.9 \pm 10	87.2 \pm 7	78.7 \pm 14	105.7 \pm 8
15	82.3 \pm 10	79.7 \pm 4	64.2 \pm 5	102.2 \pm 6	84.0 \pm 8	73.9 \pm 18	85.5 \pm 8
30	87.8 \pm 11	70.3 \pm 4	52.0 \pm 5	92.1 \pm 8	88.0 \pm 7	68.3 \pm 9	78.5 \pm 8
60	76.0 \pm 8	66.4 \pm 6	48.7 \pm 5	99.9 \pm 8	88.7 \pm 8	55.0 \pm 9	93.4 \pm 9
120	74.3 \pm 7	62.3 \pm 6	50.7 \pm 4	89.6 \pm 7	81.5 \pm 9	53.3 \pm 5	81.0 \pm 7

It can be seen from the data in Table 5-3 that borano modification using GTP α B or GTP α B + CTP α B does not increase the stability the siRNA to Exonuclease T degradation. This makes sense because the exonuclease starts at the 3' end of the RNA strand. In this sequence, the last two bases at the 3' end of the RNA are uridines, so only modification with UTP α B would be expected to show resistance to Exonuclease T digestion. This anticipated increase in stability is seen for the 3B and 4B modified sequences. The fluoro modification appeared to decrease the exonuclease stability over time, but the addition of the borano modification resulted in an increase in exonuclease stability. In fact, the HPV 16+24 AS sequence contains many U residues near the 3' end, which suggests many possible points for the modification with borano or fluoro NTPs to interfere with the enzyme. The kinetics of the Exo T digestion of natural and modified RNA is graphed in Figure 5-8.

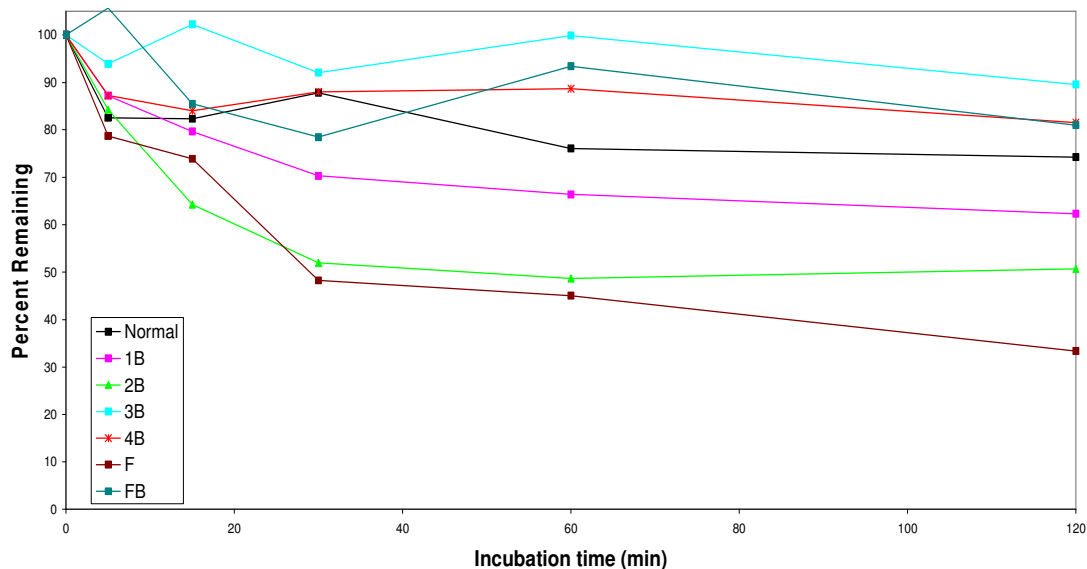


Figure 5-8. Kinetics of natural and modified RNA against Exonuclease T degradation assays. The amount of full-length transcript remaining at each time point for each sample was determined by normalization to time point 0. Each time point is the average of three separate hydrolysis experiments.

Exonuclease T is a non-processive 3'→5' exonuclease with activity against RNA and DNA substrates. (Zuo and Deutcher 2002) The enzyme uses highly positively charged residues to form a nucleic acid binding segment (NBS) and it has been shown that the Km values for the degradation of DNA are higher than the Km values for the degradation of RNA (Zuo and Deutcher 1999). The degradation of the unmodified RNA proceeded at about the same as rate the degradation of the 1B and 2B sequences. This may be explained with reference to the secondary structure data from Chapter 4. It has been shown that Exo T binds more tightly to DNA versus RNA. Since addition of the borano modification seems to shift the secondary structure to a more DNA-like conformation, Exo T may bind BP RNA more tightly than unmodified RNA. However,

it appears that the addition of the borano modification at the 3' end of the siRNA, where the exonuclease cleaves the terminal nucleotide, significantly decreases the rate of degradation. This is consistent with previous results that showed that U-U and U-A dinucleotides containing a boranophosphate linkage showed much lower rates of degradation by exonucleases as compared to the unmodified dinucleotide. (He 2000)

Since it was suggested that the fluoro modification caused the sequence to adopt a DNA conformation, it is not surprising that the 2'fluoro modified sequence showed the greatest amount of degradation, taking into account the preference of Exo T for a DNA substrate. It is interesting that inclusion of the GTP α B in the sequence restored nuclease stability. It may be that although the FB siRNA sequence was shown to adopt a more DNA-like structure, the difference in electronegativity of the BH₃ group versus the normal oxygen negatively impacted the ability of the highly positive residues of the enzyme to tightly bind the FB siRNA. Again, this reaction may be better understood when the kinetic parameters of the enzymatic hydrolysis can be obtained for the modified siRNAs. When the binding affinity can be determined for each modified sequence, it will be easier to attribute the change in enzymatic hydrolysis to the correct factor.

5.3 Lipophilicity of modified siRNA

5.3.1 Introduction

The rapid development of siRNA technology has led to many advances in gene regulation. However, the ability of the siRNA to silence gene expression is predicated on its capacity to cross the cell membrane and gain access to the RISC machinery in the cytoplasm. This cellular delivery remains the largest obstacle to siRNA therapeutics. (Wolfrum, et al. 2007; Juliano, et al. 2008) The hydrophobic cell membrane repels large, highly charged molecules like siRNA. (Alberts, et al. 2002) There have been descriptions in the literature of double stranded RNA transporters, both in *C. elegans* and human cells that can engage in active transport of RNA. (Duxbury 2005) However, this is limited to certain cell systems and has been shown to be ineffective for the transportation of short siRNAs. (Lewis and Wolf 2007) Therefore, it behooves us to find modifications that can increase the lipophilicity of siRNAs to facilitate cellular delivery through passive transport across the cell membrane.

An efficient way to determine the lipophilicity of a modified oligonucleotide has been outlined by Dagle, *et al.* This method utilizes radiolabeled oligonucleotides to measure the partitioning between 1-octanol and aqueous phases. (Dagle, et al. 1991) Earlier studies in the Shaw lab have shown that the boranophosphate modification increases the lipophilicity of thymidine dimers by eighteen-fold and increases the lipophilicity of 21mer BP-RNA containing 9 UTP α B modifications by 17.5-fold. (Huang

1994; Wan 2005) The work in this section will investigate the effect of increasing the percentage of boranophosphate modifications on the lipophilicity of borano and fluoro/borano modified siRNAs.

5.3.2 Experimental Procedures

Modified siRNA sequences were enzymatically synthesized and purified as described in Chapter 3. The sequence used for the lipophilicity experiments was the HPV 16+24 sequence (Table 2-2) with NTP α B and 2'F NTP modifications (Table 5-1). The siRNA transcripts were dephosphorylated at the 5' end with Antarctic phosphatase and subsequently labeled using PNK with [γ - 32 P] ATP and the unincorporated radiolabel was removed using YM-10 microfiltration. 1×10^5 cpm of each radiolabeled siRNA was put into RNase-free 1.5 mL cryogen tubes with screw top caps, lyophilized to powder, and then dissolved in 200 μ L of 1-octanol saturated potassium phosphate buffer. This solution was then shaken vigorously to ensure that the powder was completely dissolved, and then briefly centrifuged.

The partition coefficient was determined using a "lipophilic" phase consisting of potassium phosphate saturated 1-octanol (PSO), pH 7.5 and a "hydrophilic" phase consisting of 1-octanol saturated 1.0 M potassium phosphate buffer (OSP). In order to saturate the potassium phosphate buffer, 100 mL of 1-octanol was added to 100 mL of 1.0 M potassium phosphate buffer and the mixture was shaken vigorously at room temperature for 24 hours and then allowed to stand at room temperature for 24 hours to

allow the phases to separate. To saturate the 1-octanol, 100 mL of 1.0 potassium phosphate buffer was added to 100 mL of 1-octanol, shaken for 24 hours, and allowed to equilibrate over 24 hours. 1-Octanol is less dense than water, so it forms the top layer after equilibration. 200 μ L of PSO was added to the siRNA that was dissolved in 200 μ L of OSP. This mixture was shaken vigorously for approximately two hours at 25°C in a temperature-controlled shaker. This allowed the siRNA molecules to come to equilibrium between the two phases. After removal from the shaker, the tubes were centrifuged using the benchtop centrifuge for a few seconds to separate the OSP and PSO layers.

The lipophilicity of the natural and modified HPV 16+24 AS sequences were used, as shown in Table 5-1. The amount of radiolabeled siRNA in each layer was determined using a liquid scintillation counter. (Section 2-1) 120 μ L of the octanol layer were removed from each tube and added to liquid scintillation vials containing 15 μ L of fresh OSP buffer. 15 μ L of the potassium phosphate layer were removed from each tube and added to liquid scintillation vials containing 120 μ L fresh PSO buffer. This was done to avoid any possible differences in quenching. Five milliliters of liquid scintillation fluid was added to each vial. Three vials containing 5 mL liquid scintillation fluid, 15 μ L fresh OSP, and 120 μ L fresh PSO were used as background control samples. The amount of radioactivity in each vial was determined using a Beckman Coulter L-6000 Liquid Scintillation Counter, located in the Dong Lab in the

Department of Biology, Duke University. The partition coefficient (K_{ow}) was defined as the ratio of the amount of siRNA present in the organic phase to the amount present in the aqueous phase.

5.3.3 Results and Discussion

Single stranded HPV 16+24 antisense siRNAs were enzymatically synthesized and purified as discussed in Chapter 3 and radiolabeled using [γ - ^{32}P]-ATP as discussed in Chapter 2. For this application, it was especially important to fully remove unincorporated radiolabeled ATP from the full length RNA, because the lipophilicity of the triphosphate is much lower than that of the oligonucleotide. This disparity is caused by the difference in charge/base ratio. (Dagle, et al. 1991)

The passive transport of an oligonucleotide depends on two factors: the partition coefficient and the diffusion coefficient. (Stein 1986; Dagle, et al. 1991) The diffusion coefficient relies on membrane properties and the volume of the molecule. Consequently, the ability of modified siRNA to diffuse through plasma membranes can be regarded as solely dependent on the partition coefficient. In this work, it is assumed that the 1-octanol is similar to the plasma membrane in hydrophobicity (Dagle, et al. 1991). This assumption allows us to measure the ability of the modified siRNA to enter the hydrophobic environment via its partition coefficient, mimicking passive transport across a cell membrane. The partition coefficient (K_{ow}) was calculated by determining

the ratio of siRNA present in the octanol layer to the siRNA present in the aqueous layer. (Equation 5-1)

$$K_{ow} = \frac{RNA_{Octanol} \text{ (cpm)}}{RNA_{Phosphate \text{ buffer}} \text{ (cpm)}} \quad \text{Eqn 5-1}$$

The partition coefficients for the modified siRNAs are shown in Table 5-4. Also shown is the relative partition coefficient with respect to the normal, unmodified siRNA. Since lipophilicity is sequence-dependent, we can not directly compare the Kow of this sequence to literature values, because the lipophilicity experiments have not been performed previously. However, the Kow of the natural sequence is similar to other siRNA sequences found in literature (Dagle, et al. 1991).

Table 5-4. Partition coefficients for natural and modified ³²P-labeled HPV 16+24 siRNA. 1x10⁵ cpm of siRNA was used for each experiment. The sequences and modifications are given in Table 5-1. The Kow value is the average of at least three lipophilicity experiments.

RNA (% BP)	Kow	Relative Kow
Normal (0)	1.29 ± 5 × 10 ⁻³	1
1B (24)	2.20 ± 8 × 10 ⁻³	1.7
2B (43)	1.42 ± 3 × 10 ⁻²	11.0
3B (81)	3.24 ± 9 × 10 ⁻²	25.1
4B (100)	7.68 ± 2 × 10 ⁻²	59.6
F	1.47 ± 4 × 10 ⁻³	1.1
FB	1.90 ± 5 × 10 ⁻³	1.5

There is a clear trend that increasing the amount of boranophosphate modification increases the lipophilicity of siRNA. Figure 5-9 shows the log of the partition coefficient plotted against the percentage of linkages that are boranophosphate modified. Modification of the 2' positions does not appear to significantly impact the partition coefficient, but addition of the boranophosphate to the 2' fluoro-modified sequences increases the lipophilicity of the molecule.

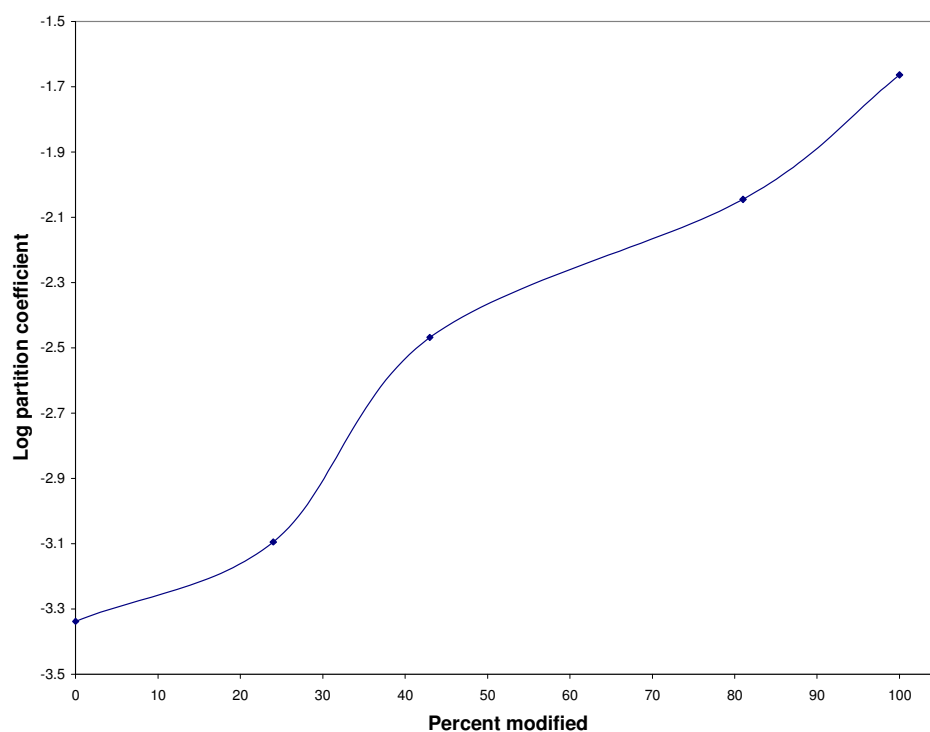


Figure 5-9. Effect of boranophosphate modification on the partition coefficients of siRNA. 5' end labeled siRNAs were shaken vigorously for several hours in the presence of 1-octanol and 1.0 M potassium phosphate buffer.

It was found earlier that an RNA sequence that was 41% modified showed an 18-fold increase in partition coefficient. (Wan 2005) The data presented here is consistent

with that previous data; the 2B sequence that is 43% modified showed an 11-fold increase in partition coefficient. Overall, the trend exhibited here suggests that increasing the amount of boranophosphate modification leads to an increase of the partition coefficient of the molecule, and consequently, increases its lipophilicity. Since it is necessary for the siRNA molecules to gain access to the RISC machinery in the cytoplasm in order to participate in the RNAi pathway, increased lipophilicity, and therefore easier delivery, of the siRNA molecules may increase their gene silencing activity.

It may be concluded that addition of the boranophosphate modification to 2'F modified RNA can increase the lipophilicity as well. However, we predict that for the 2'F RNA sequence to achieve the highest lipophilicity, it would be necessary to synthesize nucleotides that contain both the 2'F ribose modification and the α -P-boranophosphate modification. These doubly modified nucleotides could be incorporated into modified siRNA, and the lipophilicity, as well as other chemical and biological properties, could be determined.

5.4 Chapter Summary

The work described in this chapter evaluates the effect of the boranophosphate and 2' fluoro/boranophosphate modifications on the chemical, endonuclease, and

exonuclease stability of siRNA, as well as the effect on lipophilicity. As described by the chemical hydrolysis assay used in this work, the boranophosphate does not significantly impact the chemical stability of siRNA, nor does the 2' fluoro modification. Addition of the boranophosphate modification increased the stability of the siRNA to the endonuclease RNase A; however, the greatest increase to endonuclease stability was imparted by the 2' fluoro modifications. The modification of the siRNA in non-terminal positions did not significantly affect the stability of the molecule to Exonuclease T, which cleaves DNA and RNA at the 3' ends. Addition of the boranophosphate modification at the terminal position did increase the exonuclease stability. The lipophilicity of the siRNA increased with increasing percentage of boranophosphate modifications. It is hoped that this will allow for easier passive diffusion of the molecule through the plasma membrane and therefore increase cellular delivery. An increase in cellular delivery may correlate with an increase in gene silencing activity through the RNAi pathway.

6. Site specific modification of boranophosphate siRNA using T4 RNA ligase

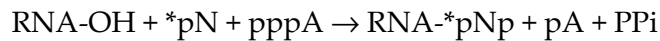
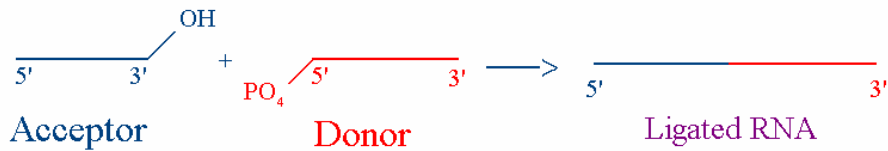
Heretofore, all BP-modified RNA has been synthesized using polymerases to uniformly introduce the modification on one or more NTPs. In this section, the ability of ligases to create boranophosphate modified RNA with site-specific modifications was investigated.

6.1 Introduction

Despite the discovery of numerous base, backbone, and sugar modifications, there has been no description of a “perfect” modification. Instead, each modification has advantages and disadvantages that must be weighed to determine its appropriateness for a given application (Kurreck 2003). The combination of modifications has allowed scientists to optimize oligonucleotides for selected tasks (Dutkiewicz, et al. 2008; Potenza, et al. 2008). It has been shown that the most potent siRNA *in vivo* are those that contain no modification in the middle of the strand (especially at residues 10 and 11, where cleavage of the mRNA target occurs) and contain modifications at the ends of the strands to prevent nuclease degradation (Manoharan 2007). For that reason, it is desirable to create these chimeras, or “gapmer” siRNA molecules to yield siRNA that has the highest potency and longest persistence in the cell. Gapmers containing 2'F and *Rp/Sp* phosphorothioate modifications have been made using chemical synthesis (Monia, et al. 1993; Manoharan 1997). However, as discussed in Chapter 3, the borane

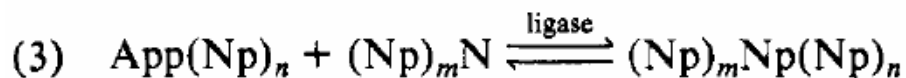
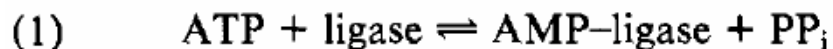
moiety does not yet lend itself well to chemical synthesis of oligonucleotides. The work discussed in the previous chapter used enzymatic transcription to create stereoregular boranophosphate-modified siRNA, which can only yield siRNAs that are modified throughout their length. Also, there has been no investigation of the effect of *Sp* and *Rp* configuration on the silencing ability of backbone modified siRNA molecules. Therefore, we turned our attention to RNA ligases, in particular T4 RNA ligase, in order to site-specifically modify boranophosphate siRNAs to increase the potency of the siRNA effect while retaining the advantages of stereoregularity, nuclease stability, and increased lipophilicity.

First described by Silber *et al* in 1972, T4 RNA ligase has the ability to form a 5'→3' phosphodiester bond between two RNA molecules (Silber, et al. 1972). The enzyme requires a donor molecule containing a 5'-phosphate and an acceptor molecule containing a 3'-hydroxyl, as shown in Scheme 6-1. The reaction requires ATP and Mg²⁺, and for every 5'-phosphate terminus rendered resistant to alkaline phosphatase, an equal amount of AMP and inorganic phosphate (PPi) are formed (Bryant, et al. 1982).



Scheme 6-1. Ligation reaction using T4 RNA ligase. Two molecules of RNA can be joined with a phosphodiester bond. The acceptor molecule contains a 3' hydroxyl and the donor molecule contains a 5' phosphate. The reaction is ATP and magnesium dependent.

The ligation reaction using normal RNA molecules can be carried out at very low RNA concentrations (i.e. 3 μM) and can give the desired product in high yield (>70%) (Uhlenbeck 1977). The enzyme can catalyze the formation of a 3'→5' phosphodiester bond with an acceptor RNA as short as trinucleotide bisphosphates and a donor mononucleoside 3', 5'-bisphosphate (Hinton, et al. 1982; Romaniuk, et al. 1982). The mechanism of the reaction is shown in Scheme 6-2.



Scheme 6-2. T4 RNA ligase mechanism. 1) Formation of adenylated enzyme. 2) Transfer adenyl group from enzyme to 5' phosphate of donor via a 5' → 5' anhydride linkage. 3) 3'-OH acceptor displaces AMP from activated donor and forms bond. Figure adapted from Bryant, et al. 1982.

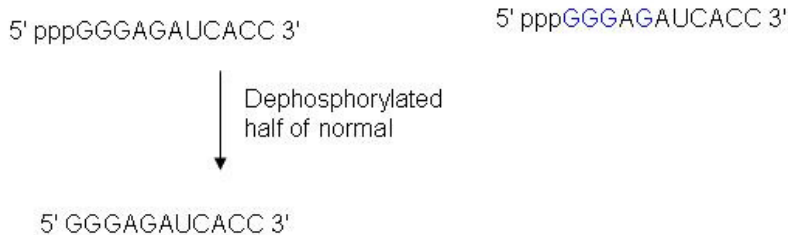
Using T4 RNA ligase is convenient for synthesis of short oligonucleotides of defined sequence and also for the addition of radioactive labels into an RNA molecule

(England, et al. 1980; Hinton, et al. 1982). The yield is directly dependent on the amount of ligase present in the reaction mixture. As a starting point for gapmer synthesis, the ligation reaction was tested using an RNA that began with GTP α B to evaluate the ability of the T4 RNA ligase to utilize a boronated RNA as a donor.

6.2 Experimental Procedures

The experiments described in this chapter are illustrated in a flow chart (Figure 6-1). An 11mer RNA transcript (5' G GGA GAU CAC C 3') was enzymatically synthesized for use in the ligation reactions. The transcriptions were carried out as described in Chapter 3. Normal and GTP α B- substituted 11mer transcription reactions were incubated at 37°C for 4 and 6 hours, respectively. The 11mer natural and boranophosphate modified RNA transcripts were purified with phenol extraction, microcolumn purification, and YM-3 filtration. Both normal RNA and GTP α B modified RNA were used to test the ligation reaction. 10 nanomoles of normal 11mer RNA was dephosphorylated on the 5' end using alkaline phosphatase. This dephosphorylated normal RNA was used as the 3' hydroxyl acceptor because it lacked the 5' phosphate that is required to act as the donor. The 5' phosphate donor molecule (in RNase-free water) was: 1) normal phosphorylated 11mer RNA of the same sequence, or 2) boranophosphate RNA that was modified with GTP α B, began with a GTP α B, and carried a 5' boranophosphate group. T4 RNA ligase (20 units/microliter) and 10X ligase

**11mer Transcription and Purification:
Normal and GTP α B modified**



**Ligation:
Normal and GTP α B modified**



**Labeling:
Normal and GTP α B modified**

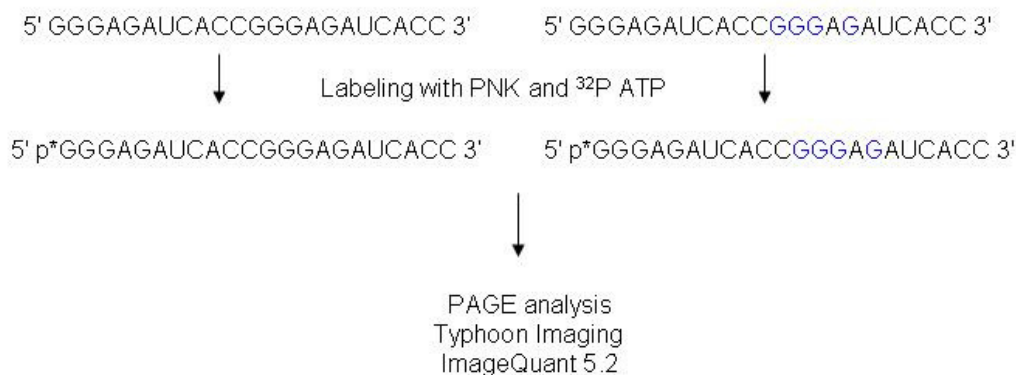


Figure 6-1. Experimental flow for the T4 RNA ligation experiments using normal and boranophosphate modified siRNA. The acceptor molecule was dephosphorylated, unmodified 11mer RNA. The donor molecule was 11mer RNA that was either unmodified or GTP α B modified. The product of the ligation reaction was radiolabeled with [γ -³²P]ATP and PNK and was separated on a 20% PAGE/7 M urea sequencing gel. The radioactivity was detected using a low-energy phosphor screen and imaged using the Typhoon instrument. The data was quantified using ImageQuant 5.2.

reaction buffer (500 mM Tris-HCl pH 7.8 at 25 °C, 100 mM MgCl₂, 10 mM ATP, and 100 mM DTT) was obtained from New England Biolabs.

The ligation reactions included the donor and the acceptor, T4 RNA ligase, and T4 RNA ligase buffer. Several sets of ligation reaction conditions were tested. The first set of conditions was taken from the ligation protocol that accompanied the T4 RNA ligase. This protocol suggested a 50 µL reaction volume with an 11mer RNA concentration of 10 µM (~1.76 µg). This concentration was determined using the Nanodrop spectrophotometer and placed in 1X ligase buffer in a 500 µL polypropylene centrifuge tube. One microliter (20 units) of ligase was added and the reaction mixture was incubated at 37°C in the Dry Bath Block Heater for 15 minutes. Longer incubations (up to 24 hours), increased ligase concentrations (60 units), and increased RNA concentrations (4 µg) at that temperature were also tested. At each time point, 5 µL of the reaction mixture was removed from the stock solution, radiolabeled, mixed with gel loading solution, and frozen for later PAGE analysis. The amount of radiolabeled, ligated product was determined using 20% PAGE/ 7M urea electrophoresis to separate the ligated 22mers from the unligated 11mer starting products. The ligation reaction time points were 0 hour, 15 min, 45 min, 1 hour, 2 hours, 4 hours, 8 hours, 12 hours, 16 hours, and 24 hours.

The second set of reaction conditions was taken from the ligation protocol found in the 2002 edition of Current Protocols in Molecular Biology. This set of conditions also

had a reaction volume of 50 μL , but required higher concentrations of RNA ($\sim 23 \mu\text{M}$) and a lower incubation temperature (22°C). Incubations were carried out using a Dry Bath Block Heater that was set up in the cold room, adjusted to the appropriate temperature, and time points were taken from the stock solution for up to 24 hours. At each time point, 5 μL of the reaction mixture was removed, radiolabeled, mixed with 2X gel loading solution and stored at -20°C for later analysis by PAGE. The time points were 0 min, 15 min, 45 min, 1 hour, 2 hours, 4 hours, 8 hours, 12 hours, 16 hours, and 24 hours.

The 20% PAGE/7 M urea sequencing gel was cast as described in Chapter 2 and pre-run in 1X TBE for two hours at 30 W for 2 hours and then loaded with the sample and run at 30 W for two hours. Afterwards, the gel was removed from the plate, wrapped in Saran wrap, and exposed to the low-energy phosphor storage screen overnight at 4°C . The screen was imaged using the Typhoon phosphoimager. Band intensities that correlated to the 11mer starting material or 22mer ligated product were measured using ImageQuant 5.2. The yield of the reaction was determined by Equation 6-1.

$$\% \text{ extended} = \frac{\text{Band intensity of } 22\text{mer}_{t=24 \text{ hours}}}{\text{Band intensity of } 11\text{mer}_{t=0}} \quad \text{Eqn 6-1}$$

6.3 Results

The ability of T4 RNA ligase to utilize GTP α B modified RNA as a donor in the RNA ligation reaction was investigated as an alternative method to enzymatically synthesize boranophosphate siRNA. The final product of the reaction should consist of a 22 nucleotide RNA with GTP α B modifications near the 3' end. (Figure 6-2)

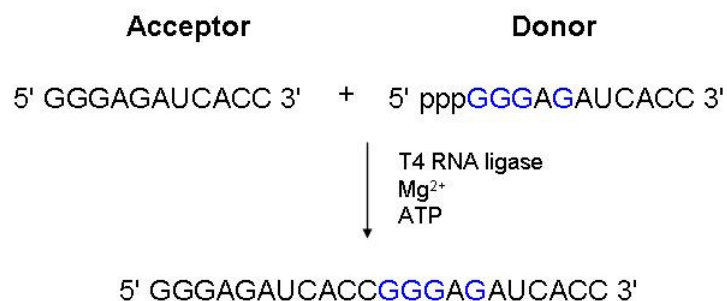


Figure 6-2. Expected product of the T4 RNA ligase reaction with 5' ppp boranophosphate donor RNA. The ligase is magnesium and ATP dependent and yields the ligated 22mer, AMP, and pyrophosphate. Boranophosphate modifications are shown in blue.

Normal and boranophosphate 11mers were prepared enzymatically and purified. From the PAGE analysis shown in Figure 6-3, it is clear that the T7 RNA pol added 1-2 extra nucleotides (non-templated addition) on the end of the 11mer transcription, since there are 3 bands, the darkest of which is where the 11mer should be, and two lighter bands above it (putatively, 12mer and 13mer). (Figure 6-3) However, the purity of the 11mer sample was not of much consideration, because extra bases on the 3' end should not influence the ligation reaction. For the normal/boranophosphate ligation, any sequence that was able to act as the donor would have to start with the 5'-

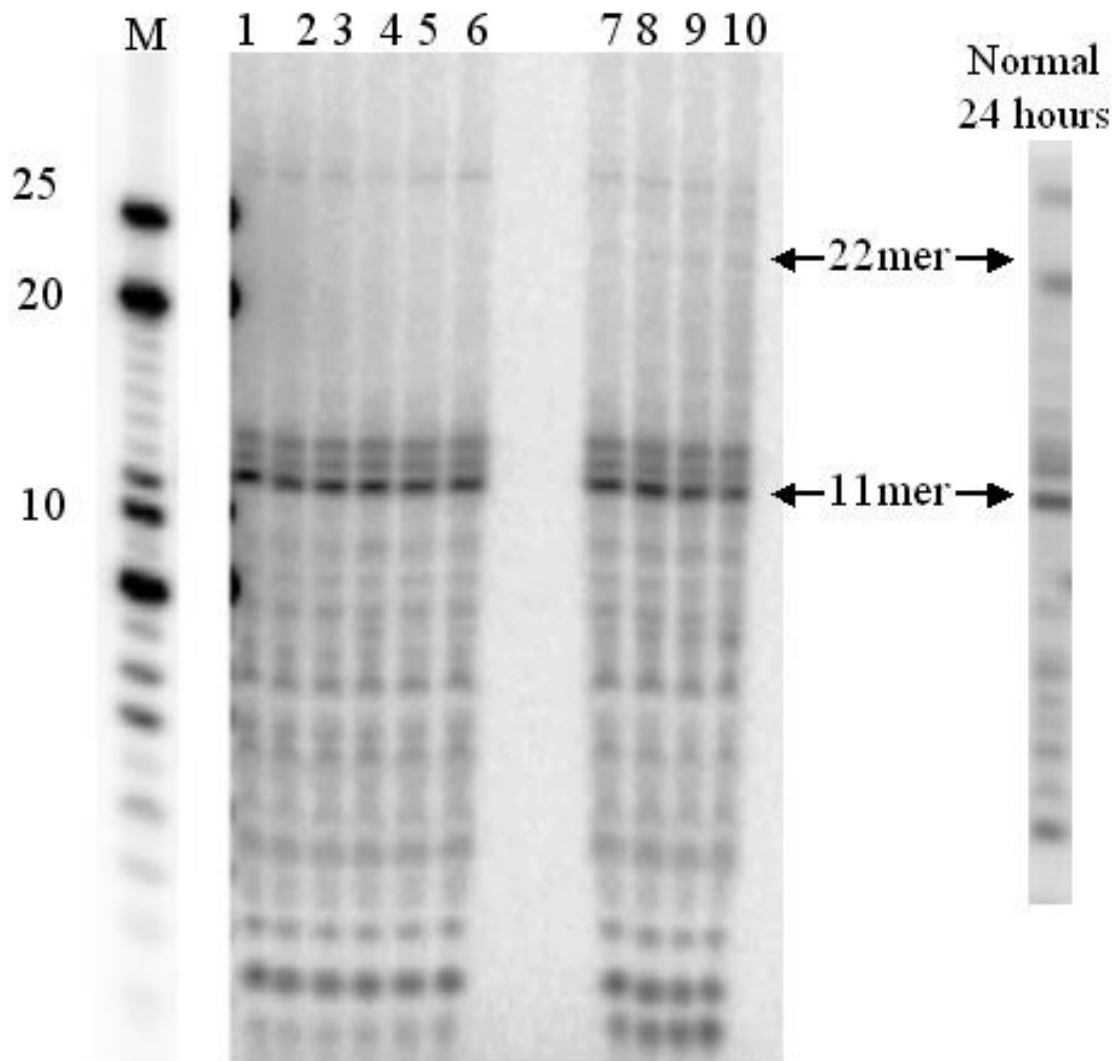


Figure 6-3. Products of ligation of a normal acceptor and a boranophosphate donor using T4 RNA ligase were run on 20% PAGE/7 M urea. The marker lane is denoted by M. Radiolabeled single stranded DNA dT standards were used as markers, 10, 20, and 25. A comparison lane is shown on the right using normal acceptor and normal donor at after 24 hours of incubation from a separate gel. Time points are: 1) 0 min, 2) 15 min, 3) 30 min, 4) 1 hour, 5) 2 hours, 6) 4 hours, 7) 8 hours, 8) 12 hours, 9) 16 hours, 10) 24 hours. The 11mer and 22mer bands were quantified using ImageQuant 5.2. Post quantification, the image was darkened to make faint bands more visible to the human eye.

GTP α B modification, as the normal 11mer was dephosphorylated to ensure it could not act as a donor. It was assumed that dephosphorylation was complete, as per the activity of the enzyme. If this was not the case, there may be a small amount of normal, phosphorylated 11mer RNA that could react as the donor in the ligation experiment.

The ligation conditions are shown in Table 6-1. The New England Biolabs protocol recommended incubation at 37°C for 15 minutes. The Short Protocols in Molecular Biology recommended incubation at 22°C for 22 hours. Both sets of reaction conditions were tested at high and low RNA and ligase concentrations over 24 hours.

Table 6-1. The four sets of ligation reaction conditions that were tested to achieve ligation of 11mer boranophosphate RNA donor molecules to 11mer unmodified acceptor molecules using T4 RNA ligase. The reaction was monitored over time and analyzed using 20% PAGE. Yields for the reactions are shown in as percent of starting materials as determined by quantification of ligated product bands shown in Figure 6-3.

Set	Donor Mod ^a	Donor RNA ^b (μ g)	Acceptor RNA (μ g)	Ligase (units)	Temp (°C)	% extended at 24 hours
1	None	1.76	1.76	20	37	0
	GTP α B	1.76	1.76	20	37	0
2	None	1.76	1.76	20	22	0
	GTP α B	1.76	1.76	20	22	0
3	None	4.0	4.0	60	37	0
	GTP α B	4.0	4.0	60	37	0
4	None	4.0	4.0	60	22	54%
	GTP α B	4.0	4.0	60	22	7%

a) Unmodified, natural RNA is referred to as "None" and boranophosphate modified RNA is referred to "GTP α B"

b) 1.76 μ g = 500 pmoles, 4.0 μ g = 1.1 moles

The RNA used under all four conditions was 11 nucleotides long. The first, second, and third sets of ligation conditions were set up as shown in Table 6-2 and described in the text. The T4 ligase reaction was incubated and 5 μ L aliquots were taken at time points for up to 24 hours. However, these reaction conditions yielded no ligated product (Table 6-1). The fourth set of reaction conditions, 4 μ g of RNA donor and acceptor, 60 units of ligase, and 22°C incubation yielded a small amount of ligated product for reactions with the normal acceptor and both the normal and the boranophosphate donor molecule. (Figure 6-3) The yield was determined as the percentage of the initial amount of the 11mer acceptor molecule that was ligated during the reaction. (Equation 6-1)

The ligation reaction using the boranophosphate donor yielded significantly less full-length product than the comparison reaction using normal donor. However, these experiments did not lend themselves to quantitative description of the yield of the ligation reaction. Yield was determined as the % ligation of the labeled, unmodified acceptors. For the normal after 24 hours, 54% of the unmodified starting material had ligated, while for the borano modified donor it was only 7%. These experiments work as proof of principle that T4 RNA ligase can accept GTP α B modified donor molecules.

6.4 Discussion

The work presented in this chapter is the first description of a successful ligation reaction using a GTP α B modified donor molecule. The yield of the ligation reactions was very low, and overall, it was appeared as if RNA modified with GTP α B was not as well tolerated by T4 RNA ligase as the unmodified donor. Still, these experiments are proof of principle only, and further studies are necessary.

The yield of the T4 RNA ligase reaction can depend on several factors that are related to the RNA and its sequence. First, the concentration and ratio of donor and acceptor molecules can affect the yield (Uhlenbeck and Cameron 1977). Second, the presence of secondary structure at the 3' terminus of the RNA will likely inhibit the RNA ligase reaction. This is unlikely in the case of small 11mer sequence used in this experiment. Third, the T4 RNA ligase shows a preference for single stranded RNA (ssRNA) versus single stranded DNA (England, et al. 1980). Also, the nucleotide sequence at the 3' terminus influences the reaction. It has been shown that oligomers with uridine in one of the three 3' terminal positions are poorer acceptors than molecules lacking uridine. For this reason, there were no uridine residues at these positions when the ligase test sequence was designed. Finally, RNA molecules with a free 5' phosphate near to the 3' ends show low reaction yields, probably due to competitive intramolecular cyclization (England and Uhlenbeck 1978). For this reason, the unmodified acceptor 11mer was dephosphorylated at the 5' end using Antarctic phosphatase, putatively to

100%, even though an intramolecular circularization was unlikely to occur with such a short sequence.

The chirality of the α -phosphorous introduced by the borano modification in the phosphodiester linkage is unlikely to be the culprit in the low reaction yield. It has been shown that T4 RNA ligase prefers phosphorothioate oligonucleotide substrates with *Rp* configuration, which is the *Sp* configuration in boranophosphate modified molecules (Bryant and Benkovic 1982). Since the T7 enzymatic transcription proceeds through a mechanism that converts the *Rp* NTP α B analogs into *Sp* BP linkages in modified oligonucleotides, T4 RNA ligase is hypothesized to accept the BP RNA on grounds of chirality.

Several factors that are related to the reaction set up can contribute to low yield, including T4 ligase inhibitors such as ammonium ions, low substrate concentration, and low enzyme concentration (England, et al. 1980). In contrast to literature, which described ligation of normal RNA at low concentrations, the ligation of boranophosphate RNA showed that increasing both substrate and ligase concentrations improved the yield of the reaction in this experiment. It is possible that the GTP α B carries triethylamine (TEA) cations as counterions due to the HPLC purification process required to separate the stereoisomers. These cations have been shown to inhibit ligase activity. (Middleton, et al. 1985) It is recommended that future experiments utilize

further methods of oligonucleotide purification to ensure that no TEA cations remain in the samples.

6.5 Chapter Summary and Future Work

The experiments described in this chapter lay the groundwork for the future synthesis of RNA that is boranophosphate modified in a site-specific manner. Four different reaction conditions were tested to determine the best parameters for the ligation experiments. Evidence favors the hypothesis that T4 RNA ligase can accept an 11mer donor molecule that is 5' modified with GTP α B and contains a BP modification on the 5' end in a reaction that contains 4 μ g of RNA and 60 units of T4 RNA ligase after incubation for 24 hours at 22°C. However, the 22mer ligated product must be analyzed to ensure that it contains boranophosphate linkages. This may be done using a 3' exonuclease, since it has been shown that boranophosphate linkages are resistant to hydrolysis by these enzymes.

In order for this work to be applicable to the site-specific modification of boranophosphate modified siRNA, the other three NTP α B analogs must also be tested to see if they can be used as donors, using optimized ligation conditions. Then all four NTP α B analogs should be tested to see if they can be used as acceptors. In this way, it will be possible to place a single boranophosphate modification anywhere in an siRNA strand, although it may take more than one ligation to produce if some NTP α B analogs

are not amenable to usage as donors or acceptors (England and Uhlenbeck 1978).

However, it has been shown that purines in the acceptor and pyrimidines in the donor result in higher reaction yields (England and Uhlenbeck 1978; Romaniuk, et al. 1982).

Further, the creation of gapmer siRNA consisting of boranophosphate modified wings with an unmodified center will require two ligations and will be facilitated if every NTP α B analog proves to be a viable substrate for T4 RNA ligase

Finally, the chirality of the linkage remains undetermined. It is recommended that NMR be used to characterize the linkage that is formed by T4 RNA ligase using boranophosphate donors. This may be done using short oligonucleotides ligated by T4 RNA ligase. It remains to be determined if the stereochemistry of the linkage significantly impacts the biological properties of the siRNA, as discussed in Chapter 4 and 5.

7. Biological Applications of Boranophosphate siRNA

The end goal of the synthesis and characterization of modified RNA is to extend the biological and pharmacokinetic properties of RNA as a therapeutic tool. This chapter will describe the biological systems in which BP-RNA has been tested. The end goal of this project is to produce boranophosphate modified RNA interference sequences to use in downregulation in gene expression in human disease, notably viruses and cancers.

7.1 Boranophosphate siRNA for use against human papillomavirus

7.1.1 Introduction

Human papillomavirus (HPV) is a member of a family of small DNA tumor viruses that can infect cervical epithelial tissue and has multiple clinical manifestations, including a subset with the potential to progress to invasive cervical cancer (zur Hausen 2003). The HPV genome encodes eight proteins: six viral proteins and two capsid proteins (Figure 7-1).

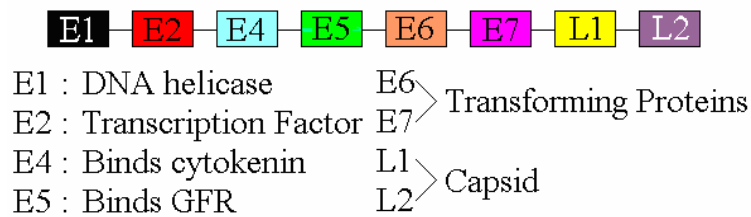


Figure 7-1. The proteins encoded by the HPV genome. HPV encodes six viral proteins and two capsid proteins. The viral oncoproteins are E6 and E7 are the target of this project.

HPV must make use of cellular replication enzymes to reproduce. It is this interference with the cell cycle that leads to the cancerous transformation. The proteins responsible are the oncoproteins E6 and E7, which are expressed bicistronically (on the same mRNA). They have varied functions, including cell immortalization, antiapoptotic effect, and enhancement of foreign DNA integration and mutagenicity (Sheffner and Whitaker 2003; zur Hausen 2003). E7 interferes with the molecules that regulate mammalian cell cycle between G1 and S phase and differentiation of tissue types. This interference is diagrammed in Figure 7-2.

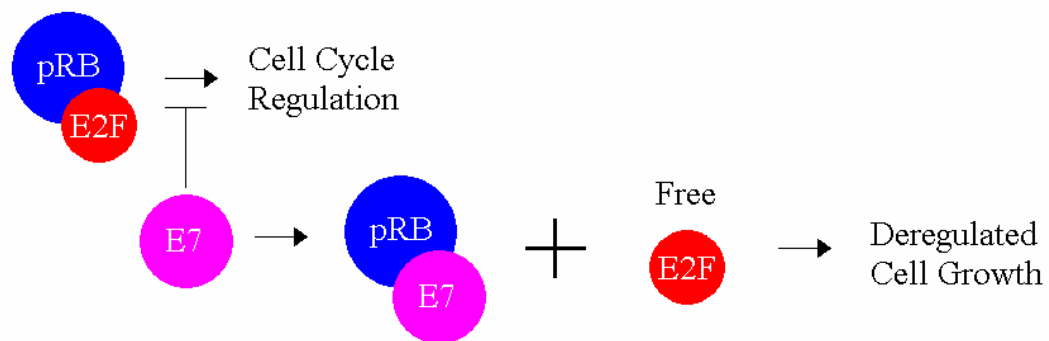


Figure 7-2. HPV oncoprotein E7 interferes with E2F, a molecule that regulates mammalian cell cycle. A cellular transcription factor, E2F is released from its inert, bound form upon E7 binding to pRB. The free E2F activates the cell cycle and leads to deregulated cell growth.

E2F is a transcription factor that activates the cell cycle. Normally it is bound to pRB, a retinoblastoma phosphoprotein localized in the nucleus, preventing E2F from promoting cellular growth. In an HPV infected cell, the viral protein E7 binds to pRB and releases E2F, which pushes the cell towards the S-phase of the cell cycle. The S-phase is when DNA replication occurs, allowing HPV to make use of cellular replication enzymes to copy its own genes. However, cells pushed towards S-phase then continue the cell cycle, leading to deregulated cell growth. In a normal cell, deregulated cell growth causes the release of cellular protein p53, a tumor suppressor that induces the cell to undergo apoptosis, or programmed cell death. The oncogenic viral protein E6 interacts with p53 to block apoptosis, leading to hypergrowth (Scheffner 2003). (Figure 7-3)

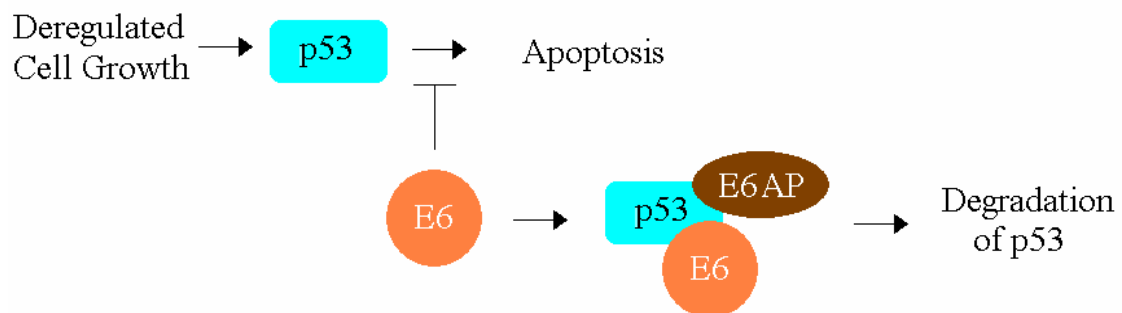


Figure 7-3. HPV oncoprotein E6 blocks programmed cell death (apoptosis) by interaction with tumor suppressor p53. E6 binds to p53 and recruits E6AP, a protein that ubiquitinates the complex, tagging it for degradation through the proteasome.

E6 binds to p53 and recruits another protein E6AP to form a trimeric complex.

The E6AP protein serves as an ubiquitinated tag, alerting the cell to break down the complex including p53 via proteasome degradation. Since cell growth is overstimulated

and the deregulated cells do not die, the cancerous transformation of the infected cells is complete.

It has been shown that siRNA can be used to silence E6 and E7 expression by targeting the mRNA that encodes both proteins (Hall and Alexander 2003). Previous work by the Alexander and Shaw lab in a reporter system using a green fluorescent protein expression in HeLa cells showed increased potency of RNAi using enzymatically boranophosphate siRNA versus unmodified, chemically synthesized double-stranded siRNA (Hall 2006). The goal of the work presented in this section was to utilize the boranophosphate modification to increase the potency and persistence of the downregulation of the HPV oncoproteins E6 and E7.

7.1.2 Experimental Procedures

The work presented in this chapter was done in collaboration with the laboratory of Dr. Kenneth A. Alexander, Department of Pediatrics, University of Chicago Medical School. The desalted DNA templates were purchased commercially from Operon as a single-stranded template and a single-stranded promoter. They were dissolved in deionized water to a concentration of 100 μ M. Equimolar amounts of template and promoter were annealed by heating to 90°C and then slowly cooling on the bench top. Klenow fragment ExoMinus DNA polymerase was used to produce fully double-stranded DNA templates to produce the required siRNA sequences. The purity of the DNA template was checked on a native 4% NuSieve agarose gel. The sequence used for

this work was the HPV 16+24+G sense and antisense siRNA and control sequences, as shown in Table 7-1. The control sequences contain the same ratio of bases as the active sequences, but contain a mismatch region in the center of the strand that should fully obviate the efficacy of mRNA target hybridization.

Table 7-1. siRNA sequences used in HeLa cell culture assays

Name	Sequence
HPV 16+24+G S	GCAGAGACAACUGAUCUCUCUU
HPV 16+24+G AS	GAGAGAU CAGUUGUCUCUGGUU
HPV 16+24+G S Control	GCAGAGAACCGAU AUCUCUCUU
HPV 16+24+G AS Control	GAGAGAU AUCGGUUCUCUGGUU

The boranophosphate siRNA sequences were modified using GTP α B, ATP α B, or GTP α B + ATP α B. The fluoro/borano siRNA sequences were modified using 2' F CTP, 2'F UTP, and GTP α B. The synthesis of the modified NTPs was discussed in Chapter 3 and was performed by Marcus Cheek and Laura Moussa. The siRNAs were transcribed and purified with phenol extraction and microcolumn purification as discussed in Chapter 3. The concentration of the final product in RNase-free water was determined by measuring the UV concentration using the Nanodrop and Varian spectrophotometers. Double stranded siRNA were prepared by dissolving equimolar amounts of the single strands in 5X annealing buffer. The mixture was heated quickly to 90°C and allowed to cool slowly on the benchtop to allow formation of the double stranded siRNA duplex.

Cell studies were performed in the Alexander lab using HeLa, SiHa, and W12E cells. The inhibition of cell growth was monitored using a cell proliferation assay that measured the amount of [³H] thymidine uptake of the cells to determine the rate of DNA synthesis and therefore the overall effect of the siRNA on cell growth. The siRNA were delivered into the cells using the cation lipids Lipofectamine 2000.

7.1.3 Results and Discussion

The work presented in this section describes the first time that single-stranded boranophosphate siRNA and fluoro/borano siRNA have been used to downregulate gene expression of a virus, in this case the oncogenes E6 and E7 of human papillomavirus. Natural, boranophosphate modified, and fluoro/borano modified siRNA with the sequence HPV 16+24+G was prepared in good yield by enzymatic transcription and purified by G-25 microcolumn. These samples are not quite as pure as those that were further purified using the YM-3 filtration, but this did not appear to affect the ability of the siRNA to show potent gene silencing effects. The products of the transcription were electrophoresed on 20% PAGE/7 M urea gels. (Figure 7-4) The siRNA samples, in RNase-free water, were sent to the Alexander lab on dry ice.

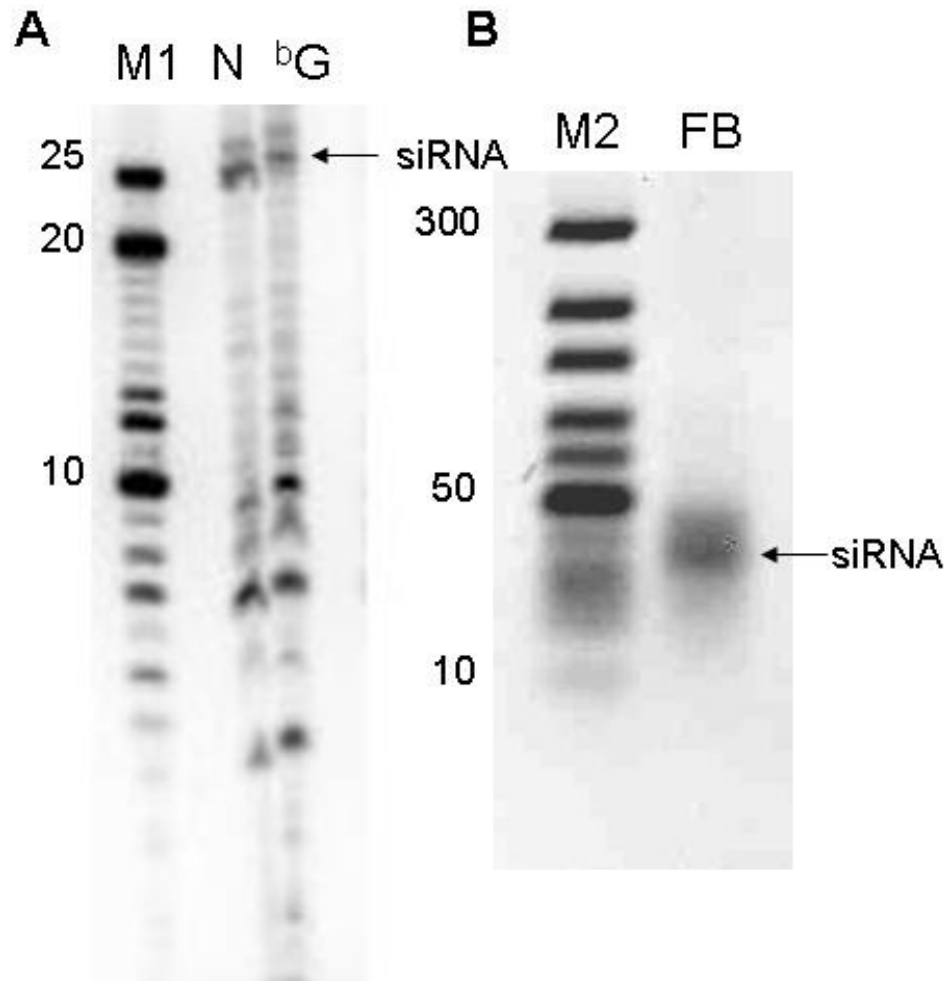


Figure 7-4. Products of T7 RNA polymerase transcription using normal and modified NTPs on 20% PAGE/7 M urea gels. A) ^{32}P -labeled normal (N) and GTP α B modified (^bG) HPV 16+24 AS single stranded siRNA is indicated. M1 is the marker lane: single stranded dT standards that were radiolabeled. The gel was quantified using the Typhoon phosphoimager B) Ethidium bromide labeled 2'fluoro/borano (FB) HPV 16+24 AS single stranded siRNA is indicated. M2 is the marker lane: GeneRuler DNA Ladder, Ultra Low Range (Fermentas)

The *in vitro* data was collected by the Alexander Lab. Two cell lines were used to assay the effects of the boranophosphate modified siRNA to ensure that the silencing that was observed was not an artifact of a particular cell line. The cell lines that were

used were SiHa and W12E cells. SiHa cells are a line of squamous cell carcinoma grade II (Friedl 1970). W12E cells are cervical epithelial cells that are infected with HPV. Both cell lines have been used previously to show that unmodified siRNA can silence expression *in vitro* of E6 and E7, restoring normal growth and morphology (Hall 2003).

Single stranded boranophosphate siRNA showed increased potency of E6 and E7 silencing compared to the unmodified double strand in W12E cells. (Figure 7-5)

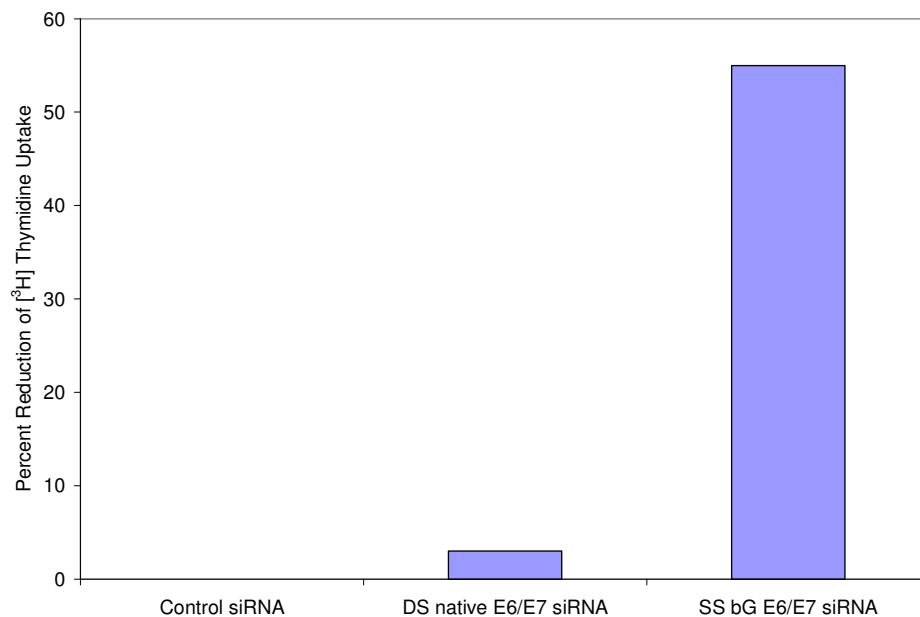


Figure 7-5. W12E cell proliferation assay after administration of 20 nM HPV 16+24+G siRNA (as shown in Table 7-1 and 7-2). Double stranded control, double stranded unmodified (native), and single stranded GTP α B modified siRNAs were transcribed in the Shaw lab and tested by the Alexander lab.

Clearly the single-stranded GTP α B modified siRNA delivered by Lipofectamine 2000 can most potently inhibit the proliferation of cervical epithelial cells infected with HPV. Since deregulated growth is the first step towards invasive cervical carcinomas,

this is an important first step in the treatment of HPV with boranophosphate modified siRNA.

Also tested were siRNAs of the same sequence modified with ATP α B or with ATP α B + GTP α B. The placement of these modifications can be seen in Table 7-2.

Table 7-2. Modifications of HPV 16+24+G siRNA used in cell proliferation assays. Boranophosphate modifications are shown in blue and 2' fluoro modifications are shown in red.

Modification	Sequence	# Mod (%)
ATP α B	GAGAGAUCAGUUGUCUCUGGUU	4 (18)
GTP α B	GAGAGAUCAGUUGUCUCUGGUU	7 (32)
ATP α +GTP α B	GAGAGAUCAGUUGUCUCUGGUU	11(50)
2'F CTP + 2'F UTP + GTP α B	GAGAGAUCAGUUGUCUCUGGUU	18 (82)

The comparison of the effect of the three boranophosphate modified siRNAs on cell proliferation of SiHa cells can be seen in Figure 7-6. The cell proliferation data can be found in Appendix II. Overall, it was determined that the sequence that showed the best downregulation of E6 and E7 promoted growth was the siRNA singly modified with GTP α B.

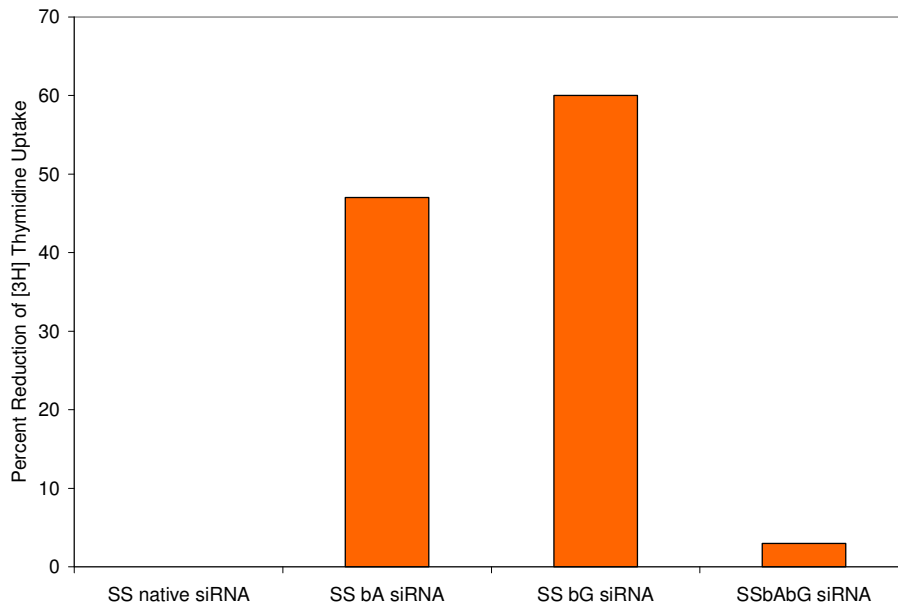


Figure 7-6. SiHa cell proliferation assay after administration of 20 nM modified single stranded siRNA. The single stranded native siRNA was unmodified. The ss bA siRNA was modified using ATP α B. The ss bG siRNA was modified with GTP α B. The ss bAbG siRNA was modified with both ATP α B and GTP α B. The single stranded siRNA was enzymatically transcribed by the Shaw lab and tested in cells by the Alexander lab. The sequences of the modified siRNAs are shown in Table 7-1 and 7-2.

The singly modified siRNA shows increased potency versus normal and doubly modified siRNAs. This data makes sense in light of the work described in previous chapters. Singly boranophosphate modified siRNA retains the ability to hybridize target unmodified RNA with affinity while increasing the nuclease stability of the strand, as demonstrated by the CD and biological stability experiments. Once the guide strand is incorporated into the RISC complex, it is protected from nuclease degradation. It has been shown that the 5' end of the siRNA strand is important for the binding of the siRNA to the RISC complex. Therefore, the increasing amounts of boranophosphate

modification at the 5' terminus may also help account for the decrease in efficacy seen when the siRNA is doubly modified.

A dose response curve performed by Shuhan Yu (K. Alexander, personal communication) showed that the IC₅₀ of the GTP α B modified siRNA was approximately 5 nanomolar. To see if this could be further improved, the 2' fluoro modification was added to the GTP α B modified sequence. However, addition of the 2' fluoro modified nucleotides C and U more than doubled the IC₅₀ to greater than 10 nanomolar. (Appendix II) This is consistent with the work described in Chapter 4, which showed significantly lowered capacity of the fluoro/borano siRNA to bind its unmodified complement and a change toward a more B-form like helix. However the increase in IC₅₀ is not as drastic as one would expect if hybridization affinity were the sole factor in determining the potency of silencing. Therefore, it may be postulated that other characteristics of the fluoro/borano siRNA can counteract the decrease in duplex stability.

The oncoproteins E6 and E7 must be suppressed or destroyed in order to reassert normal control over HPV infected cells. To this end, RNA interference (RNAi) was used to suppress the expression of these proteins by stimulating the degradation of their messenger RNAs (mRNA). In this chapter, it has been shown that the boranophosphate can deal with many of the limitations that are traditionally found when using RNAi. Further, the expected metabolites of the borane modification are non-toxic and it was

shown in Chapter 5 that boranophosphate modifications increase lipophilicity. This could enable the safe vaginal delivery of the siRNA to the target cervical cancer tissue, bypassing the first-pass filtering processes of the liver for treatment of HPV.

Preliminary testing of the boranophosphate siRNA in mouse models has also been undertaken, which should yield valuable information about the BP siRNA *in vivo*.

7.1.4 Summary

The work in this chapter described the use of four types of boranophosphate siRNA to silence the HPV oncogenes E6 and E7 and decrease their proliferative effect. This was done to greatest effect (~60% silencing) using singly modified (GMP α B at 7 positions) boranophosphate RNA and resulted in IC₅₀ values in the low nanomolar range. Attempts were made to further decrease the IC₅₀ with the addition of the 2'F NTP modifications, but the combination of modifications resulted in an increase in IC₅₀, which is not desirable.

7.2 Efforts toward cellular delivery of boranophosphate siRNA

A major stumbling block to the use of siRNA as therapeutic agents is delivery across the cell membrane. The RISC machinery is located in the cytoplasm, necessitating the ability of the RNA to get into the cell.

7.2.1 Introduction

There have been many different approaches utilized to selectively deliver antigens and antisense agents into cells. To this end, cationic lipids, nanoparticles, bioconjugation, aptamers, and many other technologies have been tested for their ability to move siRNA across the cell membrane (Cejka, et al. 2006; Chu, et al. 2006; De Paula, et al. 2007; Juliano, et al. 2008). One promising delivery approach is the liposome-protamine-DNA (LPD) nanoparticles developed in the laboratory of our collaborators in the Huang Lab at UNC. (Li and Huang 2006) It was decided that this approach would be explored to deliver BP siRNA for use in RNAi. A luciferase reporter system in melanoma cells was used to determine the potency of silencing.

LPD nanoparticles are formed by the condensation of long DNA using protamine into micelles (Li and Huang 2006). (Figure 7-7) The siRNA is mixed with the long DNA (from calf thymus) so that it is incorporated into the micelle. Addition of the liposome yields uniform, lipophilic nanoparticles, smaller than 100 μm that can be functionalized with ligands for targeted delivery.

The ultimate goal of the work presented in this section was the delivery of boranophosphate modified siRNA using LPD nanoparticles. The first step towards this goal was testing the BP siRNA in a new luciferase reporter system in melanoma cells.

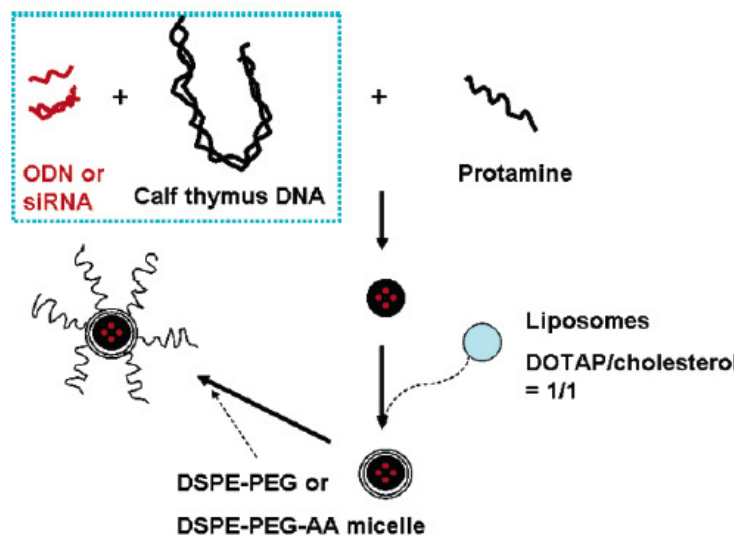


Figure 7-7. Formation of LPD nanoparticles. DNA and the antisense agent are mixed and then condensed using protamine. The micelle is formed after the addition of liposomes, and can be functionalized using ligands. In the case of lung cancer cells, the LPD nanoparticles were functionalized with anisamide (AA), which has been shown to specifically target lung cancer cells. DOTAP = cationic lipid, PEG =polyethylene glycol, DSPE= distearoylphosphatidylethanolamine. Figure from reference. (Li 2006)

7.2.2 Experimental Procedures

The work described in this section was done in collaboration with the laboratory of Dr. Leaf Huang, Department of Pharmacology, University of North Carolina at Chapel Hill. The DNA templates were purchased commercially from Operon as a single-stranded template and a single-stranded promoter. They were dissolved in deionized water to a concentration of 100 μM . Equimolar amounts of template and promoter were annealed by heating to 90°C and then slowly cooling on the bench top. Klenow fragment ExoMinus DNA polymerase (Promega) was used to produce fully double-stranded DNA templates to produce the required siRNA sequences. The purity

of the DNA template was checked on a native 4% NuSieve agarose gel. The sequence used for this work was the Luc RNA shown in Table 7-3.

Table 7-3. Luciferase sequences used in melanoma cell lines.

Name	Sequence
Luc S	CUUACGCUGAGUACUUCGAUU
Luc AS	UCGAAGUACUCAGCGUAAGUU

The boranophosphate siRNA sequences were modified using GTP α B, ATP α B, or GTP α B + ATP α B. The siRNAs were transcribed and purified as discussed in Chapter 3. The concentration of the final product was determined using the UV concentration from the Nanodrop spectrophotometer. The modified siRNA single stranded product is shown in Figure 7-8. Double stranded (ds) siRNA were prepared by dissolving equimolar amounts of the single strands in 5X annealing buffer. The mixture was heated quickly to 90°C and allowed to cool slowly on the benchtop to allow formation of the double stranded siRNA duplex.

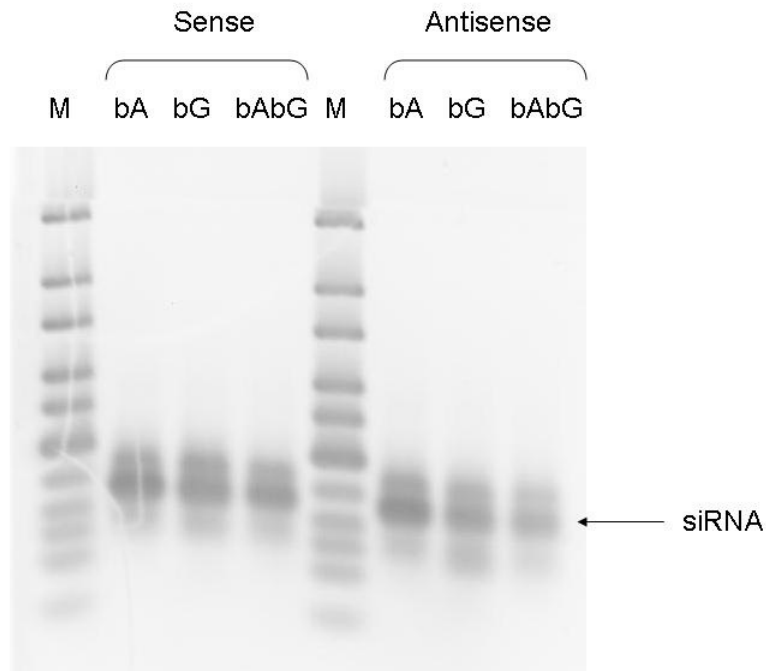


Figure 7-8. Enzymatically transcribed sense and antisense luciferase single stranded siRNA products analyzed on 20% PAGE/7 M urea. The RNA was stained with ethidium bromide and imaged using the UVP Bioimaging System.

Cell studies were performed in the Huang lab by Star Li and Sumio Cho, and assisted by Laura Moussa. The melanoma cell line B16F10 was used. The ds siRNA were delivered into the cells using the cationic lipids Lipofectamine 2000. The inhibition of cell growth was monitored using the luciferase reporter system. The cells were seeded on plates, cultured overnight and then transfected with the siRNA over 24 hours. Then the cells were washed, trypsinized, collected, and counted. 2×10^5 cells were used collected as pellets for the luciferase assays. Collected cell pellets were incubated with lysis buffer at room temperature for ten min. Ten μL of the lysate was mixed with 100 μL of the luciferase substrate (Luciferase Assay System, Promega Co., Madison, WI) and the

luminescence was measured by a plate reader. Luciferase substrate was added to the cells directly before FACS analysis and the reaction was activity was monitored for one week.

The protein concentrations of the samples were determined by using a protein assay kit (Micro BCATM protein assay kit, Pierce). Luciferase activity of a sample was normalized with the protein content and expressed as percent luminescence intensity compared to the untreated control.

7.2.3 Results and Discussion

The work presented in this chapter represents the first use of boranophosphate modified siRNA in melanoma cells. Initial experiments were done using a green fluorescent protein reporter system; however this system was determined to be unsuitable for the measurement of siRNA activity due to low signal strengths. Instead, a luciferase reporter system was used to determine the potency of silencing of boranophosphate-modified enzymatically-synthesized double-stranded siRNA in comparison to chemically-synthesized unmodified double-stranded siRNA.

The modified siRNA duplexes used in this work are shown in Table 7-4. Also, an unmodified chemically synthesized duplex with the same sequence as the unmodified enzymatically synthesized duplex was purchased from a commercial source. It should be noted that this sequence contained dTdT overhangs as opposed to the UU overhangs that were seen on the enzymatically transcribed siRNA duplexes.

Table 7-4. Enzymatically transcribed 19 nt duplexes with 3' UU overhangs used in the luciferase assays in B16F10 cells. Strand notation: sense strand = (S), antisense strand = (AS). The sense strand is shown above the antisense strand. Boranophosphate modifications are shown in pink. Modification notation: N = natural, ^bA = ATP α B, ^bG = GTP α B. Strands are shown with their polarity first and their modifications second.

Modification	Sequence	# Mod (%)
S N + AS N ^a	5' CUU ACG CUG AGU ACU UCG A UU 3' 3' UU GAA UGC GAC UCA UGA AGC U 5'	0
S N + AS ^b A	CUU ACG CUG AGU ACU UCG A UU UU G ^b AA UGC G ^b AC UCA UGA ^b AGC U	6 (27)
S N + AS ^b G	CUU ACG CUG AGU ACU UCG A UU UU G ^b AA UGC G ^b AC UCA UGA ^b AGC U	5 (23)
S N + AS ^b A ^b G	CUU ACG CUG AGU ACU UCG A UU UU G ^b AA UGC G ^b AC UCA UGA ^b AGC U	11 (50)
S ^b A + AS N	CUU ^b ACG CUG ^b AGU ^b ACU UCG ^b A UU UU GAA UGC GAC UCA UGA AGC U	4 (18)
S ^b A + AS ^b A	CUU ^b ACG CUG ^b AGU ^b ACU UCG ^b A UU UU G ^b AA UGC G ^b AC UCA UGA ^b AGC U	4 (18) 6 (27)
S ^b G + AS ^b G	CUU ACG ^b CUG ^b AGU ACU UCG ^b A UU UU G ^b AA UGC G ^b AC UCA UGA ^b AGC U	3 (14) 5 (23)
S ^b A ^b G + AS ^b A ^b G	CUU ^b ACG ^b CUG ^b AGU ^b ACU UCG ^b A UU UU G ^b AA UGC G ^b AC UCA UGA ^b AGC U	8 (36) 11 (50)

a) The enzymatically synthesized unmodified duplex was also purchased as a chemically synthesized unmodified duplex. The enzymatically synthesized duplex has UU overhangs at the 3' end, while the chemically synthesized duplex has dTdT overhangs.

Initial experiments using the boranophosphate modified duplexes yielded promising results compared to chemically synthesized unmodified duplex siRNA. It was shown that the enzymatically transcribed duplex containing the ATP α B modification on both sense and antisense strand appeared to exhibit the most potent silencing of luciferase mRNA expression. (Figure 7-9) This sequence has UU overhangs, and showed the greatest magnitude of luciferase activity reduction after one day, and the reduction lasted the longest, returning to ~60% after one week. The chemically synthesized control had returned to almost 90% after one week. Other boranophosphate modified sequences also showed greater reduction of luciferase activity; the duplex modified on both the sense and antisense strand with both ATP α B and GTP α B showed more potent silencing versus the unmodified duplex, but the effect did not last as long, returning to 130% after one week. Overall, there was clear superiority of the enzymatically-synthesized boranophosphate-modified ds-siRNA to reduce luciferase activity compared to the chemically-synthesized unmodified ds-siRNA control.

It is interesting that the singly modified (ATP α B) and doubly modified (ATP α B + GTP α B) siRNA homoduplexes showed the greatest potency of silencing. It could be that modifications in both strands of the siRNA act in some way to preferentially load the antisense guide strand into the RISC complex. This has been seen for other backbone modified siRNA duplexes. (Reynolds 2004; Ui-Tei 2004)

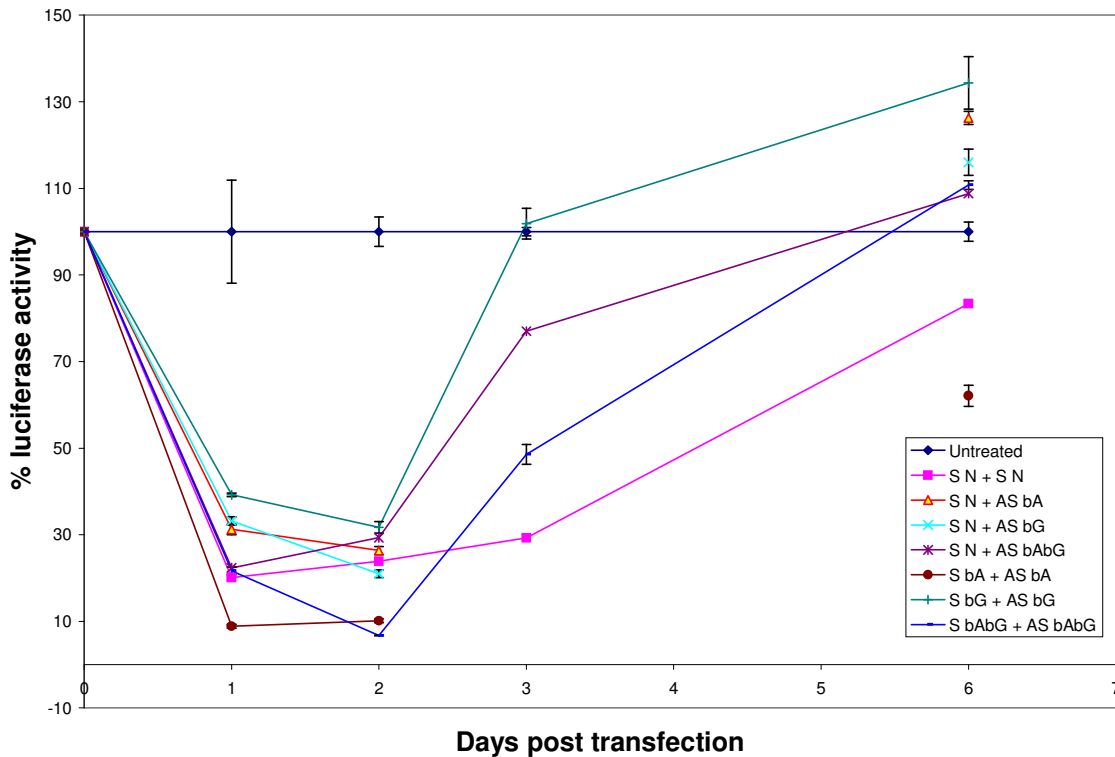


Figure 7-9. Downregulation of luciferase activity by anti-luciferase modified siRNA. The untreated cells were used to normalize the data for the treated cells. The chemically synthesized unmodified siRNA duplex, with dTdT overhangs, is shown in pink. All the other siRNA sequences were enzymatically synthesized and have UU overhangs.

However, when these experiments were repeated using the enzymatically synthesized unmodified siRNA duplex with UU overhangs as a comparison (instead of the chemically synthesized siRNA duplex with dTdT overhangs), it was found that there was no statistically significant difference between its ability to downregulate luciferase activity as compared to the boranophosphate siRNA modified on both strands with ATP α B. (Figure 7-10) This may indicate that the increased potency of the boranophosphate siRNA duplex was not due to the BP modification itself, but instead to

a difference due to enzymatic synthesis, since it is also seen for the unmodified, enzymatically synthesized siRNA.

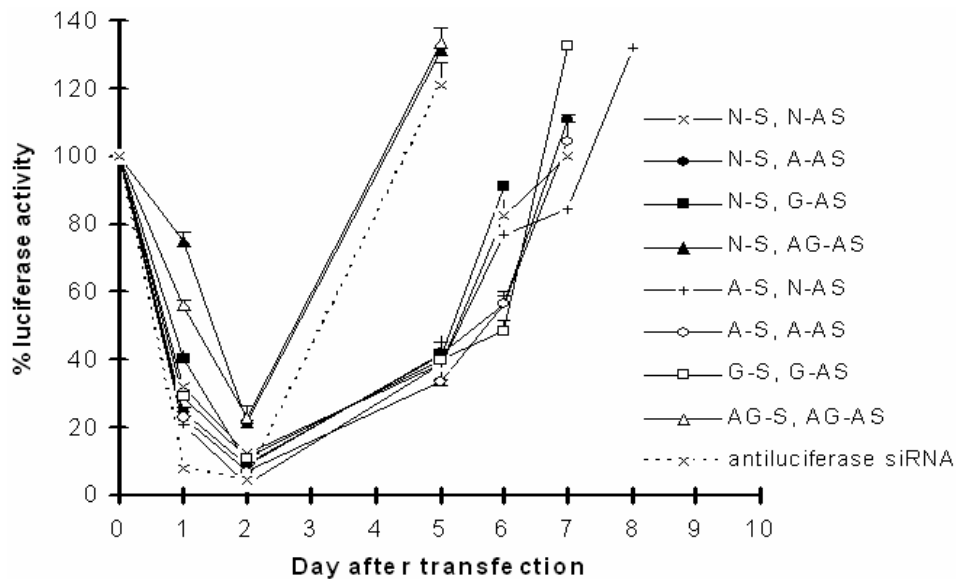


Figure 7-10. Silencing of luciferase activity by boranophosphate modified siRNA duplexes compared to chemically synthesized duplexes with dTdT overhangs (antiluciferase siRNA) and enzymatically synthesized unmodified duplexes with UU overhangs (N-S, N-AS). The boranophosphate modified siRNA duplexes were all enzymatically synthesized.

In this context, it is interesting that there is almost no difference in the *potency* of luciferase silencing between the enzymatically transcribed unmodified siRNA (with UU overhangs) and chemically synthesized unmodified siRNA duplexes (with dTdT overhangs). It is clear that the *persistence* of luciferase activity reduction is increased when using the enzymatically synthesized siRNA duplex compared to the chemically synthesized unmodified duplex. The boranophosphate modified sequences again showed an increase in persistence of silencing. This persistence might be attributed to

the greater nuclease stability exhibited by boranophosphate siRNA compared to unmodified siRNA as seen in Chapter 5.

The difference in the silencing between chemically synthesized unmodified siRNA (dTdT) and enzymatically synthesized unmodified siRNA (UU) may be attributed to the difference in the composition of the overhangs. Specifically to further investigate this hypothesis, a chemically synthesized siRNA duplex with UU overhangs was purchased from a commercial source and the silencing of the three duplexes was compared (Figure 7-8)

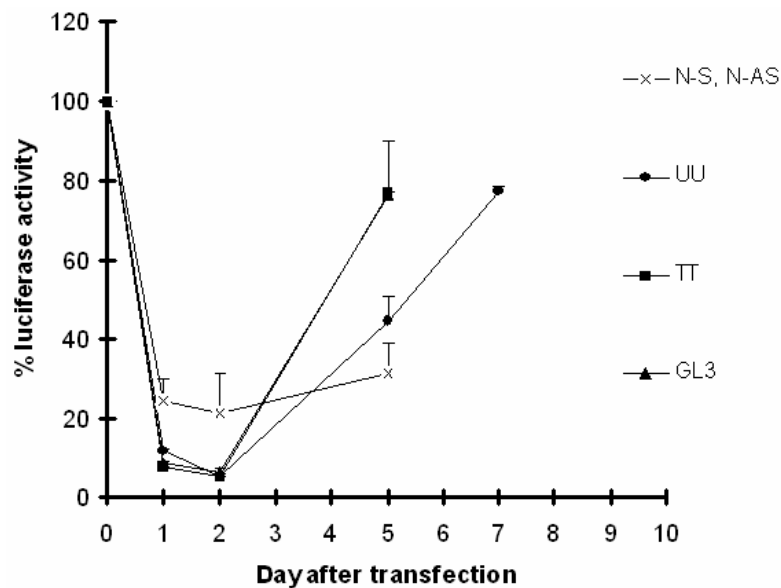


Figure 7-11. Comparison of the effect of overhang composition on luciferase activity decrease by anti-luciferase chemically and enzymatically synthesized unmodified siRNA duplexes. The X represents enzymatically synthesized unmodified ds-siRNA with UU overhangs. The • represents chemically synthesized unmodified ds-siRNA with UU overhangs. The ■ represents chemically synthesized unmodified ds-siRNA with dTdT overhangs. The Δ (GL3) represents chemically synthesized unmodified ds-siRNA with dTdT overhangs of a different sequence that also targets luciferase.

It remains to be determined whether unmodified duplexes have different silencing capabilities because of the composition of their overhangs or because of the method of synthesis. The UU overhangs showed the greatest persistence of silencing, but the dTdT overhangs showed the greatest reduction in luciferase activity. Another factor that could play a role is the presence of the 5' phosphate group on siRNA sequences that are enzymatically transcribed, but is lacking in chemically synthesized siRNA. This is one more factor that must be taken into account when designing boranophosphate modified siRNA. Further studies are necessary to determine the cause of the difference in silencing capabilities.

7.2.4 Summary

Boranophosphate modified siRNA was used to downregulate luciferase activity in a melanoma cell reporter system for the first time. This is an important system to study, since melanoma is a commonly fatal disease. Also, this system would allow the use of a new delivery system, the LPD nanoparticles, and allow comparison to Lipofectamine transfection of siRNA. This method of delivery may be able to overcome one of the main difficulties in RNAi therapeutics, the delivery of siRNA molecules into cells. However, it was decided that due to inconsistencies that were encountered in this system, it would be unlikely that the difference in luciferase activity silencing by LPD-delivered boranophosphate siRNA versus LPD-delivered unmodified siRNA could be accurately defined. Melanoma cells are a difficult system to study and there are many

variables that contribute to experimental outcome, including the method of siRNA synthesis and the composition of the overhangs of the duplex. Confounding factors would most likely remove the possibility of determining the mechanism of how the increased lipophilicity of boranophosphate siRNA could supplement cellular uptake in conjunction with the LPD system.

Ongoing work is being done to define the contribution of the 5' phosphate and the composition of the overhangs to the silencing capability of the boranophosphate modified siRNA. Ultimately, the overhangs may be removed in systems that utilize single-stranded boranophosphate siRNA, as they are not necessary without the formation of a duplex. The difference in the boranophosphate modification that showed greatest silencing illustrates the fact that for every new system that is tested, a series of singly and doubly modified siRNAs should be tested and, if possible, the duplex stability and hybridization affinity of the modified siRNA with its unmodified complement should be investigated to determine which species can yield the best results.

8. Summary and Future Work

The work presented in this dissertation encompasses the synthesis, chemical and biological characterization, and *in vitro* applications of chemically modified α -P-boranomodified siRNA, alone and in conjunction with the 2'-deoxy-2'fluoro modification. Two methods of enzymatic synthesis have been investigated; transcription with T7 RNA polymerase and ligation with T4 RNA ligase, and the conditions of each reaction were optimized to maximize the yield. The secondary structure of the boranophosphate modified siRNA was explored in homoduplexes with boranophosphate modified complements and in heteroduplexes with unmodified complements. The heteroduplex can act as a model for the hybridization affinity that a boranophosphate siRNA will have for its unmodified target mRNA. Overall, the trend that was observed showed that increasing the percentage of boranophosphate linkages shifted the secondary structure of the duplex towards a B-form helix, leading to decreases in the melting temperature. It is recommended that these experiments be followed up with NMR of boranophosphate siRNA to absolutely determine the configuration. Crystallography may also be helpful in determination of the secondary structure.

The boranophosphate modified siRNA proved to be more stable to hydrolysis by exonucleases and the combined fluoro/borano siRNA proved to be more stable to hydrolysis by endonuclease than the unmodified congener. Increasing the amount of

boranophosphate linkages in the siRNA to 100% led to a 59 fold increase in lipophilicity of the molecule versus the native.

The boranophosphate modified siRNA was tested in two biological systems, human papillomavirus and melanoma. The anti-HPV single-stranded boranophosphate modified siRNA greatly increased the potency of silencing as compared to normal siRNA. The ability of to silence a gene using only a single strand of siRNA may have advantages in terms of cellular uptake and non-immunogenicity. However, the addition of the 2' fluoro modification did not confer the expected benefits with regards to *in vitro* activity.

Silencing by boranophosphate siRNA in the melanoma system did not differ very much from silencing using enzymatically transcribed unmodified siRNA, but revealed several important factors such as overhang composition and presence of a 5' phosphate that should be investigate in future work to determine their effects in regards to BP modified siRNA. Also, it was determined that the boranophosphate modified siRNA yielded an increase in persistence of effect, possibly due to its increased nuclease stability. Finally, there may be a benefit to the stereoregularity of the BP siRNA may play a role in the biological effect.

A large amount of work remains to be done in the field of boranophosphate siRNA. Most importantly, the development of a theoretical or computational method to determine the effect of the boranophosphate modification on the secondary structure

and hybridization affinity could both save time and reduce the need to synthesize vast quantities of boranophosphate siRNA solely for the purpose of structure determination. Secondly, the expansion of the boranophosphate siRNA to other systems will give a better understanding of the types of biological systems that are best suited for our modification. Lastly, a kinetic analysis of the boranophosphate siRNA guide strand and its interactions with the programmable endonuclease Argonaute 2 should be undertaken.

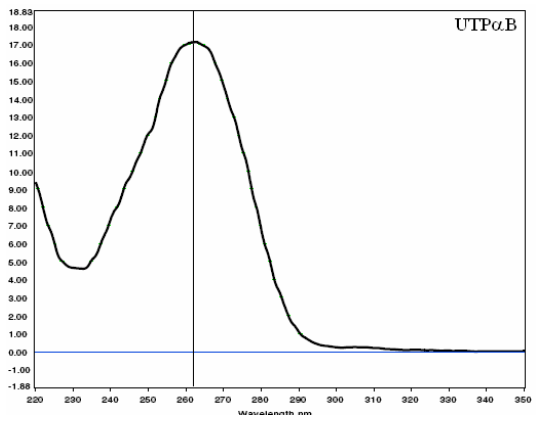
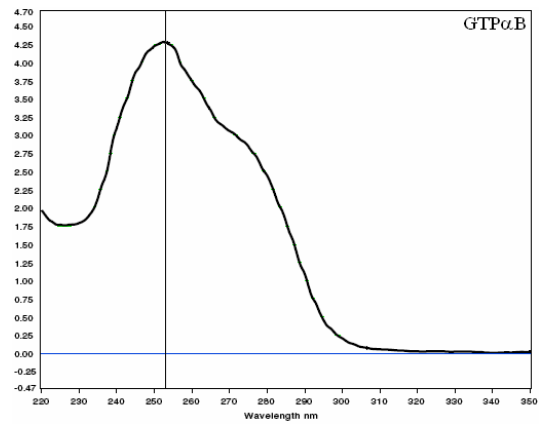
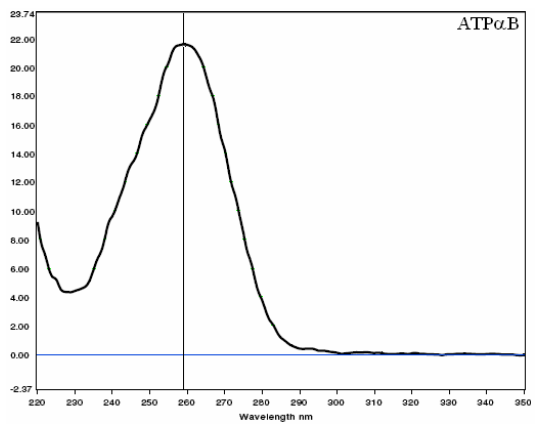
Argonaute is the catalytic engine of the RISC machinery, and it has been shown that the binding affinity of the siRNA and Argonaute as well as the catalytic efficiency of the target mRNA cleavage can depend on the type and position of backbone modifications (Preall and Sontheimer 2005). So far, kinetic experiments have only been done using unmodified siRNA molecules. This type of kinetic analysis will be more easily undertaken once the protein is available in a purified form from commercial sources, as the expression and purification of Argonaute 2 are difficult. Numerous attempts to express and purify a truncated Argonaute 2 from *E. coli* met with no success at this time.

This truncated Argonaute 2 has been shown to form a minimal RISC complex with antisense siRNA. Once the protein is in hand, it can be used to study the binding affinity (K_d) and cleavage constants (V_{max} and K_{cat}) of the mRNA cleavage reaction that is directed by a boranophosphate modified guide strand. It can also be used to

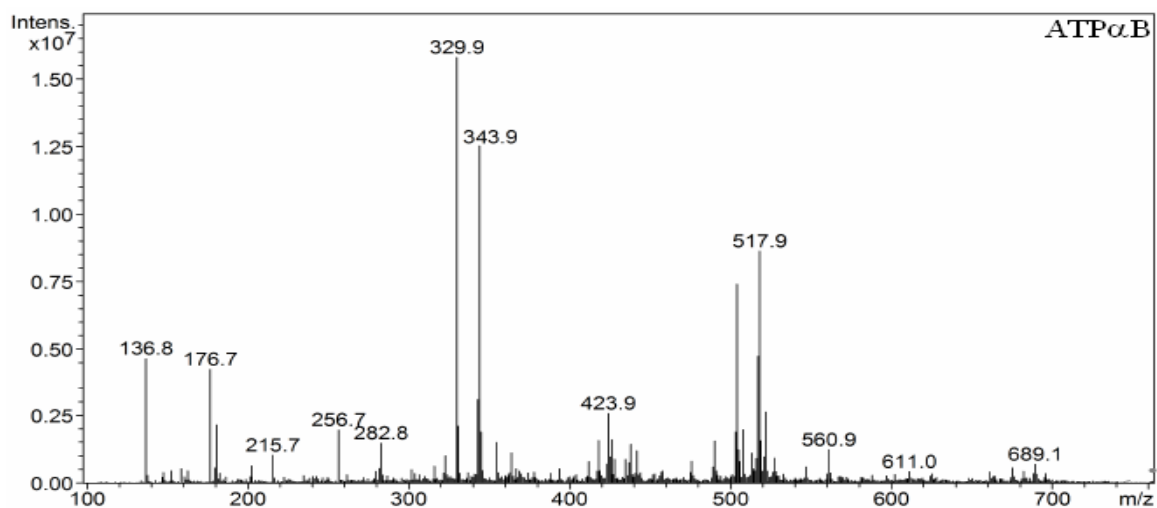
determine how the following factors influence the rate of mRNA target cleavage by RISC: 1) Presence of BP modifications, 2) Number of BP modifications, and 3) Position of BP modifications. This will yield valuable information about the nature of the interaction between boranophosphate siRNA and the RISC machinery and may be used to construct rules for rational design of boranophosphate modified siRNA.

Appendix I

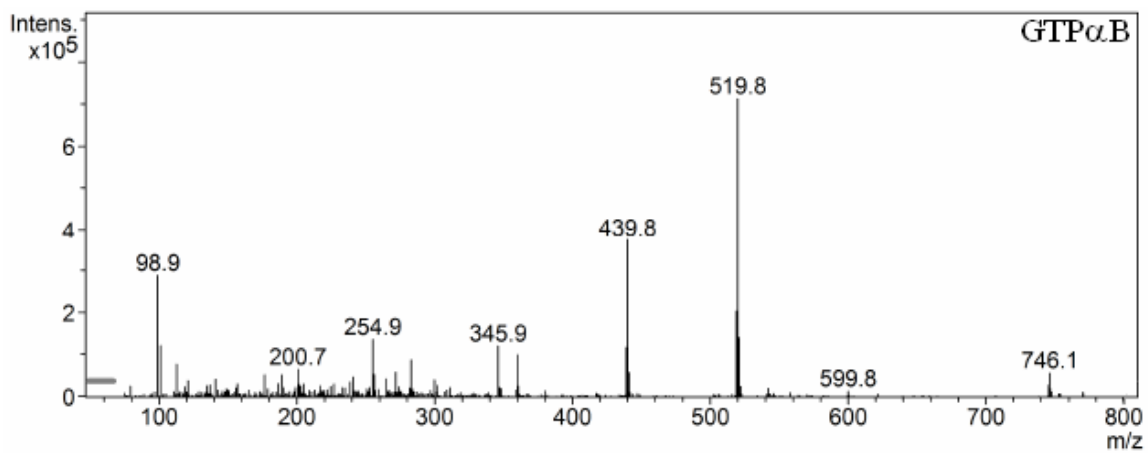
UV Spectra of NTP α B



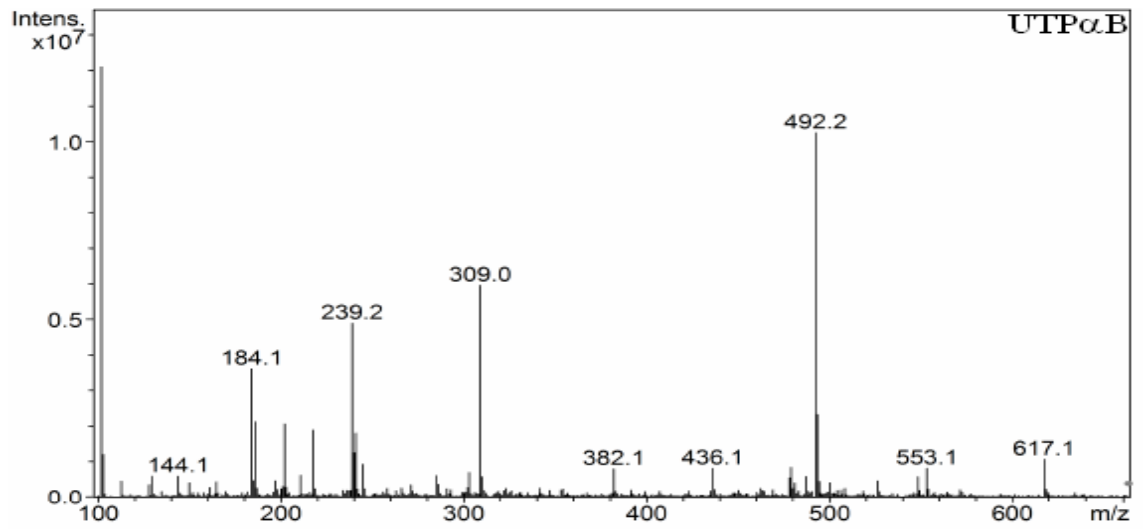
ESI-MS



Peak (m/z)	Assignment
517.9	ATP α B + Na
423.9	ADP α B
343.9	AMP α B

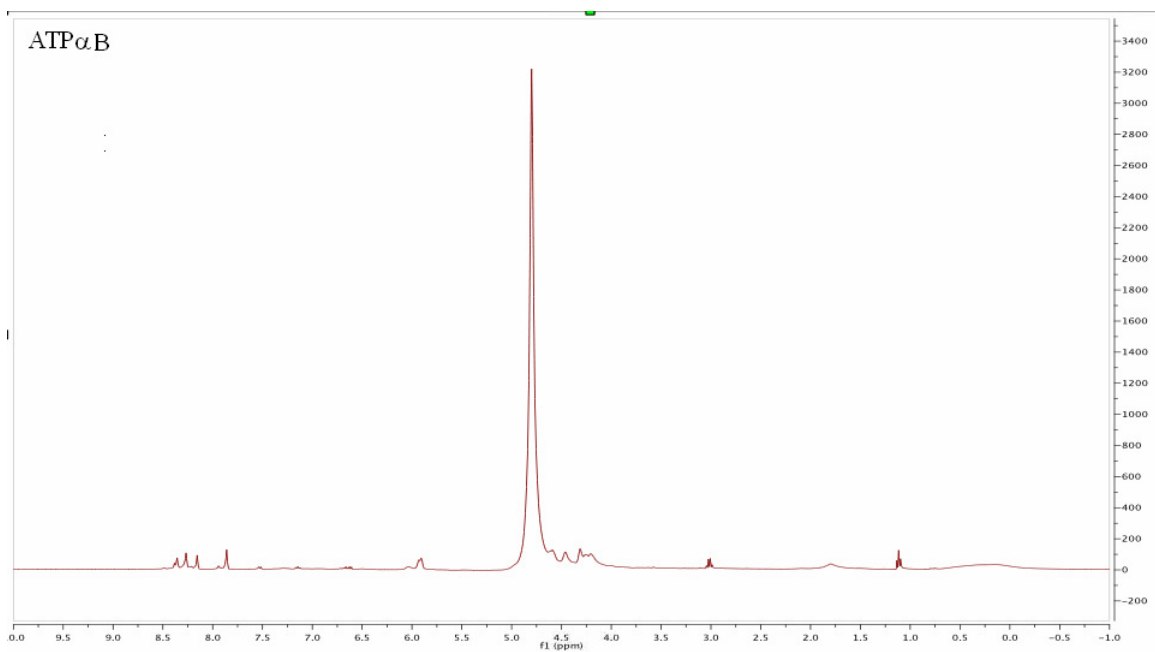
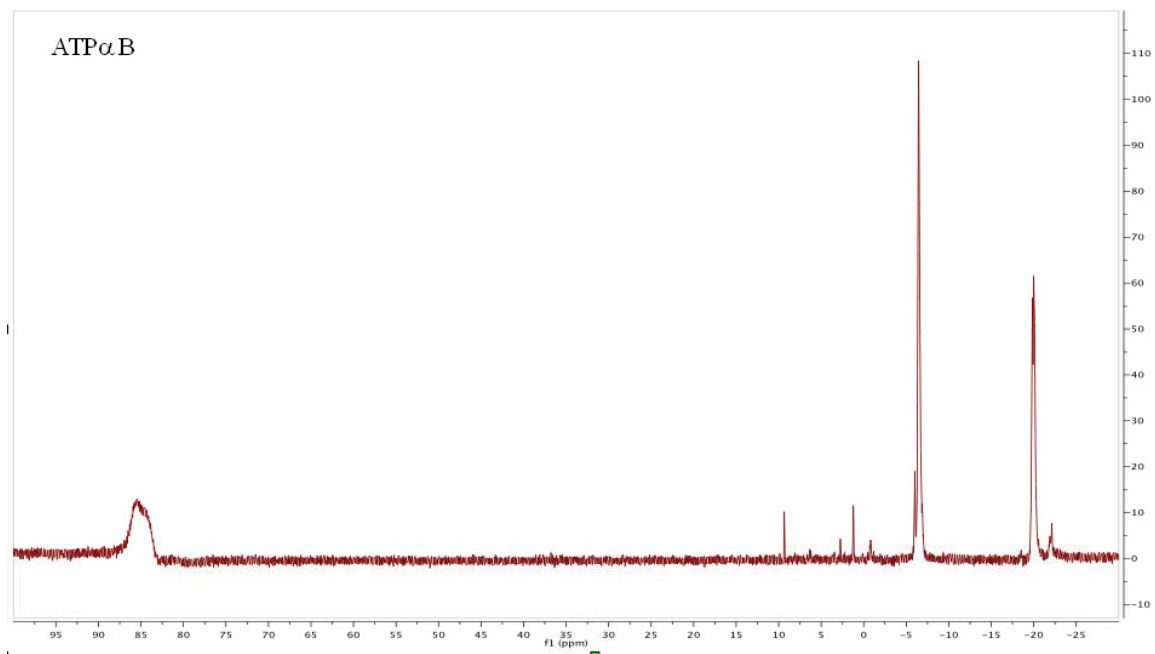


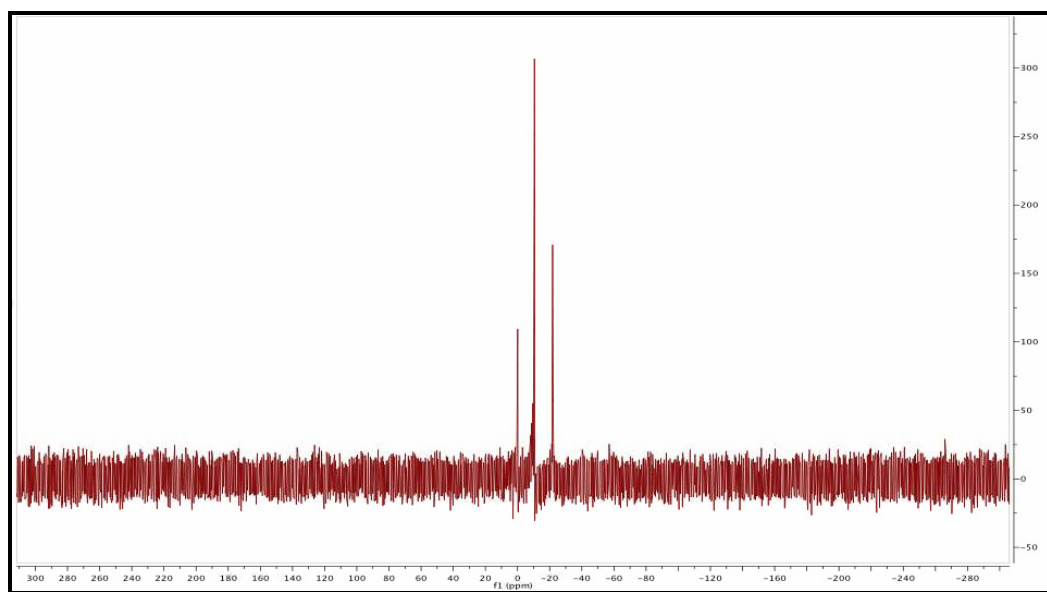
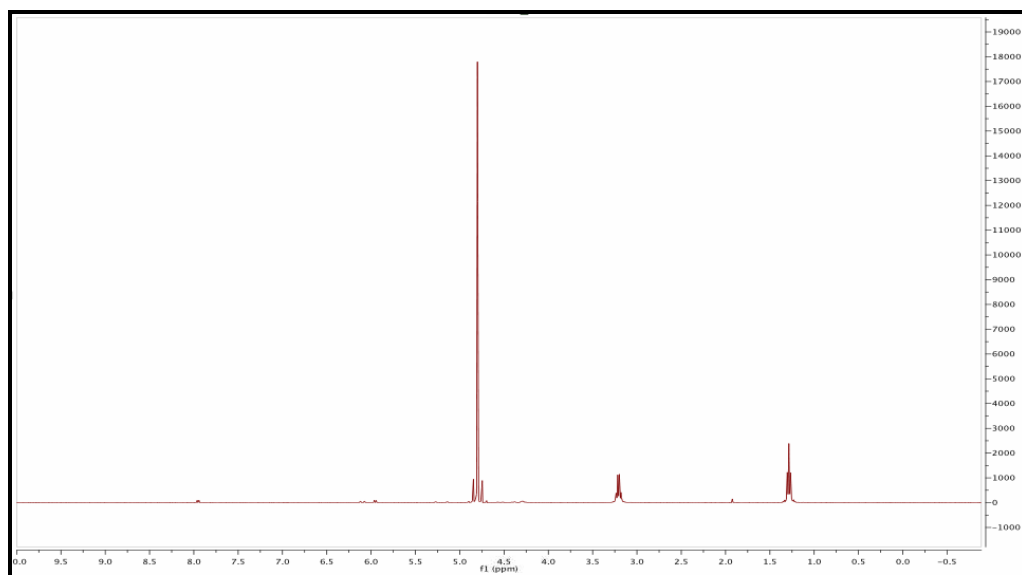
Peak (m/z)	Assignment
519.9	GTP α B
439.8	GDP α B



Peak (m/z)	Assignment
492.2	UTP α B + Na
382.4	UDP α B
309.0	UMP α B

Top: ^{31}P NMR in D_2O . Bottom: ^1H NMR in D_2O

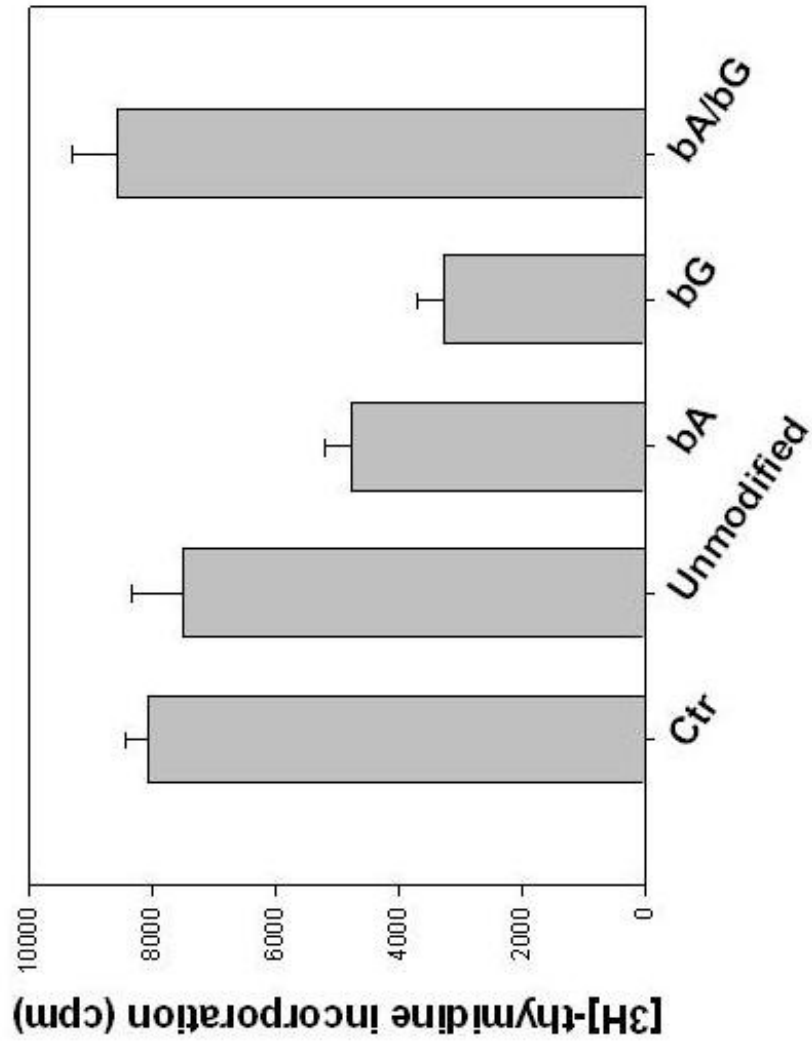




Characterization by NMR of final products from 2'F UTP synthesis. **(A)** Representative ^1H NMR profile for 2'F UTP in D_2O . **(B)** Representative ^{31}P NMR profile for 2'F UTP in D_2O

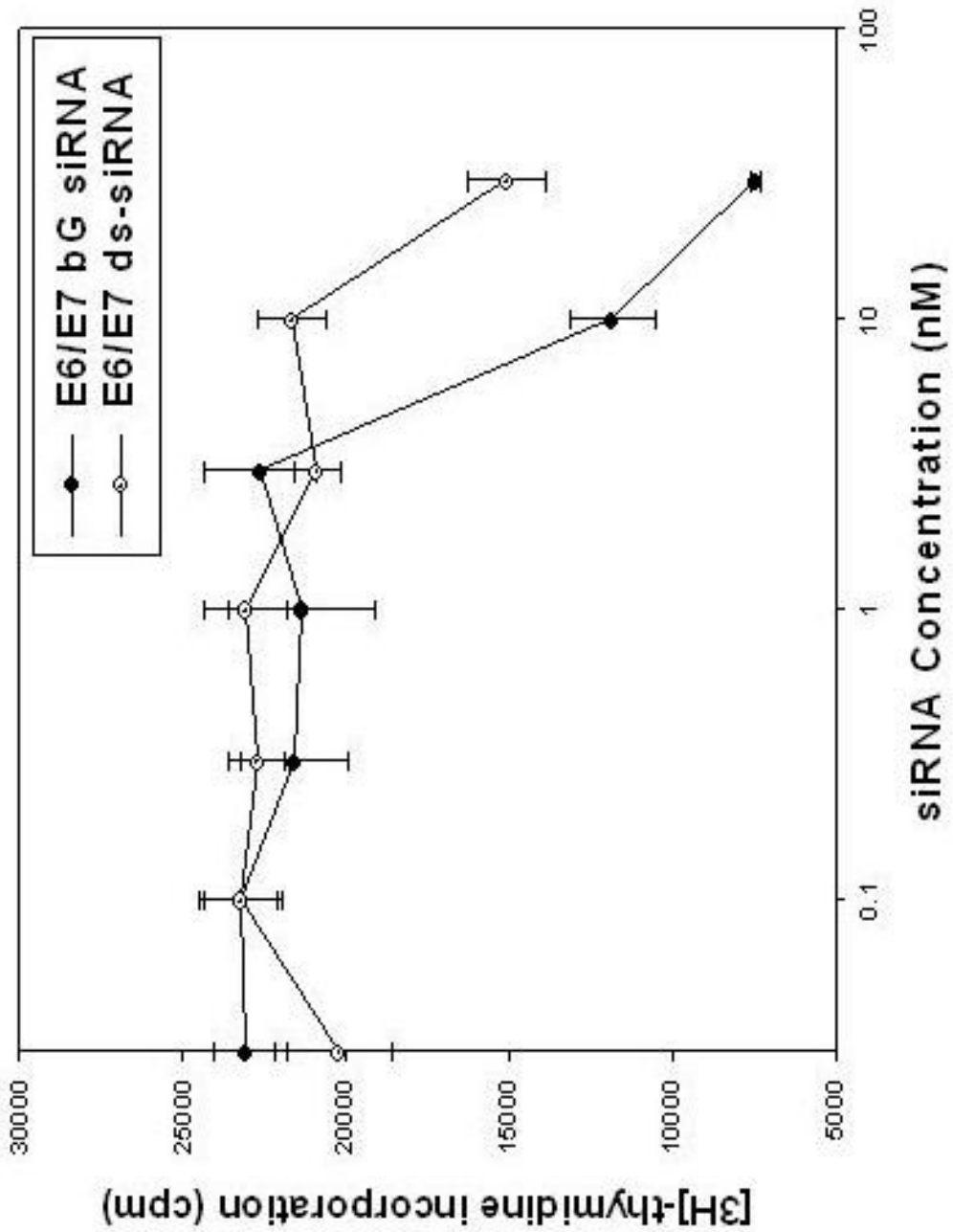
Appendix II

Effects of 20 nM Single-stranded Anti-HPV16 E6/E7BP-siRNAs on [³H] Thymidine Uptake by SiHa Cells



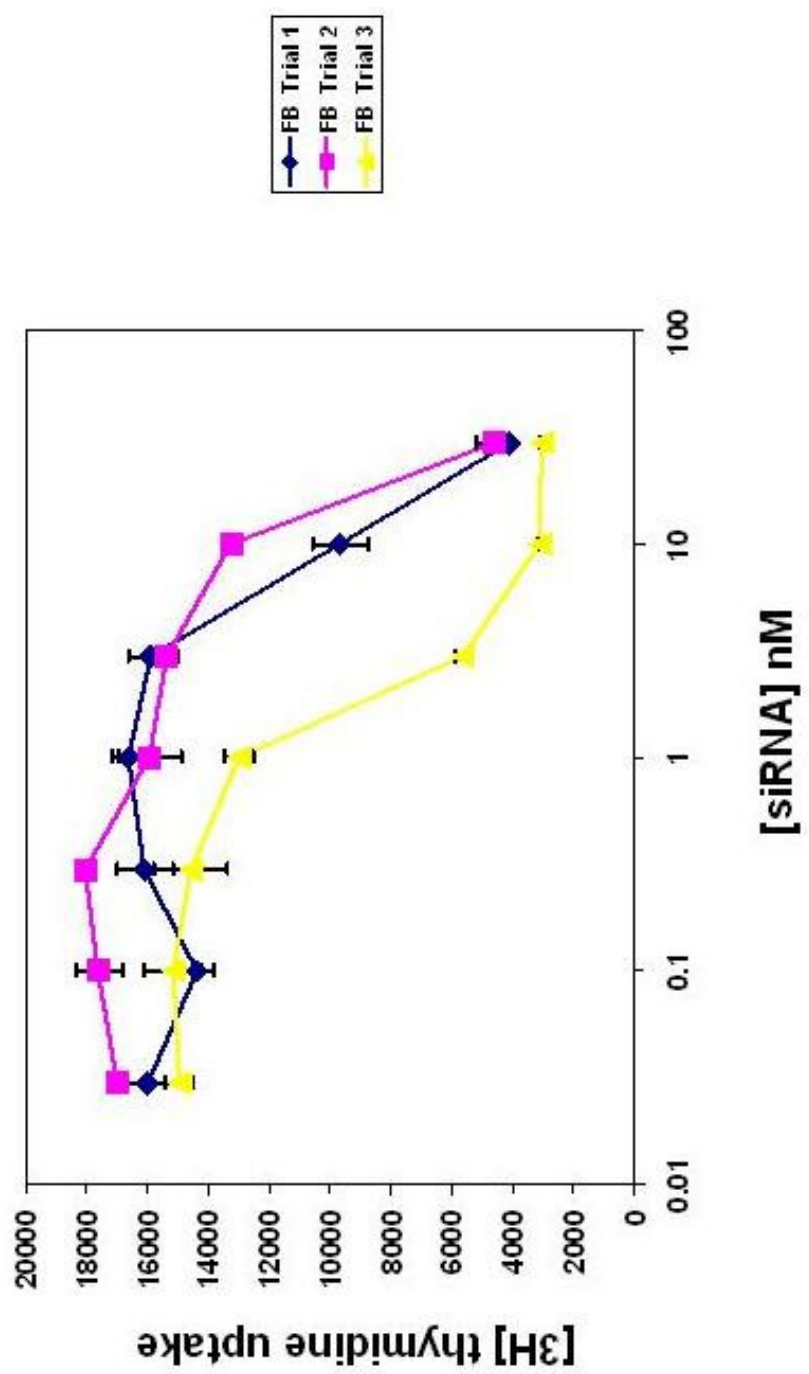
Transcription of natural and modified siRNA was done in the Shaw Lab, Duke University. Cell data collected by Alexander Lab, University of Chicago

W12-E Cell Growth Inhibition by anti-E6/E7 siRNAs



Transcription of natural and modified siRNA was done in the Shaw Lab, Duke University. Cell data collected by Alexander Lab, University of Chicago

**Testing of single-stranded
2'-Fluoro-Borano siRNAs
(GTP α B, 2'F CTP, 2'F UTP, and normal A)**



Transcription of natural and modified siRNA was done in the Shaw Lab, Duke University. Cell data collected by Alexander Lab, University of Chicago

References

- Alberts, B., Johnson, A., Lewis, J., Raff, M., Roberts, K., Walter, P. (2002). Molecular Biology of the Cell.
- Amarzguioui, M., Holen, T., Babaie, E., and Prydz, H. (2003). "Tolerance for mutations and chemical modifications in a siRNA." Nucleic Acids Research **31**(2): 589-595.
- Ambion (2003). Oligonucleotide MW and Extinction Coefficient Calculator.
- Behlke, M.A., Devor, E.J. (2005). "Chemical Synthesis of Oligonucleotides."
- Berova, N, Nakanishi, K., Woody, R.W. (2000) Circular Dichroism: Principles and Applications.
- Blidner (2007). "Fully 2'-Deoxy-2'-Fluoro Substituted Nucleic Acids Induce RNA Interference in Mammalian Cell Culture." Chem Biol Drug Design **70**: 113-122.
- Blidner (2007). "Fully 2'-Deoxy-2'-Fluoro Substituted Nucleic Acids Induce RNA Interference in Mammalian Cell Culture." Chem Biol Drug Design **70**: 113-122.
- Bloomfield, V. A., Crothers, D.M., Tinoco, I. (2000). Nucleic Acids: Structures, properties, and function.
- Bryant, F. R., Benkovic, S.J. (1982). "On the mechanism of T4 RNA ligase." Journal of American Chemical Society **103**: 696-697.
- Caberg, J. D., Hubert, P.M., Begon, D.Y., Herfs, M.F., Roncarati, P.J., Boniver, J.J., and Delvenn, P.O. (2008). "Silencing of E7 oncogene restores functional E-cadherin expression in human papillomavirus 16-transformed keratinocyte." Carcinogenesis **29**(7): 1441-1447.
- Calladine, C. R., Drew, H.R. (1992). Understanding DNA: The molecule and how it works.
- Cejka, D., Losert, D., Wacheck, V. (2006). "siRNA: tool or therapeutic?" Clinical Science **110**: 47-58.
- Chamberlin, M., McGrath, J., and Waskell, L. (1970). "New RNA Polymerase from Escherichia coli infected with Bacteriophage T7." Nature **228**(5268): 227-231.

- Chiu, Y. L., Rana, T.M. (2002). "RNAi in Human Cells: Basic Structural and Functional Features of Small Interfering RNA." Molecular Cell **10**: 549-561.
- Chiu, Y. L. a. R., T.M. (2003). "siRNA function in RNAi: a chemical modification analysis." RNA **9**: 1034-1048.
- Chu, T. C., Twu, K.Y., Ellington, A.D., Levy, M. (2006). "Aptamer mediated siRNA delivery." Nucleic Acids Research **34**: 73.
- Codington, J. F., Doerr, I.L, Fox, J.J. (1964). "Nucleosides. XVIII. Synthesis of 2'-Fluorothymidine, 2'-Fluorodeoxyuridine, and Other 2'-Halogeno-2'-Deoxy Nucleosides." Journal of Organic Chemistry **29**(3): 558-564.
- Dagle, J. M., Andracki, M.E., DeVine, R.J., Walder, J.A. (1991). "Physical properties of oligonucleotides containing phosphoramidite-modified internucleoside linkages." Nucleic Acids Research **19**(8): 1805-1810.
- Davidson, J. N., Ed. (1976). The Biochemistry of the Nucleic Acids. New York City, NY USA, Academic Press.
- de Fougerolles, A., Vornlocher, H., Maraganore, J., Lieberman, J. (2007). "Interfering with disease: a progress report on siRNA-based therapeutics." Nature Reviews: Drug Discovery **6**: 443.
- De Paula, D., Vitoria, M., Bentley, L.B., Mahato, R.I. (2007). "Hydrophobization and bioconjugation for enhanced siRNA delivery and targeting." RNA **13**: 431-456.
- Deutscher, M. P. (1993). "Promiscuous Exoribonucleases of Escherichia coli." Journal of Bacteriology **175**(15): 4577-4583.
- Deutscher, M. P., Marlors, C.W., Zaniwsky, R. (1984). "Ribonuclease T: New exoribonuclease possibly involved in end-turnover of tRNA." Proceedings of the National Academy of Sciences **81**: 4290-4293.
- Distler, A. M., Allison, J. (2001). "5-Methoxysalicylic acid and spermine: a new matrix for the matrix-assisted laser desorption/ionization mass spectrometry analysis of oligonucleotides." Journal of the American Society for Mass Spectrometry **12**(4): 456-462.
- Dutkiewicz, M., Grunert, H., Zeichhardt, H., Lenard, S.W., Wengle, J., Kurreck, J. (2008). "Design of LNA-modified siRNAs against the highly structured 5' UTR of coxsackievirus B3." **582**(20): 3061-3066.

- Duxbury, M. S., Ashley, S.W., Whang, E.E. (2005). "RNA interference: A mammalian SID-1 homologue enhances siRNA uptake and gene silencing efficacy in human cells." Biochemical and Biophysical Research Communications **331**(2): 459-463.
- Elbashir, S. M., Martinez, J., Patkaniowska, A., Lendeckel, W., and Tuschl, T. (2001). "Functional anatomy of siRNAs for mediating efficient RNAi in *Drosophila melanogaster* embryo lysate." The EMBO Journal **20**: 6877-6888.
- England, T. E., Bruce, A.G., Uhlenbeck, O.C. (1980). "Specific labeling of 3' termini of RNA with T4 RNA ligase." Methods in Enzymology **65**: 65-74.
- England, T. E., Uhlenbeck, O.C. (1978). "Enzymatic oligoribonucleotide synthesis with T4 RNA ligase." Biochemistry **17**(11): 2069-2076.
- Fasman, G. D., Ed. (1975). Handbook of Biochemistry and Molecular Biology.
- Fillopowicz, W. (2002). "RNAi: The nuts and bolts of the RISC machinery." Cell **122**: 17-20.
- Fire, A. (1999). "RNA-Triggered Gene Silencing." Trends in Genetics **15**(9): 358-363.
- Fire, A., Xu, S., Montgomery, M.K., Kostas, S.A., Driver, S. E., Mello, C.C. (1998). "Potent and Specific Genetic Interference by Double-Stranded RNA in *Caenorhabditis elegans*." Nature **391**: 806-811.
- Fire, A., Xu, S., Montgomery, M.K., Kostas, S.A., Driver, S.E., Mello, C.C. (1998). "Potent and Specific Genetic Interference by Double-Stranded RNA in *Caenorhabditis elegans*." Nature **391**: 806-811.
- Friedl, E., Kimura, I., Osato, T., Ito, Y. (1970). "Studies on a new human cell line (SiHa) derived from carcinoma of uterus. 1. Its establishment and morphology." Proceedings of the Society of Experimental Biological Medicine **135**: 543-545.
- Frier, S. M., Burger, B.J., Alkema, D., Neilson, T, Turner, D.H. (1983). "Effects of 3'-dangling end stacking on the stability of GGCC and CCGG double helices." Biochemistry **22**: 6198-6206.
- Gilar, M., Fountain, K.J., Neue, U.D., Budman, Y., Yardley, K.R., Rainville, D., Russell, R.J. Gebler, J.C. (2002). "Ion-pair reversed-phase high-performance liquid chromatography analysis of oligonucleotides: Retention prediction." Journal of Chromatography A **958**(1-2): 167-182.

- Graetzer, W. B., Richards, E. G. (1971). "Evaluation of RNA conformation from circular dichroism and optical rotatory dispersion data." Biopolymers **10**(12): 2607-2614.
- Gurevich, V. V., Pokrovskaya, I.D., Obukhova, T.A., and Zozulya, S.A. (1991). "Preparative in vitro mRNA synthesis using SP6 and T7 RNA polymerases." Analytical Biochemistry **195**: 207-213.
- Haley, P., Zamore, P.D. (2004). "Kinetic analysis of the RNAi enzyme complex." Nature Structural & Molecular Biology **11**: 599-606.
- Hall, A. S., Alexander, K. (2003). "RNA Interference of Human Papillomavirus Type 18 E6 and E7 Induces Senescence in HeLa Cells." Journal of Virology **77**(10): 6066-6069.
- Hall, A. S., Wan, J., Spesock, A., Sergueeva, Z., Shaw, B.R., Alexander, K.A. (2006). "High potency silencing by single-stranded boranophosphate siRNA." Nucleic Acids Research **34**(9): 2773-2781.
- Han, S. M., Armstrong, D.W. (1989). HPLC separation of enantiomers and other isomers with cyclodextrin-bonded phases: rules for chiral recognition. Chiral Separations by HPLC. A. M. Krstulovic.
- Harborth, J., Elbashir, S.M., Vandeburgh, K., Manninga, H., Scaringe, S.A., Weber, K., Tuschl, T. (2003). "Sequence, Chemical, and Structural Variation of Small Interfering RNAs and Short Hairpin RNAs and the Effect on Mammalian Gene Silencing." Antisense and Nucleic Acid Drug Development **13**(2): 83-105.
- He, K. (2000). Synthesis and properties of boranophosphate nucleic acids. Chemistry. Durham, Duke University. **Ph.D.**
- He, K., Hasan, A., Kryzanowska, B., Shaw, B.R. (1998). "Synthesis and Separation of Diastereomers of Ribonucleoside 5'-(alpha-P-Borano)triphosphates." Journal of Organic Chemistry **63**(17): 5769-5773.
- Heale, B. S. E., Soifer, H.S., Bowers, C., and Rossi, J.J. (2005). "siRNA target site secondary structure predictions using local stable substructures." Nucleic Acids Research **33**(3): e30.
- Hélène C., Toulmé, J. J. (1990). "Specific regulation of gene expression by antisense, sense and antigene nucleic acids." Biochimica et Biophysica Acta (BBA) - Gene Structure and Expression **1049**(2): 99-125.

- Hinton, D. M., Brennan, C.A., Gumport, R.I. (1982). "The preparative synthesis of oligodeoxyribonucleotides using RNA ligase." Nucleic Acids Research **10**: 1877-.
- Horvath, C. G., Preiss, B.A., and Lipsky, S.R. (1967). "Fast liquid chromatography. Investigation of operating parameters and the separation of nucleotides on pellicular ion exchangers." Analytical Chemistry **39** (12): 1422-1428.
- Huang, F. (1994). Synthesis and properties of boron-containing nucleic acids. Chemistry, Duke University. **Ph.D.**
- Huang, Y., Eckstein, F., Padilla, R., Sousa, R. (1997). Mechanism of Ribose 2'-Group Discrimination by an RNA Polymerase. Biochemistry **36**(27): 8231-8242.
- Jenkins Autry, L. A., Bashkin, J.K. (1997). "Transesterification of RNA by Cu(II)terypyridine." Inorganica Chimica Acta **263**: 49-52.
- Johnson, W. C. (2000). CD of nucleic acids. Circular Dichroism: Principles and Applications. N. Berova, Nakanihi, K., Woody, R.W.
- Juliano, R., Alam, M.D., Dixit, V., and Kang, H. (2008). "Mechanisms and strategies for effective delivery of antisense and siRNA oligonucleotides." Nucleic Acids Research **36**(12): 4158-4171.
- Kawasaki, A. M., Casper, M.D., Freier, S.M., Leanik, E.A., Zounes, M.C., Cummins, L.L., Gonzalez, C., Cook, P.D. (1993). "Uniformly modified 2'-deoxy-2'-fluoro phosphorothioate oligonucleotides as nuclease-resistant antisense compounds with high affinity and specificity for RNA targets." Journal of Medicinal Chemistry **36**: 831-841.
- Kirchoff, F. (2008). "Silencing HIV in vivo." Cell **134**(4): 566-568.
- Kochetkov, S. N., Rusakova, E.E., and Tunitskaya, V.L. (1998). "Recent Studies of T7 RNA Polymerase Mechanism." FEBS Letters **440**(3): 264-267.
- Krieg, P. A., Ed. (1996). A Laboratory Guide to RNA: Isolation, Analysis, and Synthesis. New York City, NY, Wiley-Liss.
- Krzyzanowska, B. K., He, K.Z., Hasan, A., Shaw, B.R. (1998). "A convenient synthesis of 2'Deoxyribonucleoside 5'-(α -P-borano)-triphosphate." Tetrahedron **54**: 5119-5128.
- Kurreck, J. (2003). "Antisense technologies: Improvements through chemical modifications." European Journal of Biochemistry **270**(8): 1628-1644.

- Lewis, D., Wolf, J.A. (2007). "Systemic siRNA delivery via hydrodynamic intravascular injection." Advanced Drug Delivery Reviews **59**(2-3): 115-123.
- Li, H., Hardin, C., Shaw, B.R. (1996). "Hydrolysis of Thymidine Boranomonophosphate and Stepwise Deuterium Substitution of the Borane Hydrogens. ³¹P and ¹¹B NMR Studies." Journal of American Chemical Society **118**(28): 6606-6614.
- Li, H., Porter, K., Huang, F.Q., Shaw, B.R. (1995). "Oligodeoxyribonucleotide 14mer Duplexes - Enzymatic Synthesis and Melting." Nucleic Acids Research **23**: 4495-4501.
- Li, P., Sergueeva, Z.A., Dobrikov, M.; Shaw, B.R. (2007). "Nucleoside and Oligonucleoside Boranophosphates: Chemistry and Properties." Chemical Reviews **107**(11): 4746-4796.
- Li, S.-D., Huang, L (2006). "Targeted delivery of antisense oligodeoxyribonucleotides and small interfering RNA into lung cancer cells." Molecular Pharmaceutics **3**(5): 579-588.
- Ludwig, J., Eckstein, F. (1989). "Rapid and efficient synthesis of nucleoside 5'-O-(1-thiotriphosphates), 5'-triphosphates and 2', 3'-cyclophosphorothioates using 2-chloro-4H-1, 3, 2-benzodioxaphosphorin-4-one." The Journal of Organic Chemistry **54**(3): 631-635.
- Manoharan, M. (1999). "2'-Carbohydrate modifications in antisense oligonucleotide therapy: importance of conformation, configuration and conjugation." Biochimica et Biophysica Acta (BBA) - Gene Structure and Expression **1489**(1): 117-130.
- Manoharan, M. (2007). "RNA interference and chemically modified small interfering RNAs." Current Opinions in Chemical Biology **8**: 570-579.
- Manoharan, M., Tivel, K.L, Inamati, G., Monia, B.P., Dean, N., Cook, P.D. (1997). "Cholesterol Conjugated Uniform and Gapmer Phosphorothioate Oligonucleotides Targeted Against PKC-alpha and C-raf Gene Expression." Nucleosides, Nucleotides and Nucleic Acids, **16**(7-9): 1139 - 1140.
- Marques, J. T., Williams, B.R.G. (2005). "Activation of the Mammalian Immune System by siRNAs." Nature Biotechnology **23**(11): 1399-1405.
- Mathews, C. K., van Holde, K.E., Ahern, K.G (2000). Biochemistry, Addison Wesley Longman.

- Maurizot, J. C. (2000). Circular dichroism of nucleic acids: nonclassical conformations and modified oligonucleotides. Circular Dichroism: Principles and Applications. Wiley-VCH.
- McGilvery, R. W. (1975). Biochemical Concepts, W.B. Saunders Company.
- McGinness, K. E., Joyce, G.F. (2002). "Substitution of Ribonucleotides in the T7 RNA Polymerase Promoter Element." Journal of Biological Chemistry **277**(4): 2987-2941.
- Melton, D. A., Krieg, P.A., Rebagliata, M.R., Maniatis, T., Zinn, R., Green, M.R. (1984). "Efficient *in vitro* synthesis of biologically active RNA and RNA hybridization probes from plasmids containing a bacteriophage SP6 promoter." Nucleic Acids Research **12**(18): 70-35-7056.
- Mergny (2003). "Analysis of Thermal Melting Curves." Oligonucleotides **13**: 515-540.
- Middleton, T., Herlihy, W.C., Schimmel, P.R., N. Munro, H.N. (1985). "Synthesis and purification of oligoribonucleotides using T4 RNA ligase and reverse-phase chromatography." Analytical Biochemistry **144**(1): 110-117.
- Monia, B. P., Lesnik, E.A., Gonzalez, C., Lima, W.F., McGee, D., Guinasso, C.J, Kawasaki, A.M., Cook, P.D., and Freier, S.M. (1993). "Evaluation of 2'-modified oligonucleotides containing 2'-deoxy gaps as antisense inhibitors of gene expression." Journal of Biological Chemistry **268**: 14514-14522.
- Pei, Y., Tuschl, T. (2006). "On the art of identifying effective and specific siRNAs." Nature Methods **3**(9): 670.
- Ponnuswamy, P. K., Gromhia, M.M. (1994). "On the conformational stability of oligonucleotide duplexes and tRNA molecules." Journal of Theoretical Biology **169**: 419-432.
- Porter, K. W., Briley, J.D., Shaw, B.R. (1997). "Direct PCR sequencing with boronated nucleotides." Nucleic Acids Research **25**(8): 1611-1617.
- Potenza, N., Moggio, L., Milano, G., Salvatore, V., Di Blasio B., Russo, A., Messere, A. (2008). "RNA Interference in Mammalian Cells by RNA-3'-PNA Chimeras." International Journal of Molecular Sciences **9**: 299-315.
- Preall, J. B., Sontheimer, E.J. (2005). "RNAi: RISC gets loaded." Cell **123**: 543-545.

- Promega (2006). Ribomax Large Scale RNA Production System - T7 and Sp6. Technical Bulletin, Promega Corporation.
- Raines, R. T. (1998). "Ribonuclease A." Chemical Reviews **98**: 1045-1065.
- Rana, T. (2007). "Illuminating the silence: Understanding the structure and function of small RNAs." Nature Reviews: Molecular and Cellular Biology **8**: 23-36.
- Reynolds, A., Leake, D., Boese, Q., Scaringe, S., Marshall, W.S., Khvorova, A. (2004). "Rational siRNA design for RNA interference." Nature Biotechnology **22**: 326 - 330.
- Roig, B., Gonzalez, C., Thomas, O. (2003). "Monitoring of phenol photodegradation by ultraviolet spectroscopy." Spectrochimica Acta Part A **59**: 303-307.
- Romaniuk, E., McLaughlin, L.W., Neilson, T., Romaniuk, P.J. (1982). "The Effect of Acceptor Oligoribonucleotide Sequence on the T4 RNA Ligase Reaction." European Journal of Biochemistry **125**(3): 639.
- Rozners, E., Moulder J. (2004). "Hydration of short DNA, RNA and 2'-OMe oligonucleotides determined by osmotic stressing." Nucleic Acids Research **23**(1): 248-254.
- Saenger, W. (1984). Principles of Nucleic Acid Structure. New York City, Springer Verlag.
- Scheffner, S., Whitkaer, N.J. (2003). "Human Papillomavirus-induced Carcinogenesis and the Ubiquitin-Proteasome System." Seminars in Cancer Biology **13**: 59-67.
- Schramm, G., Ramsey, R. (2005). "siRNA design including secondary structure target site prediction." Nature Methods **2**.
- ScienceDaily (2005). New Look At DNA Hints At Origin Of Ultraviolet Damage. ScienceDaily.
- Segueev, D., Hasan, A., Ramaswamy, M., Shaw, B.R. (1997). "Boranophosphate Oligonucleotides: New Synthetic Approaches." Nucleosides, Nucleotides, and Nucleic Acids **16**: 1533-1538.
- Sergueeva, Z. A., Segueev, D.S., Shaw, B.R. (2000). "Rapid and Selective Reduction of Amide Group by Borane-Amine Complexes in Acyl Protected Nucleosides." Nucleosides, Nucleotides, and Nucleic Acids **19**: 275-282.

- Sergueeva, Z. A., Segueev, D.S., Shaw, B.R. (2001). "Borane-Amine Complexes - Versatile Reagents in the Chemistry of Nucleic Acids and Their Analogs." Nucleosides, Nucleotides, and Nucleic Acids **20**: 941-945.
- Shaw, B. R., Dobrikov, M., Wan, X., Wang, J., He, K., Lin, J., Li, P., Rait, V., Segueeva, Z., Segueev, D. (2003). "Reading, writing, and modulating genetic information using boranophosphate mimics of nucleotides, DNA, and RNA." Annals of the New York Academy of Sciences **1002**: 12-29.
- Shaw, B. R., Sergueev, D., He, K.Z., Porter, K., Summers, J., Sergueeva, Z., and Rait, V. (2000). "Boranophosphate Backbone: A Mimic of Phosphodiester, Phosphorothioates, and Methyl Phosphonates." Methods in Enzymology **213**: 226-257.
- Sheffner, S., Whitaker, N.J. (2003). "Human Papillomavirus-induced Carcinogenesis and the Ubiquitin-Proteasome System." Seminars in Cancer Biology **13**: 59-67.
- Silber, R., Malathi, V.G., Hurwitz, J. (1972). "Purification and Properties of Bacteriophage T4-Induced RNA Ligase." Proceeding of the National Academy of Sciences **69**: 3009-3013.
- Simpson, L. (1998). Gel Electrophoresis and Photography: An Application Note, UVP, Inc.
- Sinha, N. D. (1993). Large-Scale Oligonucleotide Synthesis Using the Solid-Phase Approach.
- Smith, E. L., Hill, R.L., Lehman, I.R., Lefkowitz, R.J., Handler, P., White, A, Ed. (1983). Principles of Biochemistry: General Aspects. New York City, NY USA, McGraw-Hill.
- Snydera, L. L., Essera, J.M., Pachukb, C.J., and Steel, L.F. (2008). "Vector design for liver-specific expression of multiple interfering RNAs that target hepatitis B virus transcripts." Antiviral Research **80**(1): 36-44.
- Sood, A., Shaw, B.R., Spielvogel, B. (1990). "Boron-containing Nucleic Acids. 2. Synthesis of Oligodeoxyribonucleoside Boranophosphates." Journal of American Chemical Society **112**: 9000-9001.
- Sousa, R., Mukherjee, S. (2003). "T7 RNA Polymerase." Progress in Nucleic Acid Research and Molecular Biology **73**: 1-41.

- Stawinski, J., Ströberg, R. (2005). Di- and Oligonucleotide Synthesis Using H-Phosphonate Chemistry. Oligonucleotides Synthesis: Methods and Applications. P. Herdewijn. **288**.
- Steely, H. T., Grey, D. M., and Lang, D. (1986). "Circular dichroism of double-stranded RNA in the presence of salt and ethanol." Biopolymers **25**: 91-117.
- Stein, W. D. (1986). Simple diffusion across the membrane bilayer. Transport and diffusion across cell membranes: 69-117.
- Steitz, T. A. (2004). "The structural basis of the transition from initiation to elongation phases of transcription, as well as translocation and strand separation, by T7 RNA polymerase." Current Opinion in Structural Biology **14**(1): 4-9.
- Summers, J. S., Roe, D., Boyle, P.D., Colvin, M. (1998). "Structural studies of a borane-modified phosphate diester linkage: ab initio calculations on the dimethylboranophosphate anion and the single-crystal X-ray structure of its diisopylammonium salt." Inorganic Chemistry **37**: 4158-4159.
- Thiviyanathan, V., Vyazovkina, K.V., Gozansky, E.K., Bichenchova, E., Abramova, T.V., Luxon, B.A, Lebedev, A.V., Gorenstein, D.G. (2002). "Structure of Hybrid Backbone Methylphosphonate DNA Heteroduplexes: Effect of R and S Stereochemistry." Biochemistry **41**(3): 827-838.
- Tomasz, J., Shaw, B.R., Porter, K., Spielvogel, F., Sood, A. (1992). "5'-P-Boranosubstituted thymidine monophosphate and triphosphate." Angew Chem Int Ed Engl **31**: 1373-1375.
- Uhlenbeck, O.C., Cameron, V. (1977). "Equimolar addition of oligoribonucleotides with T4 RNA ligase." Nucleic Acids Research **4**(1):85-98.
- Ui-Tei, K., Naito, Y., Takahashi, F., Haraguchi, T., Ohki-Hamazaki, H., Juni, A., Ueda, R., Saigo, K., (2004). "Guidelines for the selection of highly effective siRNA sequences for mammalian and chick RNA interference." Nucleic Acids Research **32**(3): 938-948.
- Wan, J. (2005). Enzymatic synthesis, properties, and functions of boranophosphate RNA. Chemistry. Durham, Duke University. **Ph.D.**
- Wan, J., Shaw, B.R. (2005). "Incorporation of Ribonucleoside 5'-(α -P-borano)Triphosphates into a 20-mer RNA by T7 RNA Polymerase." Nucleosides, Nucleotides, and Nucleic Acids **24**(5-7): 943-946.

- Wang, J. X. (2004). Boranophosphate oligodeoxyribonucleotides as antisense reagents: synthesis, physicochemical and biological studies, and efforts to improve their properties. Chemistry. Durham, Duke University. **Ph.D.**
- Watson, J. D., Crick, F. H. C. (1953). "Molecular Structure of Nucleic Acids: A Structure for Deoxyribose Nucleic Acid." Nature **171**: 737-738.
- Williams, D. M., Benseler, F., Eckstein, F. (1991). "Properties of 2'-fluorothymidine-containing oligonucleotides: interaction with restriction endonuclease EcoRV." Biochemistry **30**: 4001.
- Wold, F. (1971). Macromolecules: Structure and Function.
- Wolfrum, C., Shi, S., Jayaprakash, K.N., Jayaraman, M., Wang, G., Pandey, R.K., Rajeev, K.G., Nakayama, T., Charrise, K., Ndungo, E.M., Zimmermann, T., Koteliansky, V., Manoharan, M., Stoffel, M. (2007). "Mechanisms and optimization of in vivo delivery of lipophilic siRNAs." Nature Biotechnology **25**(10): 1149-1157.
- Yu, D., Kandimalla, E.R., Roskey, A., Zhao, Q., Chen, L., Chen, J., Agrawal, S. (2000). "Stereo-enriched phosphorothioate oligodeoxynucleotides: synthesis, biophysical and biological properties." Bioorganic and Medicinal Chemistry **8**(1): 275-284.
- Zhang, H. Y., Du, Q., Wahlestedt, C., Liang, Z.C. (2006). "RNA interference with chemically modified siRNA." Current Topics in Medicinal Chemistry **6**: 893-900.
- Zuo, Y., Deutcher, M.P. (1999). "The DNase activity of ribonuclease T and its." Nucleic Acids Research **27**(20): 4077-4082.
- Zuo, Y., Deutcher, M.P. (2002). "Mechanism of Action of RNase T I. Identification of residues required for catalysis, substrate binding, and dimerization." Journal of Biological Chemistry **277**(51): 50155-50159.
- Zuo, Y., Zheng, H., Wang, Y., Chruszcz, M., Cymborowski, M., Skarina, T., Savchenko, A., Malhotra, A., Minor, W. (2007). "Crystal Structure of RNase T, an exoribonuclease involved in tRNA maturation and end-turnover." Structure **15**(4): 417-428.
- zur Hausen, H. (2003). "Papillomaviruses Causing Cancer: Evasion From Host-Cell Control in Early Events in Carcinogenesis." Journal of the National Cancer Institute **92**(9): 690-698.

Biography

Laura Moussa was born May 28, 1982 to Patricia and Wisam Moussa. She received a Bachelor of Science with Honors, Magna Cum Laude, in Chemistry from Binghamton University, Binghamton, NY, in 2003. While at Binghamton, she completed an undergraduate honor thesis in the Department of Chemistry, entitled "Electrochemical Detection in Microfluidic Analysis" under the supervision of Dr. C.J. Zhong. While in graduate school, Laura was awarded the Pharmacological Sciences Training Fellowship from 2004-2006, the 2007 Kathleen Zielek Fellowship and the 122nd NC ACS Sectional Meeting First Place Poster Award 2008.

Publications

Kariuki, Nancy N.; Luo, Jin; Han, Li; Maye, Mathew M.; Moussa, Laura; Patterson, Melissa; Lin, Yuehe; Engelhard, Mark H.; Zhong, Chuan-Jian. Nanoparticle-structured ligand framework as electrode interfaces. *Electroanalysis* (2004), 16(1-2), 120-126.

Luo, Jin; Kariuki, Nancy; Han, Li; Maye, Mathew M.; Moussa, Laura W.; Kowaleski, Scott R.; Kirk, F. Louis; Hepel, Maria; Zhong, Chuan-Jian. Interfacial Mass Flux at 11-Mercaptoundecanoic Acid Linked Nanoparticle Assembly on Electrodes. *Journal of Physical Chemistry B* (2002), 106(36), 9313-9321.

Kariuki, N.N, Moussa, L., Menard, T., Hassan, A., Han, L., Crew E., Luo, J., Zhong, C.J. Nanostructure Materials for Microfluidic Sensing Application. *Materials Research Society Symposium Proceedings* (2004), Volume Date 2003, 782 (Micro- and Nanosystems)

Moussa, Laura W. *Electrochemical Detection in Microfluidic Analysis*. Honors Thesis, 2003. Binghamton University Press.

Shaw, B.R., Moussa, L., Sharaf, M., Cheek, M., Dobrikov, M. Boranophosphate siRNA-aptamer chimeras for tumor-specific downregulation of cancer receptors and modulators. *Nucleic Acids Symposium Series* 2008 52(1):655-656